Reprinted from Mark-Bikales-Overberger-Menges:
Encyclopedia of Polymer Science and Engineering,
Vol. 8 Volume 8, Second Edition LIGHT SCATTERING 721
Copyright © 1987 by John Wiley & Sons, Inc.

19. R. B. McLaughlin, *Special Methods in Light Microscopy*, Microscope Publications, Chicago, Ill., 1977.
20. E. M. Chamot and C. W. Mason, *Handbook of Chemical Microscopy: Chemical Methods*, 2nd ed., Vol. 2, John Wiley & Sons, Inc., New York, 1940.
21. B. Kachar, *Science* **227**, 766–768 (Feb. 15, 1985).
22. A. Lewis and M. Isaacson, *Research Begets Fine Optical Microscope*, Cornell Alumni News, Mar. 1986, pp. 6,7.

T. G. ROCHOW
North Carolina State University

LIGHT SCATTERING

Study of the scattering (qv) of electromagnetic radiation from polymers and their solutions embraces a wide variety of techniques and yields information on diverse intramolecular and intermolecular properties. Methods include x-ray, neutron, and light scattering; some features of the scattering from these diverse sources can be treated with a common formalism. The molecular properties elucidated include intramolecular properties, eg, molecular weight ($\overline{M}_w$), root-mean-square radius of gyration (R_G), translational diffusion constant (D_T^0) and others obtained by extrapolation of measured quantities to infinite dilution. Data on solutions at low concentrations yield information on intermolecular properties such as the second virial coefficient A_2, and the mutual-diffusion constant D_M. The theoretical basis for deriving these parameters from scattering data is well established and generally applicable with a few exceptions. Theoretical treatment of the scattering from moderately concentrated solutions is less advanced but is developing rapidly under the impetus of new experimental methods and theoretical insights. The scattering from undiluted polymers is principally used to study the morphology of the crystalline state. Representative monographs and review articles are included in Refs. 1–26 (see also NEUTRON SCATTERING; X-RAY DIFFRACTION).

The topics covered here include only a subset of the field encompassed by electromagnetic scattering from polymer solutions. In particular, the principles of light scattering from solutions at low and moderate concentrations will be considered. A useful measure of the concentration c (weight per volume), is the product, $[\eta]c$, where the intrinsic viscosity $[\eta]$ is defined as the limiting value of $\partial \ln \eta/\partial c$ at infinite dilution, with η the solution viscosity. The product $[\eta]c$ provides a measure of the intermolecular overlap of the polymer solute inasmuch as $[\eta]M/N_A$ may be considered a hydrodynamic volume per solute molecule, with cN_A/M the number of chains per unit volume. Thus low concentrations are those for which $[\eta]c \ll 1$, and intermolecular interactions are small or suppressed in the limit as $[\eta]c$ goes to zero. For moderately concentrated solutions, $[\eta]c \approx 1$–10 and the effects of intermolecular interactions are important. Under either of these conditions, the light scattering is usually dominated by concentration fluctuations inherent in solutions, and the interpretation of the scattering is based on descriptions of the time evolution of the positions of scattering centers.

In general, the relations

$$M[\eta] = K_\eta \pi N_A R_H R_G^2 \quad (1)$$

$$R_H = kT/6\pi\eta_s D_T^0 \quad (2)$$

with η_s the solvent viscosity, provide a connection between $[\eta]$ and the parameters M, R_H, and R_G available from light scattering, where K_η depends on the nature of the solute, see below.

The incident light radiation subjects scattering centers to an alternating electric field (10^{14}–10^{15} Hz), resulting in periodic motion of the electrons in these centers which become sources of dipole radiation. The induced electric dipole moment **P** is a vector; its components (in Cartesian coordinates) may be represented as a function of the electric field **E** as the expansion ($i,j,k = 1,2,3$):

$$P_i = \alpha_{ij}E_j + \beta_{ijk}E_jE_k + \cdots \quad (3)$$

where the Einstein summation convention is employed. Interest here is limited to the polarizability tensor $\boldsymbol{\alpha}$, representing the linear response. Higher order nonlinear terms (represented here in the hyperpolarizability tensor $\boldsymbol{\beta}$) give rise to interesting and useful effects, eg, harmonically scattered light, etc. Restriction to the linear term in the expansion of **P** includes both elastic scattering, for which the frequencies ω_S and ω_L of the scattered and incident light, respectively, are equal, quasielastic scattering, for which ω_S is very slightly different from ω_L due to a Doppler effect associated with motion of the scattering centers, and inelastic scattering resulting from periodic variations of $\boldsymbol{\alpha}$ with time. The latter are associated with molecular vibrations which change the molecular structure and thereby the polarizability. Since these vibrations may be associated with normal coordinates, it is convenient to represent their effect on $\boldsymbol{\alpha}$ in the form (22):

$$\alpha_{ij} = \alpha_{ij}^0 + (\partial\alpha_{ij}/\partial Q_a)_0 Q_a + \cdots \quad (4)$$

where Q_a is the normal coordinate for the ath vibration and α_{ij}^0 represents the polarizability for the equilibrium structure ($Q_a = 0$). Since

$$E_j = E_j^0 \cos \omega_L t \quad (5)$$

$$Q_a = Q_a^0 \cos \Omega_a t \quad (6)$$

use of equations 3–6 gives

$$P_i = \alpha_{ij}^0 E_j^0 \cos \omega_L t + (\partial\alpha_{ij}/\partial Q_a)_0 Q_a^0 E_j^0 \times \{\cos[(\omega_L + \Omega_a)t] + \cos[(\omega_L - \Omega_a)t]\} \quad (7)$$

where the first term gives rise to the elastic or quasielastic light scattering, and the second term gives rise to inelastic scattering at frequencies $\omega_L \pm \Omega_a$. If the normal modes are those of a single molecule, the effect is termed Raman scattering (see RAMAN SPECTROSCOPY). It provides complementary information to that obtained by infrared absorption spectroscopy (qv). If the normal modes are associated with the vibrational modes of the entire sample, the effect is termed Brillouin scattering. In general, Brillouin scattering is shifted by 10^8–10^{11} Hz from ω_L, whereas Raman scattering is shifted by 10^{11}–10^{14} Hz. By comparison, the frequency shift with quasielastic scattering is much smaller, ie, 10–10^7 Hz.

In the following, expressions for the scattered intensity are given in a gen-

eral format to support the specific topics presented in subsequent sections dealing with treatment of elastic scattering, followed by discussion of quasielastic and Brillouin scattering. Finally, the design and use of light-scattering photometers, data treatment, and sample preparation are discussed.

Theory

Much of the discussion of light scattering is concerned with interference effects between light rays scattered from different parts of the sample; these may arise from different parts of a single solute molecule or from parts of different molecules. The topics considered here are limited to situations in which the electric field giving rise to the dipole radiation is that of the incident radiation propagating in the sample. That is, the field **E** acting on all parts of a solute is the same as that acting on the solvent. Deviations from this give rise, for example, to Mie scattering. The simplification used here is termed Rayleigh-Debye or Rayleigh-Gans scattering (8). With this simplification, the rays arriving at each scattering center bear known phase relations to each other, dependent on the position **r** of the centers at the time t of observation. Similarly, the scattered rays from each center viewed at angle θ from the incident radiation have a precisely known phase relation to the incident light. This situation is illustrated in Figure 1 for the scattering viewed in the plane containing the incident and scattered beams. The interference between rays scattered from elements i and j depends on the vector distance $\mathbf{r}_{ij} = \mathbf{r}_i - \mathbf{r}_j$, where $\mathbf{r}_i$ and $\mathbf{r}_j$ are the vectors from an arbitrary reference to elements i and j, respectively. The vectoral wave numbers $\mathbf{k}_0$ and $\mathbf{k}$, which lie in the directions of the incident and scattered light, respectively, may be used to compute the difference in the path lengths for rays scattered from centers i and j as $(\mathbf{k}_0 - \mathbf{k})\cdot\mathbf{r}_{ij}$. For elastic or quasielastic scattering,

$$|\mathbf{k}_0| = |\mathbf{k}| = 2\pi/\lambda \tag{8}$$

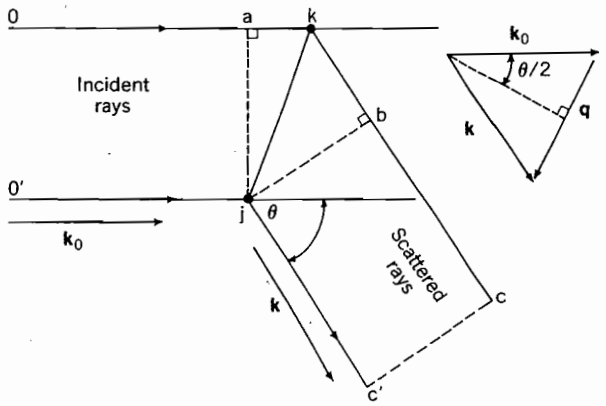

Fig. 1. Vectors $\mathbf{k}_0$ and $\mathbf{k}$ for the incident and scattered light, respectively, and the wave vector $\mathbf{q}$. Path length akb gives rise to interference effects for rays scattered from j and k.

with λ the wavelength of light in the medium; a reciprocal dimension defined as

$$\mathbf{q} = \mathbf{k}_0 - \mathbf{k} \tag{9a}$$

$$q = |\mathbf{k}_0 - \mathbf{k}| = (4\pi/\lambda) \sin \theta/2 \tag{9b}$$

with θ the scattering angle, appears in a natural way when considering interference effects.

In computing the scattered intensity, it is assumed that the solute molecules are not coupled electronically and $\boldsymbol{\alpha}$ at one site is not altered by the state of polarization at other sites. Then, with the electric field polarized along the unit vectors $\mathbf{n}_r$ and $\mathbf{n}_s$ for the incident and scattered beams, respectively, the components of the autocorrelation function of the polarizability fluctuation specified by $\mathbf{n}_r$ and $\mathbf{n}_s$ are given by (1)

$$Q_{rs}(\mathbf{q},t) = \langle \Delta\alpha^*_{rs}(\mathbf{q},0)\, \Delta\alpha_{rs}(\mathbf{q},t) \rangle \tag{10}$$

$$\Delta\boldsymbol{\alpha}_{rs}(\mathbf{q},t) = \mathbf{n}_r \cdot \left\{ \sum_{\nu}^{\eta} \boldsymbol{\alpha}_\nu(t) \exp\left[i\mathbf{q}\cdot\mathbf{r}_\nu(t)\right] \right\} \cdot \mathbf{n}_s \tag{11}$$

where ν runs over the η scattering centers in the scattering volume, and $\Delta\alpha_{rs}(\mathbf{q},t)$ represents the fourier component of the polarizability density, $\Delta\alpha_{rs}(\mathbf{r},t)$, with

$$\Delta\alpha_{rs}(\mathbf{r},t) = \mathbf{n}_r \cdot \left\{ \sum_{\nu}^{\eta} \boldsymbol{\alpha}_\nu(t)\, \delta\left[\mathbf{r} - \mathbf{r}_\nu(t)\right] \right\} \cdot \mathbf{n}_s \tag{12}$$

In these expressions, rotation and vibration of the scattering centers result in variation of $\boldsymbol{\alpha}_\nu(t)$ with t, and translation of the scattering centers results in changes of the phase factor with t. With isotropic scattering centers, the effect of rotations is nil. The quantity $Q_{rs}(\mathbf{q},0)$ is proportional to the average intensity $I(q)$ of the scattering.

For optically isotropic scattering centers, $\boldsymbol{\alpha}$ may be replaced by the average polarizability α equal to (trace $\boldsymbol{\alpha}$)/3. Although this situation is rarely, if ever, precisely realized (as shown below), it is a very good approximation for high molecular weight chains unless the chain adopts a nearly rodlike configuration. If the scattering centers are not optically isotropic and α_{ij} cannot be expressed as $\alpha\delta_{ij}/3$, it is useful to adopt the symbols $I_{Vv}(q,t)$ and $I_{Hv}(q,t)$ for the scattering obtained in the transverse scattering planes with vertically and horizontally polarized scattered light, respectively, and vertically polarized incident light, eg, $\mathbf{n}_r \cdot \mathbf{n}_s$ is unity for $I_{Vv}(q,t)$ and zero for $I_{Hv}(q,t)$.

Since digital photon-counting methods find increasing use in light scattering and are the preferred method for quasielastic light scattering studies, the presentation here is cast in terms of measurement of the number of photon counts $n(q,t;\Delta\tau)$ measured at time t over a time interval $\Delta\tau$. This information may be presented in terms of the probability density $p_1(n)$ for the count rate, or the bivariant probability density $p_2(n,n')$, where n and n' signify $n(q,t;\Delta\tau)$ and $n(q,t';\Delta\tau)$, respectively, with $t' = t + \tau$. Both $p_1(n)$ and $p_2(n,n')$ may be determined by photocounting methods, and both depend on the state of polarization used, eg, on $\mathbf{n}_r$ and $\mathbf{n}_s$; notation indicating the latter dependence is suppressed for convenience. The count rate n may be expressed in terms of the instantaneous light intensity $I(q,t;\mathbf{R})$ arriving at position $\mathbf{R}$ on a photomultiplier through the relation (1–3)

$$n(q,t;\Delta\tau) = \sigma \int_A d^2R \int_{t-\Delta\tau/2}^{t+\Delta\tau/2} dt\, I(q,t;\mathbf{R}) \tag{13}$$

where A is the area on the photomultiplier illuminated by the scattered beam, $I(q,t;\mathbf{R})$ is computed from $Q_{rs}(\mathbf{q},t)$, and σ is a constant. The average intensity $I(q)$ of the elastic scattering is independent of t, and proportional to $\Delta\tau\langle n(q,\Delta\tau)\rangle$, where

$$\langle n(q,\Delta\tau)\rangle = \int n\, p_1(n)dn \tag{14}$$

For example, $I(q)$ may be determined from the current from the photomultiplier, detected as a voltage drop across a resistor, averaged over a long time in comparison with the time for fluctuations in the instantaneous intensity, $I(q,t)$.

It is useful to express $\langle n(q,\Delta\tau)\rangle$ and $I(q)$ in terms of a quantity $\mathbf{R}(q)$ called the Rayleigh ratio, defined as

$$\mathbf{R}(q) = R^2 I(q)/VI_{\text{inc}} = R^2\langle n(q,\Delta\tau)\rangle/Vn_{\text{inc}} \tag{15}$$

where R is the distance between the scattering centers and the photomultiplier, V, the scattering volume, I_{inc}, the intensity of the incident beam, and n_{inc}, the count rate obtained with the incident beam at the $\Delta\tau$ used to determine $\langle n(q,\Delta\tau)\rangle$. The corresponding notation $\mathbf{R}_{Vv}(q)$ and $\mathbf{R}_{Hv}(q)$ will be used for the Rayleigh ratios obtained from $I_{Vv}(q)$ and $I_{Hv}(q)$, respectively; $\mathbf{R}(q)$ without subscripts always refers to $\mathbf{R}_{Vv}(q)$. In most cases, the excess Rayleigh ratio is equal to the difference of the Rayleigh ratios for solution and solvent; $\mathbf{R}(q)$, etc, refers to the excess quantity unless otherwise specified.

The photon-count distribution may also be used to obtain the quantities

$$N^{(r)}(q,\Delta\tau) = \int \frac{n!}{(n-r)!}\, p_1(n)dn \tag{16}$$

$$G^{(2)}(q,\tau;\Delta\tau) = \int nn' p_2(n,n')dndn' \tag{17}$$

where $N^{(r)}$ and $G^{(2)}$ are called the factorial moment and the photoncount correlation function, respectively, with

$$N^{(1)}(q,\Delta\tau) = \langle n(q,\Delta\tau)\rangle \tag{18}$$

For $\tau = 0$,

$$G^{(2)}(q,0;\Delta\tau) = N^{(2)}(q,\Delta\tau) + N^{(1)}(q,\Delta\tau) \tag{19}$$

Normalized functions used in the following are defined as

$$g^{(2)}(q,\tau;\Delta\tau) = \frac{G^{(2)}(q,\tau;\Delta\tau)}{G^{(2)}(q,\infty;\Delta\tau)} \tag{20}$$

$$n^{(r)}(q,\Delta\tau) = \frac{N^{(r)}(q,\Delta\tau)}{\langle n(q,\Delta\tau)\rangle^r} \tag{21}$$

where $G^{(2)}(q,\infty;\Delta\tau)$ is the limiting value of $G^{(2)}(q,\tau;\Delta\tau)$ for large τ.

Spatial and temporal integrations such as those in equation 13 complicate these relations, giving (23)

$$g^{(2)}(q,\tau;\Delta\tau,A) = 1 + f(A)[g^{(2)}(q,\tau;\Delta\tau,0) - 1] \tag{22}$$

where $f(A)$ accounts for the spatial averaging of the scattered rays from the scattering volume and (23)

$$n^{(2)}(q,\Delta\tau;A) = 1 + f(A)[n^{(2)}(q,\Delta\tau;0) - 1] \tag{23}$$

for $r = 2$. The factor $f(A)$ may be considered to be an instrument parameter dependent on the specific optical arrangements of the detector optics; typically, $f(A)$ is in the range 0.1–0.9.

In most cases, $\Delta\alpha_{rs}(\mathbf{q},\tau)$ is a Gaussian stochastic variable (1,23), and $g^{(2)}(q,\tau;\Delta\tau,0)$ may be expressed in terms of another function $g^{(1)}(q,\tau)$ given by

$$g^{(1)}(q,\tau) = \frac{Q_{rs}(q,\tau)}{Q_{rs}(q,0)} \tag{24}$$

In terms of $g^{(1)}(q,\tau)$, the temporal average over the interval $\Delta\tau$ gives (23)

$$g^{(2)}(q,\tau;\Delta\tau,0) - 1 = [p(q,\Delta\tau)g^{(1)}(q,\tau)]^2 \tag{25a}$$

where

$$p(q,\Delta\tau) = \frac{\left[\int_{t-\Delta\tau/2}^{t+\Delta\tau/2}\int_{t-\Delta\tau/2}^{t+\Delta\tau/2} |g^{(1)}(q,u-v)|^2\, du\, dv\right]^{3/2}}{\Delta\tau g^{(1)}(q,\tau)} \tag{25b}$$

Expressions for $g^{(1)}(q,\tau)$, $p(q,\Delta\tau)$, and $n^{(2)}(q,\Delta\tau;0)$ are discussed below.

Combination of equations 22, 23, and 25 shows that $f(A)$ may be evaluated as $n^{(2)}(q,0;A) - 1$ or $g^{(2)}(q,0^+;0,A) - 1$, where the symbol 0^+ designates a limit as τ tends to zero.

In studies of the static scattering, embodied in $\mathbf{R}(q)$, the light source need not exhibit long temporal and spatial coherence lengths, and any sufficiently intense (nearly) monochromatic source is suitable, eg, an emission line from a mercury arc is often used. In studies of the dynamic scattering, embodied in $G^{(2)}(q,\tau;\Delta\tau)$ or $N^{(r)}(q,\Delta\tau)$, the light source must exhibit both temporal and spatial coherence, which means that laser sources must be used. For this reason applications of dynamic scattering have increased rapidly only during the last decade as laser sources became available.

Scattering at Infinite Dilution

Static Scattering at Zero Scattering Angle. The ratio $[\mathbf{R}(0)/c]^0$ of the Rayleigh ratio divided by the concentration, extrapolated to zero angle and infinite dilution, is discussed below for several cases. Since many real systems are heterodisperse, eg, with respect to molecular weight or composition, the discussion is cast in a form to account for this feature. Thus, for isotropic scatters, $[\mathbf{R}(0)/c]^0$ is expressed in terms of a molecular weight M_{LS} appropriately averaged. In the simplest case, M_{LS} is equal to the molecular weight M_W. For an isotropic solute with identical scattering elements, heterodisperse only in chain length (and dissolved in a single component solvent), M_{LS} is equal to the weight-average molecular weight $\overline{M}_W$. More complicated examples are included. For anisotropic scatters, the results are given in terms of isotropic and anisotropic components $[\mathbf{R}_{iso}(0)/c]^0$ and $[\mathbf{R}_{aniso}(0)/c]^0$, respectively, which are expressed in terms of M_{LS}

and a molecular anisotropy δ_X^2, defined below. The presentation here is limited to a minimum of intermediate expressions with emphasis on relations useful in the interpretation of data on $[\mathbf{R}(0)/c]^0$.

Isotropic Identical Scatterers. At infinite dilution of the solution, and in the absence of long-range, eg, electrostatic, interactions, it may be assumed that spatial and orientational correlations among the solute components are nil, and only correlations among the scattering centers of a single molecule (or particle) need to be considered. However, at zero scattering angle interference effects due to these single-molecule correlations also vanish, and the excess Rayleigh ratio for isotropic scatterers may be expressed in terms of the osmotic compressibility of the C-solute molecules present in the scattering volume. (C is smaller than the number η of scattering centers for large molecules). Each solute is characterized by its concentration c_ν, molecular weight M_ν, and excess molecular polarizability $n_\nu\alpha_\nu$, where n_ν is the number of scattering centers on the ν^{th} solute, ie, each center of solute ν is assumed to have excess polarizability α_ν. A statistical mechanical treatment to relate the concentration fluctuations of the solute to thermodynamic properties gives the result (8,13,16)

$$[\mathbf{R}(0)/c]^0 = K'(2\pi N_A)^2 \sum_\nu^C w_\nu (n_\nu\alpha_\nu)^2 M_\nu^{-2} \frac{RT}{(\partial\Pi/\partial c)_\nu^0} \tag{26a}$$

where

$$[\mathbf{R}(0)/c]^0 = \lim_{\substack{q=0 \\ c=0}} \mathbf{R}(q)/c \tag{26b}$$

and

$$K' = 4\pi^2/N_A\lambda_0^4 \tag{26c}$$

Here Π is the osmotic pressure, λ_0, the wavelength of the incident light in vacuum, $w_\nu = c_\nu/c$, the weight fraction of component ν with c the total solute concentration, and $n_\nu\alpha_\nu$, making use of the Einstein summation convention for index i, is given by

$$n_\nu\alpha_\nu = \frac{(\alpha_{ii})_\nu}{3} = \left(\frac{\tilde{n}_s}{2\pi N_A}\right)\psi_\nu M_\nu \tag{27}$$

$$\psi_\nu = \left(\frac{\partial\tilde{n}}{\partial c_\nu}\right)_w^0 \tag{28}$$

The superscript 0 is used throughout to designate a quantity at infinite dilution. Here, $\tilde{n}$ is the refractive index, and the subscript s denotes the solvent. With equation 27 it is not necessary to specify n_ν or α_ν independently in terms of molecular characteristics, since only the product $n_\nu\alpha_\nu$, which may be expressed in observable terms, is of interest. In these relations, $(\partial\tilde{n}/\partial c_\nu)_w$ is determined at constant composition of all components except the ν^{th}; K' is defined for the scattering in the transverse plane with vertically polarized incident light. Equation 26, obtained by Debye (27), reveals the connection between the scattering and the osmotically dampened concentration fluctuations. Since (28)

$$\lim_{c=0} \Pi_\nu = RT\frac{c_\nu}{M_\nu} \tag{29}$$

equation 26 reduces to

$$[\mathbf{R}(0)/c]^0 = K' \tilde{n}_s^2 \left(\frac{\partial \tilde{n}}{\partial c}\right)_w^2 M_{LS} \tag{30}$$

where

$$\left(\frac{\partial \tilde{n}}{\partial c}\right)_w = \sum_\nu^C w_\nu \psi_\nu \tag{31}$$

$$M_{LS} = \left(\frac{\partial \tilde{n}}{\partial c}\right)_w^{-2} \sum_\nu^C \psi_\nu^2 w_\nu M_\nu \tag{32}$$

with $(\partial \tilde{n}/\partial c)_w$ the refractive index increment determined at constant temperature, pressure, and composition w of solute. In these relations, it is assumed that $(\partial \tilde{n}/\partial c)_w \neq 0$, otherwise $\mathbf{R}(q) = 0$ and equation 30 is not valid.

In the simplest case, with one solvent and one solute, M_{LS} reduces to the molecular weight M of the solute. If the solute comprises a homologous series with ψ_ν independent of ν and equal to $(\partial \tilde{n}/\partial c)_w$, as would usually be the case with one solvent, neglecting variation of ψ_ν for small M_ν that might occur as a result of differences between the polarizability of chain ends and middles,

$$M_{LS} = \sum_\nu^C w_\nu M_\nu = \overline{M}_w \tag{33}$$

If the system contains multiple solvent components (eg, water and salt or solvent A and solvent B with refractive indexes n_A and n_B, respectively) to a good approximation (16,17,29,30),

$$M_{LS} = \frac{(\partial \tilde{n}/\partial c)_\mu^2}{(\partial \tilde{n}/\partial c)_w^2} \overline{M}_w \tag{34}$$

where $(\partial \tilde{n}/\partial c)_\mu$ is the refractive index increment determined at constant temperature, pressure, and at osmotic equilibrium of the solvent components in the solution and the solute-free solvent mixture. Since $(\partial \tilde{n}/\partial c)_\mu$ is conveniently measured by differential refractometry on solutions dialyzed against the solvent mixture, $\overline{M}_w$ may be obtained for solutions in mixed solvents with little more effort than is required with a single-component solvent simply by use of $(\partial \tilde{n}/\partial c)_\mu$ instead of $(\partial \tilde{n}/\partial c)_w$ in equation 32. The ratio $(\partial \tilde{n}/\partial c)_\mu/(\partial \tilde{n}/\partial c)_w$ is, of course, unity with mixed solvents if all the solvent components have the same refractive index. Otherwise, with a binary solvent system this ratio may be interpreted in terms of preferential solvation of the solute by one of the solvent components. In some cases, preferential solvation depends on the solute molecular weight (30).

Isotropic Nonidentical Scatterers. If the monomer units are not all identical, provided $(\partial n/\partial c)_w \neq 0$, equation 32 becomes

$$M_{LS} = \left(\frac{\partial \tilde{n}}{\partial c}\right)_w^{-2} \sum_\nu^C w_\nu M_\nu^{-1} \left(\sum_i^{n_\nu} \psi_{i,\nu} m_{i,\nu}\right)^2 \tag{35}$$

where $\psi_{i,\nu}$ and $m_{i,\nu}$ are, respectively, the refractive-index increment and molecular weight of the i^{th} monomer on the ν^{th} chain. With the definitions

$$\Delta m_{j,\nu} = m_{j,\nu} - m_\nu \tag{36}$$

$$\Delta\psi_{j,\nu} = \psi_{j,\nu} - \psi_\nu \tag{37}$$

where $m_\nu = M_\nu/n_\nu$ and ψ_ν are properties of the ν^{th} chain, and $\Sigma\Delta m_{j,\nu}$ and $\Sigma\Delta\psi_{j,\nu}$ are each zero, equation 35 may be put in the form

$$M_{\text{LS}} = \left(\frac{\partial\tilde{n}}{\partial c}\right)_w^{-2} \sum_\nu^C w_\nu M_\nu^{-1}\left(\psi_\nu M_\nu + \sum_j^{n_\nu} \Delta\psi_{j,\nu}\Delta m_{j,\nu}\right)^2 \tag{38}$$

If either $\Delta\psi_j$ or Δm_j are zero for all ν, M_{LS} reduces to the relation for a blend of homopolymers. For example, if the solute comprises a blend of two homogeneous components with refractive-index increments ψ_A and ψ_B, weight-average molecular weights $\overline{M}_{w,A}$ and $\overline{M}_{w,B}$ present at weight fractions W_A and $W_B = 1 - W_A$, then [for a single solvent and $(\partial\tilde{n}/\partial c)_w \neq 0$], M_{LS} is given by (16)

$$M_{\text{LS}} = \overline{M}_w(1 + 2pY + qY^2) \tag{39}$$

where

$$Y = \left[\frac{\psi_A - \psi_B}{(\partial n/\partial c)_w}\right] \tag{40}$$

$$p = w_A w_B(\overline{M}_{w,A} - \overline{M}_{w,B})/\overline{M}_w \tag{41}$$

$$q = w_A w_B\left(\frac{\overline{M}_{w,A} + \overline{M}_{w,B}}{\overline{M}_w} - 1\right) \tag{42}$$

Consequently, M_{LS} is a parabolic function of Y, being equal to $\overline{M}_w$ for $Y = 0$.

For a copolymer comprising scattering elements with refractive index increment ψ_A or ψ_B and molecular weight m_A and m_B, respectively, with $W_{A,\nu}$ and $W_{B,\nu} = 1 - W_{A,\nu}$ the weight fractions of the two monomers in component ν, and

$$\Delta w_\nu = w_{A,\nu} - w_A = w_B - w_{B,\nu} \tag{43}$$

Equation 35 may be expressed in the form (16,31–33)

$$[\mathbf{R}(0)/c]^0 = K'\tilde{n}_s^2 \sum_\nu^C w_\nu M_\nu[\psi + (\psi_A - \psi_B)\Delta w_\nu]^2 \tag{44}$$

with $\psi = (\partial\tilde{n}/\partial c)_w$. If $\psi \neq 0$, then $[\mathbf{R}(0)/c]^0$ may be represented by equation 30 with M_{LS} given by equation 39, where Y is given by equation 40 and

$$p = \sum_\nu^C w_\nu M_\nu \Delta w_\nu/\overline{M}_w \tag{45}$$

$$q = \sum_\nu^C w_\nu M_\nu(\Delta w_\nu)^2/\overline{M}_w \tag{46}$$

For a strictly alternating copolymer or a copolymer with random placements of the monomers, $\Delta w_\nu = 0$ and $M_{\text{LS}} = \overline{M}_w$. Similarly, for regular block copolymers, $\Delta w_\nu = 0$, and $M_{\text{LS}} = \overline{M}_w$ if the composition is identical for all components. If the copolymer is homogeneous in molecular weight, or if the composition is independent of molecular weight, p vanishes and q, falling in the range $0 \leq q \leq w_A w_B$, depends on the dispersion of the composition, where $w_A = \Sigma w_{A\nu} w_{B\nu}$, and $w_B = 1 - w_A$. If $\psi = 0$, then equation 44 becomes

$$[\mathbf{R}(0)/c]^0 = K'\tilde{n}_s^2\, c(\psi_A - \psi_B)^2 \sum_{\nu}^{C} w_\nu M_\nu (\Delta w_\nu)^2 \tag{47}$$

On the other hand, if a solvent is selected for which, say $\psi_B = 0$, equation 30 applies, with

$$M_{LS} = \overline{M}_n \frac{\overline{M}_{w,A}}{\overline{M}_{n,A}} \tag{48}$$

where $\overline{M}_{w,A}$ and $\overline{M}_{n,A}$ are the weight- and number-average molecular weights of polymer A (ie, $\overline{M}_{w,A} = n_{w,A} m_A$, etc) and $\overline{M}_n$ is the number-average molecular weight of the copolymer.

Anisotropic Identical Scatterers. As implied in the preceding discussion, equation 26 may be obtained by developing a statistical mechanical treatment to relate concentration fluctuations of the solute to thermodynamic properties (13). Alternatively, relations for the light scattering intensity may be developed in terms of molecular distribution functions. Use of the latter is especially appropriate if the scattering centers comprising the solute molecules are not optically isotropic. In such a case (1,13),

$$[\mathbf{R}_{Vv}(0)/c]^0 = [\mathbf{R}_{iso}(0)/c]^0 + \tfrac{4}{3}[\mathbf{R}_{aniso}(0)/c]^0 \tag{49}$$

$$[\mathbf{R}_{Hv}(0)/c]^0 = [\mathbf{R}_{aniso}(0)/c]^0 \tag{50}$$

with $[\mathbf{R}_{iso}(0)/c]^0$ given by equation 30 and $[\mathbf{R}_{aniso}(0)/c]^0$ given in terms of the orientational correlation among the scattering centers on one molecule. Thus, for a solution with concentration c_ν of solute, each having n_ν identical scattering centers and molecular weight M_ν (5),

$$[\mathbf{R}_{aniso}(0)/c]^0 = \tfrac{1}{15}K'(2\pi N_A)^2 \sum_{\nu}^{c} w_\nu \langle \gamma_\nu^2 \rangle M_\nu^{-1} \tag{51}$$

where $\langle \cdots \rangle$ indicates an ensemble average, and $\langle \gamma_\nu^2 \rangle$ is the mean-square optical anisotropy per molecule of component, ν with

$$\gamma_\nu^2 = \{\tfrac{3}{2}[(\alpha_{11} - \alpha_{22})^2 + (\alpha_{11} - \alpha_{33})^2 + (\alpha_{22} - \alpha_{33})^2] + 3(\alpha_{12}^2 + \alpha_{13}^2 + \alpha_{23}^2)\}_\nu \tag{52}$$

If the scattering centers are optically isotropic, then $\alpha_{ij} = (\alpha/3)\delta_{ij}$, $\langle \gamma_\nu^2 \rangle = 0$ and $[\mathbf{R}_{aniso}(0)/c]^0$ is zero. Detailed calculation of $\langle \gamma^2 \rangle$ is possible in some cases. For example, $\langle \gamma^2 \rangle$ has been calculated for chain molecules using bond polarizabilities and relative energies of rotational isomeric states (5).

If the polarizabilities of the scattering centers of a particular chain are identical, and all possess cylindrical symmetry, so that in diagonal form, $\alpha_{11} \neq \alpha_{22} = \alpha_{33}$; where α_{11} is directed along a chain bond, equation 51 can be written in the form (with $\psi_\nu \neq 0$):

$$[\mathbf{R}_{aniso}(0)/c]^0 = \frac{3}{5}K'\tilde{n}_s^2 \left(\frac{\partial \tilde{n}}{\partial c}\right)_w^2 \overline{M}_w \delta_x^2 \tag{53}$$

with

$$\delta_x^2 = \frac{\Sigma w_\nu M_\nu \delta_\nu^2}{\overline{M}_w} \tag{54}$$

where δ_ν is given by the relation (5,34)

$$\delta_\nu^2 = \frac{\delta_0^2}{n_\nu^2} \sum_i^{n_\nu} \sum_j \frac{3\langle \cos^2 \beta_{ij} \rangle - 1}{2} \tag{55}$$

with β_{ij} the angle between the major axes of the polarizability ellipsoids associated with scattering elements i and j on a chain having n_ν elements. The ensemble average indicated by $\langle \cdots \rangle$ is over all conformations available to the molecules, and δ_0 is given by

$$\delta_0 = \frac{\alpha_\parallel - \alpha_\perp}{\alpha_\parallel + 2\alpha_\perp} \tag{56}$$

where $\alpha_\parallel$ and $\alpha_\perp$ are the principal polarizabilities for the scattering elements. For rodlike chains, $\beta_{ij} = 0$ for all i and j and as a consequence $\delta_\nu = \delta_0$ and

rod:
$$[R_{\text{aniso}}(0)/c]^0 = \frac{3}{5} K' \tilde{n}_s^2 \left(\frac{\partial \tilde{n}}{\partial c} \right)_w^2 \delta_0^2 \overline{M}_w \tag{57}$$

For a chain comprising n_ν elements which are orientationally uncorrelated and optically identical, only terms with $i = j$ contribute to the summation in equation 55 and $\delta_\nu^2 = \delta_0^2/n_\nu$; equation 53 becomes

random coil:
$$[R_{\text{aniso}}(0)/c]^0 = \frac{3}{5} K' \tilde{n}_s^2 \left(\frac{\partial \tilde{n}}{\partial c} \right)_w^2 \delta_0^2 m_0 \tag{58}$$

where $m_0 = M_\nu/n_\nu$ is the molecular weight of the statistically independent scattering elements. In effect, because of the absence of orientational correlation among the scattering centers, $[\mathbf{R}_{\text{aniso}}(0)/c]^0$ takes on the value that would obtain if the n_ν centers were not connected in a polymer chain.

Unlike the relation for $[\mathbf{R}_{\text{iso}}(0)/c]^0$, it is necessary to attribute specific properties to the scattering centers, eg, δ_0 and m_0, which appear in the expression for $[\mathbf{R}_{\text{aniso}}(0)/c]^0$. Comparison of equations 30 and 58 shows that $[\mathbf{R}_{\text{aniso}}(0)/c]^0 \ll [\mathbf{R}_{\text{iso}}(0)/c]^0$ for flexible chains, for which $m_0 \ll \overline{M}_w$. This is the usual circumstance with, for example, vinyl polymers or other flexible chain polymers. As a consequence, the contribution of $[\mathbf{R}_{\text{aniso}}(0)/c]^0$ to $[\mathbf{R}_{V\nu}(0)/c]^0$ is usually negligible for such molecules.

Additional chain models that have been used to estimate $[\mathbf{R}_{\text{aniso}}(0)/c]^0$ include those for chains with free rotation about n_ν bonds connected with fixed valence angle $\pi - \alpha$ and wormlike chains with persistence length ρ and contour length $L_\nu = \overline{M}_\nu/M_L$ (13). With these models (35),

$$\delta_\nu^2/\delta_0^2 = \frac{1}{n_\nu} \left[\frac{1+b}{1-b} - \frac{2b}{n_\nu} \frac{1-b^{n_\nu}}{(1-b)^2} \right] \tag{59}$$

$$\delta_\nu^2/\delta_0^2 = (2/3Z_\nu)\{1 - (3Z_\nu)^{-1}[1 - \exp(-3Z_\nu)]\} \tag{60}$$

where $b = (3a^2 - 1)/2$ with $a = \cos \alpha$ and $Z_\nu = L_\nu/\rho$. Plots of $(\delta_\nu/\delta_0)^2$ vs $(1-a)n_\nu/a$ with equation 59 and $(\delta_\nu/\delta_0)^2$ vs Z_ν with equation 60 superimpose for most a and n_ν of interest (35) (Fig. 2) showing the equivalence of these models for the computation of δ_ν/δ_0. The results in Figure 2 show that the expected crossover from rodlike to coillike behavior occurs for L/ρ about equal to unity.

Static Scattering at Arbitrary Angle. The value $[\mathbf{R}(q)/c]^0$ of the Rayleigh ratio at q divided by the concentration, extrapolated to infinite dilution, is considered below for a range of q. For isotropic scatterers, $[\mathbf{R}(q)/c]^0$ is expressed in

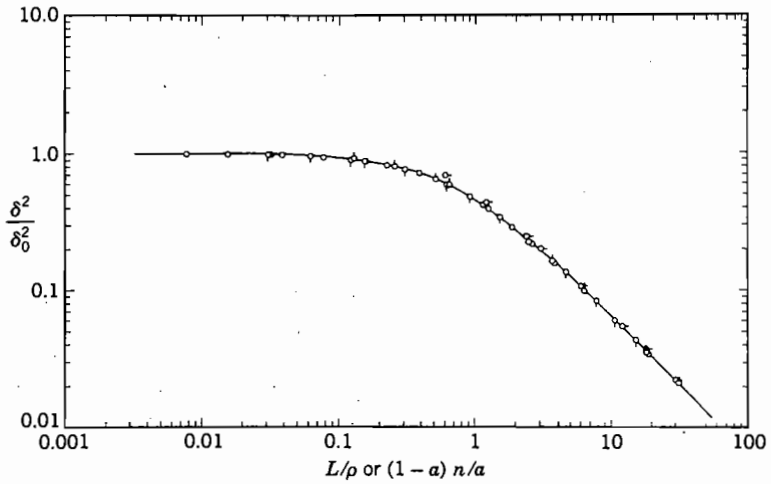

Fig. 2. Anisotropy factor δ^2/δ_0^2 as a function of chain length. The points give δ^2/δ_0^2 vs $(1 - a)\ n/a$ according to equation 59, with a = cos α, where α is ○, 5°; ♀, 10°; ♁, 20°; ○–, 40°. The curve gives δ^2/δ_0^2 vs L/p according to equation 60, with L the contour length and ρ the persistence length (35).

terms of the product $M_{LS}P_X^0(q)$, where $P_X^0(q)$, defined below, accounts for interference effects among the rays scattered from a solute. First, an expansion of $P_X^0(q)$ for small q as a Taylor series in $R_{G,X}^2q^2$ is given, where $R_{G,X}^2$ is an average mean-square radius of gyration. Examples of $R_{G,X}^2$ are given for a variety of solute architectures. Following this, certain analytical expressions for $P_X^0(q)$ are given for a few frequently encountered cases. Finally, the asymptotic behavior of $P_X^0(q)$ for large q is discussed. Methods to account for molecular weight heterodispersity are included throughout. Anisotropic scatters are treated similarly.

Isotropic Scatterers for Small q. For $\theta > 0$, the effects of interference between rays scattered from different centers on one molecule must be included. Comparable intermolecular interference effects are neglected here since only solutions at infinite dilution are considered. For a system with C-solute molecules, each characterized by a number n_ν of scattering elements, the expression for $[\mathbf{R}(q)/c]^0$ for an optically isotropic molecule, with $(\partial n/\partial c)_w \neq 0$, is (16)

$$[\mathbf{R}(q)/c]^0 = K'\tilde{n}_s^2\left(\frac{\partial\tilde{n}}{\partial c}\right)_w^2 M_{LS}P_X^0(q) \tag{61}$$

where M_{LS} is given by equation 32 (or for copolymers by equations 39, 45, and 46), and

$$P_X^0(q) = \frac{\sum_\nu^C w_\nu M_\nu^{-1}\left(\sum_j\sum_k^{n_\nu} \psi_j\psi_k m_j m_k \left\langle \frac{\sin q|r_{jk}|}{q|r_{jk}|}\right\rangle\right)}{\sum_\nu^C w_\nu M_\nu^{-1}\left(\sum_j^{n_\nu} \psi_j m_j\right)^2} \tag{62}$$

where it is assumed that the molecules in solution exhibit no preferential orientation in carrying out an ensemble average of $\langle \exp i\mathbf{q}\cdot\mathbf{r}_{jk}\rangle$ to give the factor $\langle\cdots\rangle$; as previously, the symbol $\langle\cdots\rangle$ indicates an average over all conformations.

The subscript X is adopted to designate the indicated average over ν. For small q, the factor $\langle \cdots \rangle$ may be expanded in a power series in q to give the result (6,13,16,36)

$$P_X^0(q) = 1 - \tfrac{1}{3}R_{G,X}^2 q^2 + \cdots \tag{63}$$

$$R_{G,X}^2 = \frac{\sum_\nu^C w_\nu M_\nu^{-1}\left(\sum_j^{n_\nu}\sum_k^{n_\nu} \psi_j\psi_k m_j m_k \langle r_{jk}^2\rangle\right)}{2\sum_\nu^C w_\nu M_\nu^{-1}\left(\sum_j^{n_\nu} \psi_j m_j\right)^2} \tag{64}$$

For a homopolymer with m_i and ψ_i identical for all scattering elements, $M_{LS} = \overline{M}_w$ (eq. 33), and equation 62 becomes

$$P_X^0(q) = \frac{1}{\overline{M}_w}\sum_\nu^C w_\nu M_\nu P_\nu^0(q) \tag{65}$$

$$P_\nu(q,c) = \frac{1}{n_\nu^2}\sum_j^{n_\nu}\sum_k^{n_\nu}\left\langle \frac{\sin q|r_{jk}|}{q|r_{jk}|}\right\rangle \tag{66a}$$

$$P_\nu^0(q) = \lim_{c=0} P_\nu(q,c) \tag{66b}$$

Expansion of $P_\nu^0(q)$ for small q gives equation 63 with

$$R_{G,X}^2 = \frac{\sum_\nu^C w_\nu M_\nu R_{G,\nu}^2}{\overline{M}_w} \tag{67}$$

$$R_{G,\nu}^2 = \frac{1}{2n_\nu^2}\sum_j^{n_\nu}\sum_k^{n_\nu}\langle r_{jk}^2\rangle \tag{68}$$

where $R_{G,\nu}$ is the rms radius of gyration of component ν. Examples of R_G for models of typical interest are given in Table 1 (86). Of these, the wormlike chain model results in the relation (13)

$$R_{G,\nu}^2 = \frac{L_\nu\rho}{3}S(\rho/L_\nu) \tag{69a}$$

$$S(Z) = 1 - 3Z + 6Z^2 - 6Z^3[1 - \exp(-Z^{-1})] \tag{69b}$$

$$S(Z) \approx (1 + 4Z)^{-1} \tag{69c}$$

where ρ is the persistence length characteristic of the particular chain and $L_\nu = M_\nu/M_L$, the chain contour length, with M_L the mass-per-unit length. Equation 69c is a useful approximation, being exact for very small or very large Z. With equation 69, the relations

$$\lim_{\rho/L\nu=0} R_{G,\nu}^2 = \frac{\rho L_\nu}{3} \tag{70}$$

$$\lim_{\rho/L\nu=\infty} R_{G,\nu}^2 = \frac{L_\nu^2}{12} \tag{71}$$

provide expressions for a random-flight coil or a rodlike chain, respectively.

Table 1. Radius of Gyration and Hydrodynamic Radius for Some Model Structures

	Characteristic lengths	R_G^2	R_H/R_G
persistent coil	L = contour length ρ = persistence length d = diameter	$\frac{L\rho}{3} S(\rho/L)^a$	$3^{1/2}\left(1 + \frac{L}{4\rho}\right)^{1/2}\left(\frac{27L}{16\rho} + \ln^2 \frac{3L}{2d}\right)^{-1/2\,b}$
coil ($\rho/L \ll 1$)	$b = 2\rho$ = step length $L = nb$	$\frac{L\rho}{3} = \frac{nb^2}{6}$	$\frac{2}{3}\left(\frac{9\pi^{1/2}X}{6 + 16X}\right)^c$
rod ($\rho/L \gg 1$)	L = rod length d = rod diameter	$\frac{L^2}{12}$	$\sqrt{3}/\ln (3L/2d)$
disk	R = radius	$\frac{1}{2}R^2$	$\sqrt{2}/\pi$
sphere	R = radius	$\frac{3}{5}R^2$	$\sqrt{\frac{5}{3}}$
spheroid	$2R_1$ = length of unique axis		$\left[\frac{5(p^2 - 1)}{2 + p^2}\right]^{1/2} \frac{1}{\ln \{p[1 + (1 + p^{-2})^{1/2}]\}}$; $p > 1$
	$2R_2$ = length of transverse axis $p = R_2/R_1$	$\left(\frac{2 + p^2}{5}\right)R_1^2$	$\left(\frac{1 - p^2}{2 + p^2}\right)^{1/2} \frac{1}{\arctan(p^{-2} - 1)^{1/2}}$; $p < 1$

[a] Equation 69.
[b] An approximate relation (37).
[c] $\pi^{3/2}X = (L/R_G)(\zeta/6\pi\eta_s d)$ with ζ the friction factor per step length.

Calculation of $R_{G,X}^2$ may be illustrated by the use of the two-parameter exponential relation (36)

$$w_\nu = \frac{(yn_\nu)^h}{n_n\Gamma(h)} \exp(-yn_\nu) \tag{72}$$

With this relation, the number, weight, z and $z + 1$, etc, averages of n are given by (38)

$$n_n = (\Sigma\, w_\nu n_\nu^{-1})^{-1} = h/y \tag{73}$$

$$n_w = \Sigma w_\nu n_\nu = (h + 1)/y \tag{74}$$

$$n_z = \frac{\Sigma w_\nu n_\nu^2}{n_w} = (h + 2)/y \tag{75}$$

$$n_{z+1} = \frac{\Sigma\, w_\nu n_\nu^3}{n_w n_z} = (h + 3)/y \tag{76}$$

etc

Calculation of $R_{G,X}^2$ with the help of equations 69 and 72 (with $M_\nu = n_\nu m_0$), gives

$$R_{G,X}^2 = \frac{L_z\rho}{3}\,\overline{S}(\rho/L_z) \tag{77a}$$

$$\overline{S}(Z) = 1 - 3Z + 6Z^2\frac{h + 2}{h + 1} - 6Z^3\frac{(h + 2)^2}{h(h + 1)^2} \times \left\{1 - \left[1 + \frac{1}{Z(h + 2)}\right]^{-h}\right\} \tag{77b}$$

$$\bar{S}(Z) \approx \left(1 + 4Z\frac{h+2}{h+3}\right)^{-1} \tag{77c}$$

where $L_z = M_z/M_L = n_z m_0/M_L$ and equation 77c is a useful approximation, being exact for very small or very large Z.

In many cases, it is adequate to represent $R^2_{G,\nu}$ in the form

$$R^2_{G,\nu} = r\, n_\nu^{1+\epsilon} \tag{78}$$

with r and ϵ constants, eg, ϵ is 0, 1, or $-\frac{1}{3}$ for models of the random-flight coil, rodlike chain, and sphere, respectively. With the use of equations 67 and 78 (38)

$$R^2_{G,X} = r\, n_z^{1+\epsilon\omega_\epsilon} \tag{79}$$

where

$$\omega_\epsilon = \frac{n_z}{n_w}\frac{\Sigma\, w_\nu n_{Z\nu}^{2+\epsilon}}{n_z^{2+\epsilon}} \tag{80}$$

Use of equation 72 gives

$$\omega_\epsilon = \frac{\Gamma(3+h+\epsilon)}{(h+2)^\epsilon\Gamma(3+h)} \tag{81}$$

and therefore

coil: $$R^2_{G,X} = r\, n_z \tag{82}$$

rod: $$R^2_{G,X} = r\, n_z n_{z+1} \tag{83}$$

sphere: $$R^2_{G,X} = r\, n_z^{2/3}\frac{\Gamma(3+h+\epsilon)}{(h+2)^{2/3}\Gamma(2+h)} \tag{84}$$

With copolymers comprising units with refractive indexes ψ_A and ψ_B and monomer molecular weights m_A and m_B for the respective homopolymers, the expansion of $\langle \sin(q|r_{jk}|)/q|r_{jk}|\rangle$ can be used for small q, and the definition of $R^2_{G,X}$ given by equation 64

$$[\mathbf{R}(q)/c]^0 = K'\bar{n}_s^2\left[\sum_\nu^C w_\nu M_\nu^{-1}\left(\sum_j^{n_\nu}\psi_j m_j\right)^2\right](1 - \tfrac{1}{3}R^2_{G,X}q^2 + \cdots) \tag{85}$$

Provided $(\partial\bar{n}/\partial c)_w \neq 0$, this may be expressed in the form of equation 61, with M_{LS} represented by equations 30 and 38 as discussed above. With $R^2_{G,A}$ and $R^2_{G,B}$ the values of $R^2_{G,X}$ that obtain for ψ_B and ψ_A, respectively, equal to zero (and for $\psi = (\partial\bar{n}/\partial c)_w \neq 0$) (32)

$$R^2_{G,X} = x\, R^2_{G,A} + (1-x)R^2_{G,B} + x(1-x)\Delta^2_{AB} \tag{86}$$

where $x = w_A\psi_A/\psi$ and Δ_{AB} is the root-mean-square separation of the centers of gravity of the structures comprising only A or B units. In general, use of this relation is complicated by the dependence of $R_{G,A}$, $R_{G,B}$, and Δ_{AB} on solvent. For copolymers with random placement of the A and B monomers, or strict alternation of these placements, $\Delta_{AB} = 0$. With diblock copolymers, ie, $A\cdots AB\cdots B$, Δ_{AB} may be comparable to $R^2_{G,A}$ and $R^2_{G,B}$. For example if the diblock components may be treated as random-flight chains, eg, $R^2_{G,A}$ proportional to the number of scat-

tering elements in the A block, then for the diblock chain

$$\Delta_{AB}^2 = 2(R_{G,A}^2 + R_{G,B}^2) \tag{87}$$

As the number of blocks increases, Δ_{AB} decreases, reaching zero for an alternating copolymer. Values of Δ_{AB} are available for a few other copolymer configurations (32). Since X may be positive, zero, or negative, $R_{G,X}^2$ may itself be positive, zero, or negative, in distinction to the geometric radius of gyration $R_{G,geo}^2$ which must be positive. For copolymers

$$R_{G,geo}^2 = w_A R_{G,A}^2 + (1 - w_A)R_{G,B}^2 + w_A(1 - w_A)\Delta_{AB}^2 \tag{88}$$

Isotropic Scatterers for Large q. The ensemble average $\langle(\sin q|r_{jk}|)q|r_{jk}|\rangle$ in equation 66 may be completed for several chain models. Results for models with n_ν identical scattering elements that find frequent use (9,15,16,39,40) give

coil:
$$P_\nu^0(q) = \frac{2}{u_\nu^2}[u_\nu - 1 + \exp(-u_\nu)] \tag{89}$$

rod:
$$P_\nu^0(q) = \frac{2}{x_\nu^2}[x_\nu Si(x_\nu) - 1 + \cos x_\nu] \tag{90}$$

disk:
$$P_\nu^0(q) = \frac{2}{z_\nu^2}[1 - J_1(2z_\nu)/z_\nu] \tag{91}$$

sphere:
$$P_\nu^0(q) = \frac{9}{y_\nu^6}(\sin y_\nu - y_\nu \cos y_\nu)^2 \tag{92}$$

for random-flight coils, thin rods, thin disks, and spheres, respectively. In these expressions, $u_\nu = R_{G,\nu}^2 q^2$, $x_\nu^2 = 12u_\nu$, $z_\nu^2 = 2u_\nu$, and $y_\nu^2 = 5u_\nu/3$. The Bessel function of 1st order $J_1(z)$ and the sine integral

$$\mathrm{Si}(z) = \int_0^z \frac{\sin t}{t}\, dt \tag{93}$$

may be found in standard tabulations; $P_\nu^0(q)$ is shown as a function of $qR_{G,\nu}$ for several models in Figure 3. Relations for $P_\nu^0(q)$ for a variety of other shapes are available, including branched random-flight coils, non-Gaussian coils, wormlike chains, disks, oblate and prolate ellipsoids, cylinders of finite radius, cylindrical shells, particles of nonuniform density, and assemblages of simple geometrical shapes (9,15,16,40). In the calculation of $P_\nu^0(q)$ for random-flight coils, $\langle r_{jk}^2\rangle$ is proportional to the number of scattering elements n_{jk} along the chain contour between elements j and k. In certain approximate treatments for non-Gaussian chains, this result is modified by multiplying by n_{jk}^ϵ, where ϵ is taken to be an empirical parameter ranging from 0 to the upper bound ⅕, corresponding to the limiting behavior expected for excluded volume interactions among nonadjacent chain elements (13).

Although equation 89 is the result of calculations for linear random-flight chains, it represents a useful approximation to $P_\nu^0(q)$ for a variety of branched random-flight chains (15) and to $P_\nu^0(q)$ for a more realistic model based on a rotational-isomeric state model (5), provided that the value of $R_{G,\nu}^2$ corresponding to the specific model is used. For each of these models $R_{G,\nu}^2$ may be represented by equation 79, with $\epsilon = 0$ and r specific to the model. Of course, use of $R_{G,\nu}^2$

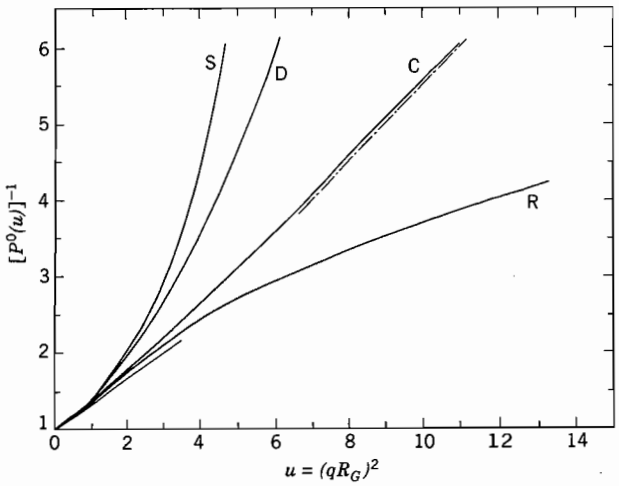

Fig. 3. Reciprocal scattering factor for a S, sphere; D, disk, C, random-flight coil; and R, thin rod. The solid line is the initial tangent for all curves; — - — - indicates the asymptotic behavior for the coil for large u.

ensures correspondence of the approximate and exact $P_\nu^0(q)$ for small q, and therefore deviations increase progressively with increasing q. An example for one type of branched chain is shown in Figure 4, where the branched chains are comblike with branches attached along a linear backbone (16); the fraction ϕ of monomers

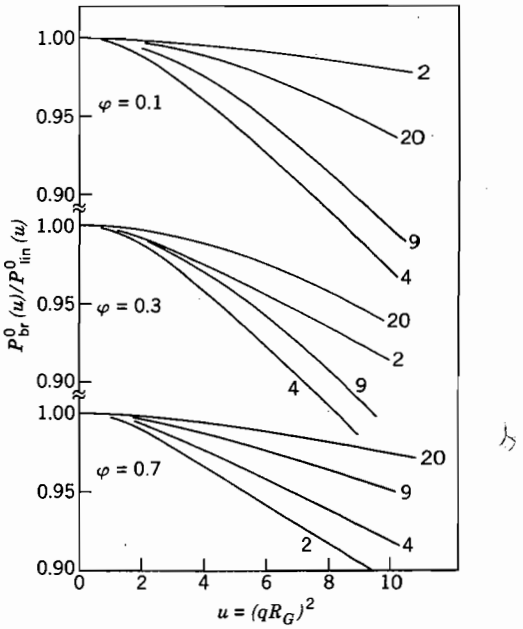

Fig. 4. Reciprocal scattering factors for comb-branched polymers and for a linear chain with the same radius of gyration. The number of branches is given at the right and the fraction φ of monomers in the backbone is given on the left (16).

in the backbone ranges from 0.1–0.7 for the examples in Figure 4. For the range of structures represented, $P_\nu^0(q)$ for the branched structure is closely approximated by equation 89, and $R_{G,\nu}^2$ represents the value for the branched chain.

Expansion of equation 89 as a power series for $[P_\nu^0(q)]^{-1}$ or $[P_\nu^0(q)]^{-1/2}$ in q^2 gives relations that are more nearly linear for small q^2 than is equation 63 (16,36):

$$[P_\nu^0(q)]^{-1} = 1 + \tfrac{1}{3}u_\nu + \tfrac{1}{36}u_\nu^2 + 0(u_\nu^3) \tag{94}$$

$$[P_\nu^0(q)]^{-1/2} = 1 + \tfrac{1}{6}u_\nu + 0(u_\nu^3) \tag{95}$$

Thus, experimental data for $[\mathbf{R}(q)/c]^0$ vs q^2 are frequently analyzed by using plots of $[c/\mathbf{R}(q)]^0$ or $\{[c/\mathbf{R}(q)]^0\}^{1/2}$ vs q^2 (see below); as shown in Figure 5, the latter provides a more nearly linear relation to somewhat larger q than the former, if equation 89 is valid (16).

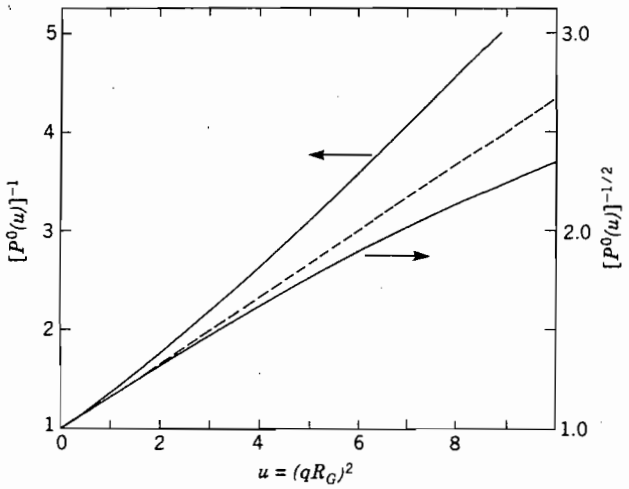

Fig. 5. Comparison of $[P^0(u)]^{-1}$ with $[P^0(u)]^{-1/2}$ for a random-flight chain. ------- represents the initial tangent for both plots (16).

For a heterodisperse system in which ψ_i and m_i are identical for all scattering centers, equation 65 and $P_\nu^0(q)$ for a random-flight coil (with $R_{G,\nu}^2$ given by equation 78 with $\epsilon = 0$) gives (36,38)

$$P_X^0(q) = \frac{2}{q^2 r n_w}\left\{1 - \frac{1}{q^2 r n_n}\left[1 - n_n \sum_\nu^C n_\nu^{-1} w_\nu \exp(-rq^2 n_\nu)\right]\right\} \tag{96}$$

Equation 72 for w_ν gives (36,38)

$$P_X^0(q) = \frac{2}{q^2 r n_w}\left\{1 - \frac{1}{q^2 r n_n}\left[1 - \left(1 + \frac{q^2 r n_n}{h}\right)^{-h}\right]\right\} \tag{97}$$

For the special case of $h = 1$, ie, $n_w/n_n = 2$,

$$[P_X^0(q)]^{-1} = 1 + \tfrac{1}{3}q^2 r n_z \tag{98}$$

exactly. For a randomly branched random-flight chain, such as may be obtained in certain polymerizations (15), the result for $P_X^0(q)$ is given by equation 98,

provided the value of r appropriate for the branched chain is used (ie, $r = R^2_{G,X}/n_z$) where $R^2_{G,X}$ is the averaged radius of gyration of the branched chain. With $P^0_\nu(q)$ for rodlike chains (with $R^2_{G,\nu}$ given by equation 78 where $\epsilon = 1$) and equation 72 for w_ν, ($h > 0$) (35,41)

$$P^0_X(q) = \frac{2}{(h+1)z}\left\{\arctan z + \sum_{j=1}^{h-1}\left(\frac{1}{h-j} - \frac{1}{h}\right) \times (1+z^2)^{\frac{j-h}{2}} \sin\left[(h-j)\arctan z\right]\right\} \quad (99)$$

where $z = qn_w r/(h+1)$

In some cases, the behavior of $P^0_\nu(q)$ for large q is of interest. Unfortunately, in such cases, relations such as equations 89 or 90 may be inadequate, since these do not contain any information on the short-distance correlations on the chain. Such deficiency may be particularly important for the scattering of x rays or neutrons, but may be less troublesome with light scattering. For large q in random-flight chain molecules, $P^0_\nu(q)$ given by equation 66 may be expressed in the form (16)

$$\lim_{qR_{G,\nu}\gg 1} [P^0_\nu(q)]^{-1} = C + \tfrac{1}{2}u_\nu + 0(u_\nu^{-1}) \quad (100)$$

where C depends on the chain model. For example, with linear random-flight chains, equation 89 gives $C = \frac{1}{2}$, but for branched random-flight chains C depends on the chain structure (16).

For linear or branched random-flight chains, use of equation 100 to compute $P^0_X(q)$ gives

$$\lim_{qR_{G,X}\gg 1} [P^0_X(q)]^{-1} = \frac{1}{2}\frac{n_w}{n_n}[2C + q^2 r n_n + 0(q^{-2})] \quad (101)$$

Consequently, linear extrapolation of $\{[R(q)/c]^0\}^{-1}$ vs q^2 from the asymptotic behavior at large q is expected to yield M_n from the intercept $(\mathbf{R}(0)/c)^0$ and rn_n from $\partial[c/\mathbf{R}(q)]^0/\partial q^2$ divided by the intercept (in comparison with M_w and $rn_z/3$ for these quantities evaluated from $\{[R(q)/c]^0\}^{-1}$ at small q). For rodlike chains with length L_ν (16)

$$\lim_{qR_{G,\nu}\gg 1} [P^0_\nu(q)]^{-1} = \frac{2}{\pi^2} + \frac{qL_\nu}{\pi} + 0(q^{-1}) \quad (102)$$

Consequently, for large enough q, the quantity $\partial\{[R(q)/c]^0\}^{-1}/\partial q$ is proportional to $M_L^{-1} = L_\nu/M_\nu$, and does not contain any information on the overall molecular size.

Equations 100–102 illustrate the principle that for $qR_G \gg 1$, the dependence of scattering on q does not provide information on the overall dimensions of a solute. For example, with $R^2_{G,\nu}$ given by equation 78, in the limit for large qR_G, equation 66 gives equation 103 for threadlike solute components.

$$\lim_{qR_G\gg 1} \mathbf{R}(q) \propto (q^2 R^2_{G,\nu}/M_\nu^{1+\epsilon})^{-1/(1+\epsilon)} \approx (q^2 r)^{-1/(1+\epsilon)} \quad (103)$$

Thus, in the limit with $qR_G \gg 1$, the parameter $\partial \ln \mathbf{R}(q)/\partial \ln q$ depends on short-range features of the solute shape, eg, $-\partial \ln \mathbf{R}(q)/\partial \ln q$ is 2 for a random-flight

coil, between 2 and 5/3 for flexible coil chains with excluded volume, and 1 for a rod.

For a monodisperse copolymer (31,33)

$$P_X^0(q) = x^2P_A^0(q) + (1 - x)^2P_B^0(q) + 2x(1 - x)P_{AB}^0(q) \tag{104}$$

where $x = w_A\psi_A/\psi$, as in equation 86, and

$$P_A^0(q) = \frac{1}{n_A^2}\sum_j^{n_A}\sum_k^{n_A}\left\langle\frac{\sin q|r_{jk}|}{q|r_{jk}|}\right\rangle \tag{105a}$$

$$P_B^0(q) = \frac{1}{n_B^2}\sum_j^{n_B}\sum_k^{n_B}\left\langle\frac{\sin q|r_{jk}|}{q|r_{jk}|}\right\rangle \tag{105b}$$

$$P_{AB}^0(q) = \frac{1}{n_An_B}\sum_j^{n_A}\sum_k^{n_B}\left\langle\frac{\sin q|r_{jk}|}{q|r_{jk}|}\right\rangle \tag{105c}$$

Expansion of equation 105 for small q yields the result $1 - R_{G,X}^2q^2/3 + \cdots$ with $R_{G,X}^2$ given by equation 86. This relation has been studied for diblock copolymers (31,32).

Anisotropic Scatterers. For nonzero q, equations 49 and 50 become (1)

$$[\mathbf{R}_{Vv}(q)/c]^0 = [\mathbf{R}_{iso}(q)/c]^0 + \tfrac{4}{3}[\mathbf{R}_{aniso}(q)/c]^0 + [\mathbf{R}_{cross}(q)/c]^0 \tag{106}$$

$$[\mathbf{R}_{Hv}(q)/c]^0 = [\mathbf{R}_{aniso}(q)/c]^0 \tag{107}$$

The term $[\mathbf{R}_{cross}(q)/c]^0$ vanishes for zero q, but must be retained otherwise. As explained previously, for chain molecules $[\mathbf{R}_{aniso}(0)/c]^0$ is small unless the conformation deviates significantly from that for a random-flight coil. Chain molecules having identical scattering elements (ie, ψ_i and m_i do not vary among the elements) with cylindrical symmetry can be represented in terms of δ_ν and $R_{G,\nu}^2$, with $(\partial n/\partial c)_w \neq 0$

$$[\mathbf{R}_{Vv}(q)/c]^0 = K'\tilde{n}_s^2\left(\frac{\partial\tilde{n}}{\partial c}\right)_w^2\overline{M}_w\left(1 + \frac{4}{5}\delta_X^2\right)P_{V,A}^0(q) \tag{108}$$

$$[\mathbf{R}_{Hv}(q)/c]^0 = \frac{3}{5}K'\tilde{n}_s^2\left(\frac{\partial\tilde{n}}{\partial c}\right)_w^2\overline{M}_W\delta_X^2P_{H,A}^0(q) \tag{109}$$

where δ_X^2 is defined by equation 54 and

$$P_{V,A}^0(q) = \frac{\Sigma\, w_\nu M_\nu(1 + \frac{4}{5}\delta_\nu^2)P_{V,\nu}^0(q)}{(1 + \frac{4}{5}\delta_X^2)\overline{M}_w} \tag{110}$$

$$P_{H,A}^0(q) = \frac{\Sigma\, w_\nu M_\nu\delta_\nu^2P_{H,\nu}^0(q)}{\delta_X^2\overline{M}_w} \tag{111}$$

In these expressions, $P_{V,\nu}^0(q)$ and $P_{H,\nu}^0(q)$ are both unity for $q = 0$, in which case the relations given previously for $[\mathbf{R}_{Vv}(0)/c]^0$ and $[\mathbf{R}_{Hv}(0)/c]^0$ are recovered. For small q, power-series expansions may be used for $P_{V,\nu}^0(q)$ and $P_{H,\nu}^0(q)$:

$$P_{V,\nu}^0(q) = 1 - \tfrac{1}{3}J(\delta_\nu)u_\nu + \cdots \tag{112}$$

$$P_{H,\nu}^0(q) = 1 - \tfrac{3}{7}(f_{3,\nu}\delta_\nu)^2u_\nu + \cdots \tag{113}$$

where $u_\nu = R_{G,\nu}^2q^2$ and δ_ν, $f_{3,\nu}$ and $J(\delta_\nu)$ depend on the model. Results for rodlike chains, wormlike chains, and coils with free rotation about fixed valence angles

may be expressed in the form (35):

$$J(\delta_\nu) = \frac{1 - \frac{4}{5}f_{1,\nu}\delta_\nu + \frac{4}{7}(f_{2,\nu}\delta_\nu)^2}{1 + \frac{4}{5}\delta_\nu^2} \tag{114}$$

with $f_{1,\nu}$, $f_{2,\nu}$, and $f_{3,\nu}$ given in Figure 6, and δ_ν given by equations 59 or 60. A useful feature of this form is that estimates of the molecular weight and the mean-square radius of gyration are usually close to those obtained with the relation for isotropic scatterers, unless $\delta_\nu \approx \delta_0$, in which case, the three functions $f_{i,\nu}$ are all essentially unity for cases of practical interest. For example, if $\delta_\nu \ll \delta_0$, then $J(\delta_\nu) \approx 1$, whatever the value of δ_0. It may be noticed that with these relations for $[\mathbf{R}_{V\upsilon}(q)/c]^0$ and $[\mathbf{R}_{H\upsilon}(q)/c]^0$, the cross-term $[\mathbf{R}_{\text{cross}}(q)/c]^0$ defined by equation 106 is not zero unless $q = 0$, ie, $[\mathbf{R}_{\text{cross}}(q)/c]^0 \propto q^2$ for small q.

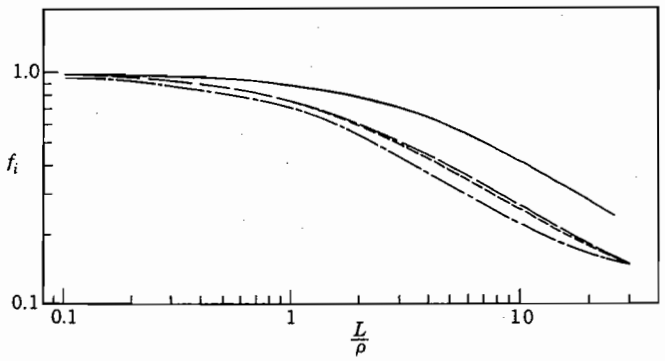

Fig. 6. The functions f_i appearing in the reciprocal scattering factors for anisotropic chains as a function of the contour length L divided by the persistence length ρ (eqs. 112 and 113). ———, f_1; — - — - —, f_2; ---------, f_3; – – – – – – –, f_4.

For monodisperse rodlike chains, $[\mathbf{R}_{V\upsilon}(q)/c]^0$ and $[\mathbf{R}_{H\upsilon}(q)/c]^0$ can be expressed as linear combinations of the three functions

$$p_1(x) = -\frac{2}{x^2}(1 - x\text{Si}(x) - \cos x) \tag{115}$$

$$p_2(x) = \frac{2}{x^3}(x - \sin x) \tag{116}$$

$$p_3(x) = \frac{4}{3x^5}(x^3 + 3x\cos x - 3\sin x) \tag{117}$$

where Si( ) is the sine integral and $x^2 = 12u = 12R_G^2q^2$. The function $p_1(x)$ is recognized as $P^0(q)$ for the isotropic rod. With

$$q_1 = p_1 = 1 - \tfrac{1}{3}u + \cdots \tag{118}$$

$$q_2 = 3p_2 = 1 - \tfrac{3}{5}u + \cdots \tag{119}$$

$$q_3 = \tfrac{15}{8}(p_2 + \tfrac{3}{2}p_3) = 1 - \tfrac{15}{28}u + \cdots \tag{120}$$

$$q_4 = 6q_3 - 5q_2 = 1 + \tfrac{3}{14}u + \cdots \tag{121}$$

$$m_1 = q_1 - q_2 = {}^4\!/_{15}u + \cdots \tag{122}$$

$$m_2 = p_1 - p_2 - 5p_3 = {}^{16}\!/_{105}u + \cdots \tag{123}$$

the relations for $P^0_{V,\nu}(q)$ and $P^0_{H,\nu}(q)$ become

$$(1 + {}^4\!/_5\delta^2)P^0_{V,\nu}(q) = q_1(x_\nu) + {}^4\!/_5\delta^2 q_4(x_\nu) + (\delta - 2\delta^2)m_1(x_\nu) + {}^{27}\!/_8\delta^2 m_2(x_\nu) \tag{124}$$

$$P^0_{H,\nu}(q) = {}^2\!/_3 q_3(x_\nu) + {}^1\!/_3 q_4(x_\nu) + {}^{15}\!/_{16}(1 - \cos\theta)m_2(x_\nu) \tag{125}$$

where $\delta = \delta_0$ is independent of the rod length L_ν. With these expressions, $(\mathbf{R}_{\text{cross}}(q)/c)^0$ is not zero unless $q = 0$ (or $\delta = 0$), and $P^0_{H,\nu}(q)$ depends explicitly on θ. Equations 124 and 125 reduce to equations 112 and 113, respectively, for small q with $f_i = 1$. Values of $P^0_{V,A}(q)$ and $P^0_{H,A}(q)$ have been computed with these relations using equation 72 for w_ν (33).

Dynamic Scattering at Arbitrary Angle. Interpretation of the normalized photon-count correlation function $g^{(2)}(q,\tau;\Delta\tau)$ and second factorial moment $n^{(2)}(q,\Delta\tau)$ is given below for data extrapolated to infinite dilution. These are usually related to the function $g^{(1)}(q,\tau)$; the latter is more directly amenable to calculation and is emphasized in the following discussion. If q is small enough (made precise below), then $g^{(1)}(q,\tau)$ is related to center-of-mass translation of the solute. Relations needed to analyze such data are given, including representations of a hydrodynamic radius for several solute models. The effects of internal intramolecular dynamics on $g^{(1)}(q,\tau)$ are considered, although seldom important in the scattering from polymer solutions. The effect of optical anisotropy is considered briefly, followed by a discussion of electrophoretic scattering.

Center of Mass Translation for Isotropic Scatterers. If solutions are sufficiently dilute that intermolecular correlations may be ignored, the function $g^{(1)}_\nu(q,\tau)$ for the ν^{th} solute is given by (1)

$$g^{(1)}_\nu(q,\tau) = \frac{S_\nu(q,\tau)}{S_\nu(q,0)} \tag{126}$$

$$S_\nu(q,\tau) = \frac{1}{n_\nu^2}\left\langle \sum_{i}^{n_\nu}\sum_{j} \exp i\,\mathbf{q}\cdot[\mathbf{r}_i(\tau) - \mathbf{r}_j(0)] \right\rangle \tag{127}$$

where the brackets $\langle\cdots\rangle$ designate an average over the space–time distribution, in contrast to earlier usage where only the equilibrium spatial average was required. In equation 126 it is assumed that ψ_i and m_i are identical for all scattering elements and that the elements are optically isotropic. Relations for copolymers for which the latter condition is relaxed have been developed (42). It is convenient to express $\mathbf{r}_i$ in terms of the vector $\mathbf{s}_i$ of the element to the center of mass, and vector $\mathbf{S}$ from the center of mass to the arbitrary coordinate center:

$$\mathbf{r}_i = \mathbf{S} + \mathbf{s}_i \tag{128}$$

Then (1)

$$S_\nu(q,\tau) = \left\langle \exp i\,\mathbf{q}\cdot[\mathbf{S}_\nu(\tau) - \mathbf{S}_\nu(0)]\,\frac{1}{n_\nu^2}\sum_{j}^{n_\nu}\sum_{k} \exp i\,\mathbf{q}\cdot[\mathbf{s}_j(\tau) - \mathbf{s}_k(0)] \right\rangle \tag{129}$$

For $qR_G \ll 1$, (the long-wave limit), equation 129 may be greatly simplified, since then the probing radiation is insensitive to the shorter scale correlations embodied in the double summation, which may be factored from $\langle\cdots\rangle$. Such a fac-

torization is exact for rigid spherical particles at infinite dilution. The result of this operation is given by

$$S_\nu(q,\tau) = S_\nu(q,0)\ \langle \exp i\ \mathbf{q}\cdot[\mathbf{S}_\nu(\tau) - \mathbf{S}_\nu(0)]\rangle \tag{130}$$

showing that $g_\nu^{(1)}(q,\tau)$ is related to the center of mass translation. Complications that result, for example, with chain models for larger q are discussed below.

In terms of the Van-Hove self space–time correlation function

$$G_{s,\nu}(\mathbf{R},\tau) = \langle \delta\{\mathbf{R} - [\mathbf{S}_\nu(\tau) - \mathbf{S}_\nu(0)]\}\rangle \tag{131}$$

giving the probability density that a spherical particle undergoes a displacement $\mathbf{R}$ in time τ, (1)

$$\langle \exp i\mathbf{q}\cdot[\mathbf{S}_\nu(\tau) - \mathbf{S}_\nu(0)]\rangle = \int d^3R G_{s,\nu}(\mathbf{R},\tau)\ \exp(i\mathbf{q}\cdot\mathbf{R}) \tag{132}$$

With this expression, it can be seen that $G_{s,\nu}(\mathbf{R},\tau)$ is given by

$$G_{s,\nu}(\mathbf{R},\tau) = \frac{1}{(2\pi)^3}\int d^3q\ \exp(-i\mathbf{q}\cdot\mathbf{R})\ S_\nu(\mathbf{q},\tau)/S_\nu(\mathbf{q},0) \tag{133}$$

and in principle, $G_{s,\nu}(\mathbf{R},\tau)$ may be determined if $S_\nu(\mathbf{q},\tau)/S_\nu(\mathbf{q},0)$ is known for all $\mathbf{q}$. In practice, such data are rarely available because of the limited range of q available experimentally and inaccuracies in the estimate of $g^{(1)}(q,\tau)$ for large τ.

Given that the center of mass translation is a diffusion process, a reasonable approximation to $G_s(\mathbf{R},\tau)$ may be obtained from the diffusion equation:

$$\frac{\partial G_s(\mathbf{R},\tau)}{\partial\tau} = D_T^0\ \nabla^2 G_s(\mathbf{R},\tau) \tag{134}$$

where D_T^0 is the diffusion constant for center of mass translation and ∇^2 is the Laplacian. Then

$$g_\nu^{(1)}(q,\tau) = \exp(-\gamma_\nu\tau) \tag{135}$$

where $\gamma_\nu = q^2 D_{T,\nu}^0$ plays the role of an inverse coherence time. It is frequently useful to express $D_{T,\nu}^0$ in terms of a hydrodynamic radius $R_{H,\nu}$ defined by equation 2, ie:

$$R_{H,\nu} = kT/6\pi\eta_s D_{T,\nu}^0 \tag{136}$$

where η_s = solvent viscosity. The relation between $R_{H,\nu}$ and $R_{G,\nu}$ for several models is given in Table 1.

The translational diffusion constant (at infinite dilution) may be expressed in terms of a molecular-friction coefficient Ξ_ν^0 and the osmotic pressure by the relation (13)

$$D_{T,\nu}^0 = \frac{M_\nu}{N_A\Xi_\nu^0}\left(\frac{\partial\Pi}{\partial c}\right)_\nu^0 = \frac{kT}{\Xi_\nu^0} \tag{137}$$

For $g_\nu^{(1)}(q,\tau)$ given by equation 135, a combination of equations 22 and 25 gives (23,43)

$$g^{(2)}(q,\tau;\Delta\tau,A) = 1 + f(A)[g^{(2)}(q,\tau;\Delta\tau,0) - 1] \tag{138a}$$

$$g^{(2)}(q,\tau;\Delta\tau,0) - 1 = [p(q,\Delta\tau)g^{(1)}(q,\tau)]^2 \tag{138b}$$

$$[p(q,\Delta\tau)g^{(1)}(q,\tau)]^2 = \sum_{\nu}^{C}\sum_{\mu} r_\nu r_\mu \left\{\frac{\sin h[\gamma_\nu + \gamma_\mu)\Delta\tau/2]}{(\gamma_\nu + \gamma_\mu)\Delta\tau/2}\right\} \exp[-(\gamma_\nu + \gamma_\mu)k\Delta\tau] \quad (138c)$$

where a Gaussian stochastic $\Delta\alpha_{rs}(\mathbf{q},t)$ is assumed in equation 138b.

In equation 138, r_ν is the fraction of the scattered light associated with $g_\nu^{(1)}(q,\tau)$ and $\tau = k\Delta\tau$ with k an integer. For $\Delta\tau$ in the range usually preferred to study $g^{(2)}(q,\tau;\Delta\tau,A)$, $p(q,\Delta\tau)$ is essentially unity, ie, $\gamma\Delta\tau < 1$, and equation 138c may be written in the form

$$p(q,\Delta\tau)g^{(1)}(q,\tau) = \sum_{\nu}^{C} r_\nu \exp(-\gamma_\nu k\Delta\tau) \quad (139)$$

With the use of equation 139 for $g_\nu^{(1)}(q,\tau)$ (23,42)

$$n^{(2)}(q,\Delta\tau;A) = 1 + f(A)\sum_{\nu}^{C}\sum_{\mu} r_\nu r_\mu h(\gamma_\nu + \gamma_\mu) \quad (140)$$

$$h(y) = \frac{2}{y} - \frac{2}{y^2}(1 - \exp - y) \quad (141)$$

For a monodisperse solute, these relations simplify and permit evaluation of D_T^0 by several methods. Thus for a monodisperse solute

$$-\lim_{\gamma\Delta\tau<1} \frac{\partial \ln [g^{(2)}(q,\tau;\Delta\tau,A) - 1]}{\partial\tau} = 2q^2D_T^0 \quad (142)$$

$$-\lim_{\gamma\Delta\tau>1} \frac{\partial \ln [n^{(2)}(q,\Delta\tau;\Delta\tau,A) - 1]}{\partial\Delta\tau} = q^2D_T^0 \quad (143)$$

$$-\lim_{\gamma\Delta\tau>1} \frac{\partial \ln [g^{(2)}(q,\Delta\tau;\Delta\tau,A) - 1]}{\partial\Delta\tau} = 2q^2D_T^0 \quad (144)$$

where equation 144 includes the effects of $p(q,\Delta\tau)$.

For heterodisperse samples, these measures give different averages over the γ_ν set (44,45). The method of cumulants is based on the expansion (46)

$$\ln\{[g^{(2)}(q,\tau;0) - 1]^{1/2}\} = K_1\tau + \frac{1}{2!}K_2\tau^2 + \cdots \quad (145)$$

$$K_i = (-1)^i\left\{\frac{\partial^i \ln [g^{(2)}(q,\tau;0) - 1]^{1/2}}{\partial\tau^i}\right\}_{\tau=0} \quad (146)$$

Thus with equation 139

$$K_1 = \sum_{\nu}^{C} r_\nu\gamma_\nu \quad (147)$$

$$K_2 = \sum_{\nu}^{C} r_\nu\gamma_\nu^2 - K_1^2 \quad (148)$$

For example, $K_1 = q^2D_T^0$ and $K_2 = 0$ if the solute is monodisperse. Estimates based on $n^{(2)}(q,\Delta\tau)$ result in an average $\langle\gamma\rangle_{n^{(2)}}$ given by (47)

$$\langle\gamma\rangle_{n^{(2)}} = K_1(1 + K_2/2K_1^2)^{1/2} \quad (149)$$

Using $g^{(2)}(q,\Delta\tau;\Delta\tau,A)$ gives a different average (47).

In the preceding expressions, r_ν is equal to $w_\nu M_\nu P_\nu^0(q)/\overline{M}_w P_X^0(q)$ in the infinite dilution limit (with identical scattering elements). If the dependence on $P_\nu^0(q)$ is neglected, ie, $P_\nu^0(q)/P_X^0(q) \approx 1$ and with $R_{H,\nu} = \underline{d}R_{G,\nu}$, then with $R_{G,\nu}$ given by equation 78 and w_ν given by equation 72, $g^{(2)}(q;\tau;\Delta\tau,A)$ may be evaluated to give the results in Figure 7 (calculated for $\epsilon = 0$). As shown in this example, $g^{(2)}(q,\tau)$ exhibits increased nonexponential behavior as the heterodispersity is increased and the dependence on A and $\Delta\tau$ is suppressed. The horizontal line in Figure 7 indicates the typical lower bound experimentally accessible for $g^{(2)}(q,\tau)$. Attempts to determine the molecular-weight distribution by some suitable inversion of the data on $g^{(2)}(q,\tau)$ are hampered by the loss of information at large τ. A number of methods devised to determine estimates of the molecular-weight distribution are discussed in Refs. 4 and 25; a simple procedure useful in some cases is discussed later.

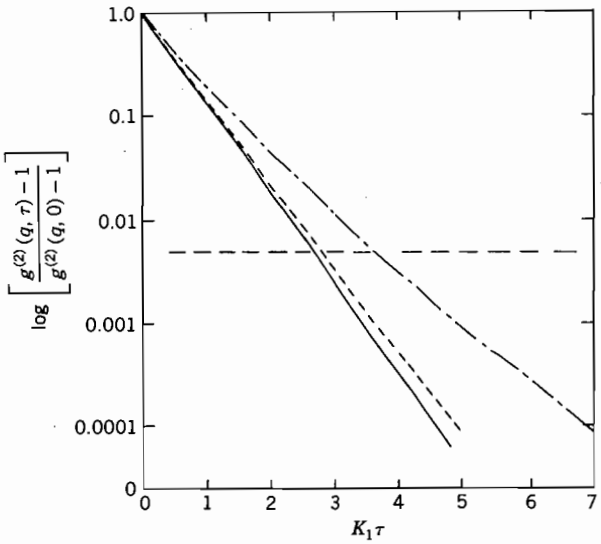

Fig. 7. Normalized photon-count correlation functions calculated for a random-flight coil for $\overline{M}_w/\overline{M}_n = 1$, 1.1, and 11 for the solid, dashed, and chain curves, respectively; K_1 is the first cumulant and the horizontal line shows the typical smallest value for which $g^{(2)}(q,\tau)$ may be determined experimentally.

Values of K_1 and K_2 may be calculated for the examples described in the preceding paragraph with the result

$$K_1 = (q^2kT/6\pi\eta_s)[\underline{d}\, r\overline{M}_w^\alpha H_{(1-\alpha)}(h + 1)]^{-1} \tag{150}$$

$$K_2 = K_1^2(\beta - 1)/2 \tag{151}$$

where $\alpha = (1 + \epsilon)/2$, $H_\mu(x) = x^\mu\Gamma(x)/\Gamma(x + \mu)$ with $\Gamma(\ )$ the gamma function, $h^{-1} = (\overline{M}_w/\overline{M}_n) - 1$, and $\beta = H_{(1-\alpha)}(h + 1)/H_{(1-2\alpha)}(h + 1)$. For $\alpha = 1$, approximating a rodlike chain, $K_1 \propto \overline{M}_w^{-1}$, and

$$\frac{K_2}{K_1^2} = [(\overline{M}_w/\overline{M}_n) - 1]/2 \tag{152}$$

For $\alpha = 1/2$, as with a random-flight chain, $K_1 \propto \overline{M}_w^{-1/2}/H_{1/2}(h + 1)$, where $H_{1/2}(h + 1) \approx 1$, eg, $H_{1/2}(\infty) = 1$ and $H_{1/2}(1.1) = 1.117$. In this case K_2 is small, even for a rather broad molecular-weight distribution, eg, K_2/K_1^2 is 0.005 and 0.12 for $h = 10$ and $h = 0.1$, respectively.

In some cases, a reference beam is mixed with the scattered light in such a way that a fraction r_0 of the total count rate is due to the reference beam. Under these circumstances (1,23,43) with $p(q,\Delta\tau) = 1$:

$$g^{(2)}(q,\tau;A) = 1 + 2r_0(1 - r_0)f^{1/2}(A)g^{(1)}(q,\tau) + (1 - r_0)^2 f(A)[g^{(2)}(q,\tau;0) - 1] \quad (153)$$

$$n^{(2)}(q,\Delta\tau;A) = 1 + 2r_0(1 - r_0)f^{1/2}(A)\sum_{\nu}^{C} r_\nu h(2\gamma_\nu) + (1 - r_0)^2 f(A)\sum_{\nu}^{C}\sum_{\mu}^{C} r_\nu r_\mu h(\gamma_\nu + \gamma_\mu) \quad (154)$$

where $g^{(2)}(q,\tau;0)$ and $g^{(1)}(q,\tau)$ are given by equations 25 and 139, respectively. As mentioned previously, $\Delta\alpha_{rs}(\mathbf{q},\tau)$ is usually a Gaussian stochastic variable, permitting the use of equation 25 for $g^{(2)}(q,\tau;\Delta\tau,0)$ in terms of $g^{(1)}(q,\tau)$. Even if this condition is not met, the limiting form of equation 153 for small $1 - r_0$ may be used to express $g^{(2)}(q,\tau;\Delta\tau,A)$ in terms of $g^{(1)}(q,\tau)$, with the latter given by equation 139 (23,43).

The Effect of Internal Dynamics. If the molecules are large enough that $qR_{G,\nu}$ exceeds about unity, and if they have asymmetric instantaneous conformations, equation 130 for $S_\nu(q,\tau)$ is not adequate. In such cases, the double sum in equation 127 cannot be factored to give $S_\nu(q,0)$, but rather contributes terms to $S_\nu(q,\tau)$ deriving from correlations among the scattering elements comprising one molecule. Consideration of such effects requires a detailed model for the intramolecular dynamics, and results in a more complicated representation for $g_\nu^{(1)}(q,\tau)$ than that given by equation 135. With several such treatments (1,48,49)

$$g_\nu^{(1)}(q,\tau) = \exp(-\Omega_\nu\tau)D(\Omega_\nu\tau) \quad (155)$$

where Ω_ν and $D(\Omega_\nu\tau)$ have the properties

$$\lim_{q=0} \Omega_\nu = \gamma_\nu = q^2 D_{T,\nu}^0 = \frac{kT}{6\pi\eta_s}\frac{u_\nu}{(R_{H,\nu}R_{G,\nu}^2)} \quad (156)$$

$$\lim_{q=0} D(\Omega_\nu\tau) = \lim_{\tau=0} D(\Omega_\nu\tau) = 1 \quad (157)$$

with $u_\nu = (qR_{G,\nu})^2$. Thus with equation 155, generally the second cumulant $K_2 \neq 0$, even for a monodisperse solute.

For several models for small u_ν, $g_\nu^{(1)}(q,\tau)$ may be represented by equation 155 with $\Omega_\nu = \gamma_\nu$ and

$$D(\Omega_\nu\tau) = 1 - u_\nu^2 s_\nu^{(2)}(u_\nu)[1 - \exp(-k_\nu^{(2)}\gamma_\nu u_\nu^{-1}\tau)] + \cdots \quad (158)$$

$$\left[\frac{\partial \ln D(\Omega_\nu\tau)}{\partial\tau}\right]_{\tau=0} = -k_\nu^{(2)}\gamma_\nu s_\nu^{(2)}(0)u_\nu + 0(u_\nu^2) \quad (159)$$

where $[k_\nu^{(2)}\gamma_\nu u_\nu^{-1}]^{-1}$ is a time constant $\tau_\nu^{(2)}$ given by

$$\tau_\nu^{(2)} = 6\pi\eta_s R_{H,\nu}R_{G,\nu}^2/k_\nu^{(2)}kT \quad (160)$$

In these relations, $s_\nu^{(2)}(u_\nu)$ depends on the structure and $k_\nu^{(2)}$ is a constant that depends on structure and hydrodynamical features. With these relations

$$K_1 = \sum_\nu^C r_\nu \left\{ \gamma_\nu - \left[\frac{\partial \ln D(\Omega_\nu \tau)}{\partial \tau} \right]_{\tau=0} \right\} \tag{161}$$

$$K_1 = \sum_\nu^C r_\nu \gamma_\nu [1 + k_\nu^{(2)} s_\nu^{(2)}(0) u_\nu + 0(u_\nu^2)] \tag{162}$$

As shown by equation 162, the effects of intramolecular dynamics on K_1 become important as $u_\nu > [k_\nu^{(2)} s_\nu^{(2)}(0)]^{-1}$.

For rodlike chains $s_\nu^{(2)}(0) = 1/45$ and $\tau_\nu^{(2)} = (6D_{R,\nu}^0)^{-1}$, with $D_{R,\nu}^0$ the rotational diffusion constant (1). Since

$$D_{R,\nu}^0 = 9D_{T,\nu}^0/L_\nu^2 \tag{163}$$

for rodlike chains

$$\tau_\nu^{(2)} = (4/3)\eta_s[\eta]_\nu M_\nu/RT$$

rod: (164)

$$k_\nu^{(2)} = 9/2$$

Thus $k_\nu^{(2)} s_\nu^{(2)}(0) = 1/10$, and in this case, the rotational motion is not important in K_1 for $qR_{G,\nu}$ less than ca 1.

For flexible coil chains, $s_\nu^{(2)}(0) = 1/45$, and $\tau_\nu^{(2)}$ is the time constant for the longest relaxation mode, given by (1, 48)

$$\tau_\nu^{(2)} = k(X_\nu)\eta_s[\eta]_\nu M_\nu/RT$$

coil: (165)

$$k_\nu^{(2)} = 6/k(X_\nu)$$

where $k(X_\nu)$ $6/\pi^2 \approx 0.61$ or 0.42, respectively, in the limits as X_ν tends to zero or infinity. Here (13)

$$\pi^{1/2} X_\nu = (L_\nu/R_{G,\nu})(\zeta/6\pi\eta_s d) \tag{166}$$

with ζ and d the friction factor and diameter of the chain elements, respectively, and therefore $\zeta/6\pi\eta_s d \approx 1$. In obtaining equation 165, the following relation is used (13)

$$R_{H,\nu} = R_{G,\nu} \frac{9\pi^{1/2} X_\nu}{9 + 24X_\nu} \tag{167}$$

for the random-flight chain. With equation 165, $k_\nu^{(2)} s_\nu^{(2)}(0) \approx 0.2$–$0.3$, depending on X_ν; therefore the effects of internal dynamics on K_1 may be neglected for $qR_{G,\nu}$ less than $\sim$ unity.

The q-dependence of the effects of internal dynamics and rotational motions on $g^{(1)}(q,\tau)$ for $qR_{G,\nu} > 1$ may not be described by the linearized equations 161 and 162, and the truncated expression in equation 158 may be inadequate for larger τ. Effects of this sort are discussed extensively in reference (48). Such behavior might be especially important with neutron scattering, for which q is large enough that behavior may be unavoidably influenced by higher order terms.

For this range of q, the expansion in equation 158 does not converge rapidly enough to be convenient. For an important intermediate q regime with $qR_{G,\nu} > 1$, but q^{-1} much larger than the dimension of a scattering unit, Ω_ν is given by (48,50)

$$\lim_{\substack{X_\nu=0 \\ qR_G>1}} \Omega_\nu = (u_\nu/\pi)^2/2\tau_\nu^{(2)} = \gamma_\nu u_\nu/2 = \frac{kT}{6\pi\eta_s}(\rho/6)q^4 \tag{168}$$

$$\lim_{\substack{X_\nu=\infty \\ qR_G>1}} \Omega_\nu = (u_\nu/\pi)^{3/2}/1.16\tau_\nu^{(2)} = \frac{3\pi^{1/2}}{8}\gamma_\nu u_\nu^{1/2} = \frac{kT}{6\pi\eta_s}q^3 \tag{169}$$

for the hydrodynamic model for flexible coil chains mentioned above; ρ is the persistence length (eg, eq. 70) and $\zeta/6\pi\eta_s d$ is set to unity.

Equations 168 and 169 show that for large q, Ω_ν does not depend on the overall dimensions of the solute, reflecting the short range of the correlations probed by the scattering at large q. For threadlike molecules, if $\sigma = \partial \ln R_H/\partial \ln R_G$, then for large q, $\Omega_\nu \propto q^{2+\sigma}$.

For the flexible coil models discussed above, for $qR_G > 1$, $g_\nu^{(1)}(q,\tau)$ is not an exponential function of τ (48,49). For $\tau > \tau_\nu^{(2)}$,

$$\lim_{\substack{\tau>\tau_\nu^{(2)} \\ X_\nu=0 \\ qR_G>1}} g_\nu^{(1)}(q,\tau) \propto \exp\left[-(4\Omega_\nu\tau/\pi)^{1/2}\right] \tag{170}$$

$$\lim_{\substack{\tau>\tau_\nu^{(2)} \\ X_\nu=\infty \\ qR_G>1}} g_\nu^{(1)}(q,\tau) \propto \exp\left[-(1.575\Omega_\nu\tau)^{2/3}\right] \tag{171}$$

where Ω_ν is given by the appropriate Ω_ν from equations 168 and 169. This behavior is difficult to observe experimentally by light scattering, both because it is difficult to reach large enough q and because $g_\nu^{(1)}(q,\tau)$ is small in the range of interest.

Effect of Optical Anisotropy. If the scattering centers are optically anisotropic, $I_{Hv}(q,t)$ provides information on orientation fluctuations. In this case, the autocorrelation $g_{Hv}^{(2)}(\tau)$ of the intensity can be represented in the form (1)

$$g_{Hv}^{(2)}(q,\tau) - 1 = [g_{Hv}^{(2)}(q,0) - 1]\left\{\sum_\nu^C r_{Hv,\nu} \exp\left[-(q^2D_{T,\nu}^0 + 6D_{R,\nu}^0)\tau\right]\right\}^2 \tag{172}$$

for rodlike chains, where the $r_{Hv,\nu}$ may depend on q and $\Sigma\, r_{Hv,\nu} = 1$. For larger qR_G, the relations are more complex. It may be noted that with equation 172, $g_{Hv}^{(2)}(\tau)$ at zero q depends on $D_{R,\nu}^0$, but not $D_{T,\nu}^0$.

The Effect of an External Field. In the presence of an appropriate external field, eg, an electric field, the solute may undergo a uniform translation with velocity **v**. In this case, equation 134 is changed to (1,19,26)

$$\frac{\partial G_s(\mathbf{R},\tau)}{\partial\tau} + \mathbf{v}\cdot\nabla\, G_s(\mathbf{R},\tau) = D_T^0\nabla^2 G_s(\mathbf{R},t) \tag{173}$$

With this modification, and with a fraction r_0 of the light derived from a reference beam, equation 153 becomes

$$g^{(2)}(q,\tau;A) = 1 + 2r_0(1 - r_0)f^{1/2}(A)\sum_{\nu}^{C} r_\nu \cos(\Delta\omega_\nu\tau)\exp(-\gamma_\nu\tau) + (1 - r_0)^2 f(A)\left[\sum_{\nu}^{C} r_\nu \exp(-\gamma_\nu\tau)\right]^2 \quad (174)$$

where $\Delta\omega_\nu = \mathbf{q}\cdot\mathbf{v}_\nu$. Evaluation of $\Delta\omega_\nu$ from $g^{(2)}(q,\tau)$ requires $r_0 > 0$, eg, the presence of a reference beam. If the external field is an electric field $\mathscr{E}$, then

$$\mathbf{v}_\nu = \mu_\nu\mathscr{E} \quad (175)$$

$$\Delta\omega_\nu = \mathbf{q}\cdot\mathbf{v}_\nu = \mu_\nu q\mathscr{E}\cos\phi \quad (176)$$

where ϕ is the angle between $\mathbf{q}$ and $\mathscr{E}$, and μ_ν is the electrophoretic mobility of solute ν. For many systems, the relation

$$\mu_\nu = \frac{Z_{\mathrm{eq},\nu}}{\Xi_\nu^0} = D_{T,\nu}^0 Z_{\mathrm{eq},\nu}/kT \quad (177)$$

may be used for μ_ν, where $Z_{\mathrm{eq},\nu}$ is the effective change on the solute. With the Debye-Hückel-Henry theory of the ion atmosphere (26,29)

$$Z_{\mathrm{eq}} = Z\frac{X_H(\kappa a)}{1 + \kappa a} \quad (178)$$

where a is the ionic radius, Z is the charge on the solute, $X_H(\kappa a)$ is called the Henry function, and κ is given in terms of the dielectric constant ϵ, the ionic strength I(mol/L), and the electron charge e (in esu):

$$\kappa^2 = \frac{8\pi N_A e^2}{\epsilon kT}(I/1000) \quad (179)$$

As shown in equation 174, evaluation of $\Delta\omega_\nu$ requires use of a reference beam in such a way that for small $1 - r_0$,

$$g^{(2)}(q,\tau;A) \approx 1 + 2r_0(1 - r_0)f^{1/2}(A)\sum_{\nu}^{C} r_\nu \cos(\Delta\omega_\nu\tau)\exp(-\gamma_\nu\tau) \quad (180)$$

Even in this case $g^{(2)}(q,\tau)$ is complicated and a more useful form is given by the Fourier transform $\hat{G}^{(2)}(q,\omega;A)$ of $G^{(2)}(q,\tau;A) = \langle n(q)\rangle^2 g^{(2)}(q,\tau;A)$ calculated with equation 180, where ω is usually in the range from 0 to a few kHz; ω represents the shift in frequency of the scattered light from that of the incident beam:

$$\hat{G}^{(2)}(q,\omega;A) = \frac{1}{2\pi}R_e\left[\int_{-\infty}^{\infty} G^{(2)}(\mathrm{q},\tau;A)\exp(i\tau\omega)d\tau\right] \quad (181)$$

$$\hat{G}^{(2)}(q,\omega;A) = \langle n(q)\rangle^2\left\{\delta(0) + r_0(1 - r_0)f^{1/2}(A)\sum_{\nu}^{C} r_\nu\gamma_\nu \times\left[\frac{1}{(\omega - \Delta\omega_\nu)^2 + \gamma_\nu^2} + \frac{1}{(\omega + \Delta\omega_\nu)^2 + \gamma_\nu^2}\right]\right\} \quad (182)$$

Therefore $\hat{G}^{(2)}(q,\omega;A)$ exhibits a series of peaks, each centered at a frequency $\Delta\omega_\nu$, with intensities weighted by r_ν. If r_0 is zero (a self-beating experiment), the

scattering provides no information on the uniform translation. Examples of $G^{(2)}(q,\tau;A)$ and $\hat{G}^{(2)}(q,\omega;A)$ for a hypothetical heterodisperse sample are illustrated in Figure 8 where two components are present, with $r_1 = 1 - r_2 = 0.1$, $\gamma_1 = 0.1$, and $\gamma_2 = 0.01$, and $K_1 = 0.091$, $\Delta\omega_1 = 1.0$, and $\Delta\omega_2 = 0.1$; the summation in equation 182 gives 0.376 for $\omega = 0$. In Figure 8, $\hat{G}^{(2)}(q,0^+;A)$ represents the limit of $\hat{G}^{(2)}(q,\omega;A)$ for small, but nonzero ω. The example in Figure 8 shows that $\Delta\omega_\nu$ is much more easily deduced from $\hat{G}^{(2)}(q,\omega;A)$ than from $G^{(2)}(q,\tau;A)$.

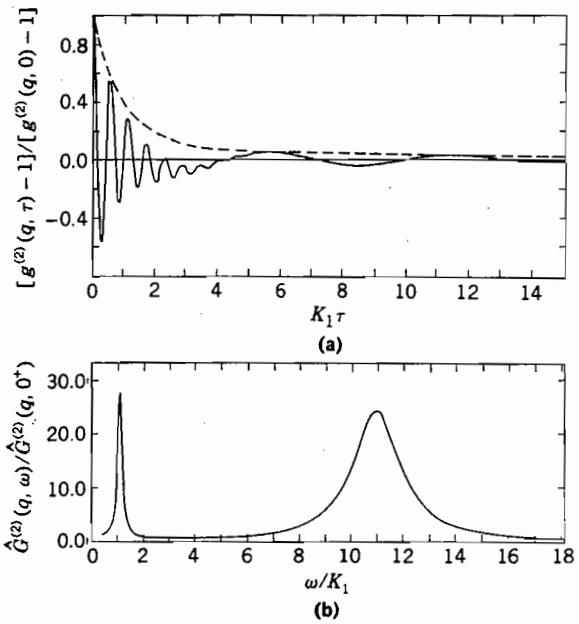

Fig. 8. (a) Photon-count correlation function for a two-particle system in an electrophoretic light-scattering experiment (see text for a description of the particles). Dashed curve represents behavior in the absence of an electric field; K_1 is the first cumulant; (b) fourier transform of the data in (a).

Scattering at Arbitrary Concentration

Static Scattering at Zero Scattering Angle. The Rayleigh ratio $\mathbf{R}(0)$ at zero angle is considered below as a function of concentration, principally for isotropic scatterers. The discussion is separated into two broad regimes with $[\eta]c$ smaller or larger than unity. The product $[\eta]c$ provides a measure of the potential for intermolecular interactions. For small $[\eta]c$, expansion of $\mathbf{R}(0)/c$ in a Taylor series in c (a virial expansion) is useful. Several models for the second virial coefficient A_2 are given, along with discussion of the effects of molecular-weight heterogeneity. The behavior for larger $[\eta]c$ is discussed next with emphasis on semiempirical analytical relations for $\mathbf{R}(0)$, along with the development of a correlation length. The latter reduces to R_H for small $[\eta]c$, but can be expressed as a function of $[\eta]c$ for large $[\eta]c$. Finally, the effect of concentration on $\mathbf{R}_{\text{aniso}}(0)/c$ is briefly considered.

Isotropic Scatterers. For C-solute molecules, where the ν^{th} solute has n_ν identical, isotropic scattering centers, equations 10 and 15 give (13,16)

$$\mathbf{R}(0) = KcM_{LS}[1 - c\mathbf{B}(c)] \tag{183}$$

$$\mathbf{B}(c) = \frac{\sum_{\mu}^{C}\sum_{\substack{\nu \\ \nu\neq\mu}}^{C} \psi_\nu w_\nu M_\nu \psi_\mu w_\mu M_\mu B_{\nu\mu}(c)}{\sum_{\nu}^{C} \psi_\nu^2 w_\nu M_\nu} \tag{184}$$

where $K = K' n_s^2 (\partial\tilde{n}/\partial c)_w^2$. The interaction term $B_{\nu\mu}$, which may depend on M_ν and M_μ, as well as c, is given formally by (13,16)

$$B_{\nu\mu}(c) = \frac{N_A}{VM_\nu M_\mu}\int g_2(\nu,\mu)d(\nu)d(\mu) \tag{185}$$

The symbols $d(\nu)$ and $d(\mu)$ represent integration over the positions of the n_ν and n_μ scattering elements, respectively, of components ν and μ in the volume V. The radial distribution function $g_2(\nu,\mu)$, given by (13,16)

$$\begin{aligned} g_2(\nu,\mu) &= F_2(\nu,\mu) - F_1(\nu)F_1(\mu) \\ &= F_1(\nu)F_1(\mu)[\exp(-U_{\nu\mu}/kT) - 1] \end{aligned} \tag{186}$$

may depend on c. Here, $F_1(\nu)d(\nu)/V$ is the probability that molecule ν occupies the set of coordinates symbolized by (ν) within $d(\nu)$, with a similar meaning for $F_1(\mu)d(\mu)/V$; $F_2(\nu,\mu)d(\nu)d(\mu)/V^2$ is the probability that molecules ν and μ occupy the joint set of coordinates symbolized by (ν,μ) within $d(\nu)d(\mu)$; and $U_{\nu\mu}$ is a potential associated with the joint configuration. An alternative form of equation 183 used below is given by

$$\mathbf{R}(0) = KcM_{LS}[1 + c\Gamma(c)]^{-1} \tag{187}$$

$$\Gamma(c) = \frac{\mathbf{B}(c)}{1 - c\mathbf{B}(c)} \tag{188}$$

Behavior for Small $[\eta]c$. For a monodisperse solute, $\mathbf{B}(c)$ and $\Gamma(c)$ may be expanded in a power series in c with concentration-independent coefficients (13,16,28)

$$\Gamma(c) = 2\Gamma_2 + 3\Gamma_3 c + \cdots \tag{189}$$

$$\mathbf{B}(c) = 2\Gamma_2 + (3\Gamma_3 - 4\Gamma_2^2)c + \cdots \tag{190}$$

where $\Gamma_2 = A_2\mathrm{M}$, $\Gamma_3 = A_3 M$, etc. Such expansions are useful at low concentrations, eg, for $c[\eta] < 1$. With equation 189,

$$\mathbf{R}(0) = KcM(1 + 2A_2Mc + 3A_3Mc^2 + \cdots)^{-1} \tag{191}$$

or, equivalently, an extension of equation 26:

$$\mathbf{R}(0) = K\frac{RTc}{(\partial\Pi/\partial c)} \tag{192}$$

That is,

$$c\Gamma(c) = \frac{M}{RT}\frac{\partial \Pi}{\partial c} - 1 \tag{193}$$

For $A_2 > 0$, equation 191 may be expressed in the forms

$$\frac{Kc}{\mathbf{R}(0)} = \frac{1}{M}[1 + 2A_2Mc + 3q_3(A_2Mc)^2 + \cdots] \tag{194}$$

$$\left[\frac{Kc}{\mathbf{R}(0)}\right]^{1/2} = \left(\frac{1}{M}\right)^{1/2}[1 + A_2Mc + \tfrac{1}{2}(3q_3 - 1)(A_2Mc)^2 + \cdots] \tag{195}$$

where $q_3 = A_3/A_2^2M$. If $q_3 \approx \frac{1}{3}$, $[Kc/\mathbf{R}(0)]^{1/2}$ is more nearly a linear function of c than $Kc/\mathbf{R}(0)$ (16,28)

It is convenient to express A_2 in terms of the excluded volume per molecule U defined as (13,28)

$$A_2M = \frac{N_A}{M}\frac{U}{2} \tag{196}$$

For particles with a hard-core potential, U, which represents the volume excluded by one particle to all other particles, may be calculated exactly based on geometric considerations. Such calculations have been completed for spheroids, disks, and rods (13), with the following results (V_p is the volume of the particle in every case) for cylinders of length L and diameter d and spheroids with unique axis of length R_1 and transverse axes of length R_2 (ie, $R_1 > R_2$ for prolate ellipsoids and $R_2 > R_1$ for oblate ellipsoids):

$$U = 8V_pf \tag{197}$$

cylinder:
$$4f_{cyl} = 1 + (L/d)(1 + d/2L)(1 + \pi d/2L) \tag{198}$$

rod:
$$\lim_{L \gg d} f_{cyl} = L/4d \tag{199}$$

disk:
$$\lim_{d \gg L} f_{cyl} = \pi d/16L \tag{200}$$

spheroid:
$$4f_{sp} = 1 + \frac{3}{4}\left[1 + (1 - \epsilon^2)^{-1/2}\frac{\arcsin \epsilon}{\epsilon}\right]\left[1 + \frac{1 - \epsilon^2}{2\epsilon}\ln\left(\frac{1 + \epsilon}{1 - \epsilon}\right)\right] \tag{201a}$$

$$\epsilon^2 = (R_2^2 - R_1^2)/R_2^2 \tag{201b}$$

sphere:
$$(f_{sp})_{R_1 = R_2} = 1 \tag{202}$$

More realistic intermolecular potentials exhibit both repulsive and attractive terms. Thus U, or A_2, may be zero or negative, in contrast to the case for the hard-core potential for which $U > 0$. With flexible chain polymers, it is useful to express A_2M in the form (13,28)

$$A_2M = \frac{N_AR_G^3}{M}\Psi(U/R_G^3) \tag{203}$$

where $\Psi(x)$ is a function with the properties

$$\lim_{x=0} \Psi(x) = 0 \tag{204}$$

$$\lim_{x=\infty} \Psi(x) = \Psi_\infty \tag{205}$$

with $\Psi_\infty \approx 6$–7 for linear flexible chain polymers. Various models have been developed for Ψ (13,28,51–53). In the limit with $\Psi \approx \Psi_\infty$, equation 1 with $K_\eta \approx 3.2$ and $R_H \approx 2R_G/3$ for linear flexible chain polymers gives $A_2M/[\eta] \approx 1$ for large U/R_G^3. Insofar as $a = \partial \ln [\eta]/\partial \ln M$ is a constant, this result gives $\partial \ln A_2/\partial \ln M \approx a - 1$ if $A_2M/[\eta]$ is large enough that Ψ is near its asymptotic limit Ψ_∞.

For heterodispersed systems in which $\Psi_\nu = \Psi$ for all ν, equation 184 becomes (13,16)

$$\mathbf{B}(c) = \frac{1}{\overline{M}_w} \sum_{\nu}^{C} \sum_{\substack{\mu \\ \mu \neq \nu}}^{C} w_\nu w_\mu M_\nu M_\mu B_{\nu\mu}(c) \tag{206}$$

With expansion of $B_{\nu\mu}$ in a power series in c, for small c, equation 206 becomes

$$\mathbf{R}(0) = Kc\overline{M}_w(1 + 2A_2^R\overline{M}_w c + \cdots)^{-1} \tag{207}$$

$$A_2^R = \frac{1}{\overline{M}_w^2} \sum_{\nu}^{C} \sum_{\substack{\mu \\ \mu \neq \nu}}^{C} w_\nu w_\mu M_\nu M_\mu B_{\nu\mu}^0 \tag{208}$$

By comparison, for such a heterogeneous mixture,

$$\Pi = RTc\overline{M}_n^{-1}(1 + A_2^\Pi \overline{M}_n c + \cdots) \tag{209}$$

$$A_2^\Pi = \sum_{\nu}^{C} \sum_{\substack{\mu \\ \mu \neq \nu}}^{C} w_\nu w_\mu B_{\nu\mu}^0 \tag{210}$$

In this case, equation 192 is not valid. In general, $A_2^R \leqslant A_2^\Pi$. For example, if $B_{\nu\mu}^0 = (B_{\nu\nu}^0 B_{\mu\mu}^0)^{1/2}$, then (38)

$$\frac{A_2^R}{A_2^\Pi} = \left(\frac{\sum_{\nu}^{C} w_\nu M_\mu B_{\nu\nu}^0}{\overline{M}_w \sum_{\nu}^{C} w_\nu B_{\nu\nu}^0} \right)^2 \tag{211}$$

If $B_{\nu\nu}^0 \propto bM_\nu^{-\gamma}$, then for w_ν given by equation 72 (38)

$$\frac{A_2^R}{A_2^\Pi} = \frac{1}{n_w^2} \left(\frac{\sum_{\nu}^{C} w_\nu n_\nu^{1-\gamma/2}}{\sum_{\nu}^{C} w_\nu n_\nu^{-\gamma/2}} \right) = \left(\frac{1 + h - \gamma/2}{1 + h} \right)^2 \tag{212}$$

Behavior for $[\eta]c > 1$. If $c[\eta] > 1$, the power-series expansions in equations 189 and 190 are not applicable. For monodisperse solute, equation 192 may be coupled with the expression for Π to provide a relation for $\mathbf{R}(0)$. As c approaches the density of the solute, contributions to $\mathbf{R}(0)$ not included in equation 192 must be

taken into account (52,53). In some cases, analytical expressions are available for Π, and hence for $\mathbf{R}(0)$. For example, for homogeneous spheres with radius R interacting through a hard-core potential (54),

$$\frac{\Pi M}{RTc} = \frac{1 + \phi + \phi^2 - \phi^3}{(1 - \phi)^3} \tag{213}$$

where $\phi = (4\pi/3)N_A R^3 c/M$, so that with equations 193 and 213

$$c\Gamma(c) = \frac{8\phi - 2\phi^2}{(1 - \phi)^4} \tag{214}$$

If the solute species are charged, the intermolecular interaction can result in very large $\Gamma(c)$.

For flexible chain polymers in systems for which U/R_G^3 is large, as shown by equation 194, A_2Mc forms a natural dimensionless variable for $M\Pi/RTc$, or $\mathbf{R}(0)/KcM$. For A_2Mc in the range 1–10, it is expected that Π should depend on c, but not on M (28,50). Thus retaining the form based on the dimensionless variable A_2Mc,

$$\frac{\Pi M}{RTc} = P(A_2Mc) \tag{215}$$

the condition $\partial\Pi/\partial M = 0$ requires that $(\partial \ln P/\partial \ln M) - 1 = 0$. Making use of the relation $\partial \ln A_2/\partial \ln M = a - 1$ with $a = \partial \ln [\eta]/\partial \ln M$, this condition gives the result (55)

$$1 + p = \frac{\partial \ln P(A_2Mc)}{\partial \ln A_2Mc} = \frac{1}{a} \tag{216}$$

For large A_2Mc, for which a tends to $\frac{4}{5}$, p goes to $\frac{1}{4}$ (50). The power-series expansion valid for small A_2Mc and the power-law representation may be combined in the semiempirical relation (55)

$$\frac{\Pi M}{RTc} = 1 + Z\left(1 + \frac{q_3}{p}Z\right)^p \tag{217}$$

where $Z = A_2Mc$. Numerically similar relations have been derived using renormalization group methods (52,53). This relation provides a semiempirical representation for Π over the range from infinite dilution to large $[\eta]c$, but should not be used if $c/\hat{\rho}$ is larger than ca 0.5 (with $\hat{\rho}$ the solute density), as then $\Pi M/RTc$ may not scale with A_2Mc (52).

With equation 192, this expression for Π gives (55)

$$\mathbf{R}(0) = KcM\left\{\left[1 + 2Z\left(1 + \frac{q_3}{p}2Z\right)^p\right]H(Z)\right\}^{-1} \tag{218}$$

where $H(Z) \approx 1$. This is a special form of equation 187 with

$$c\Gamma(c) \approx 2A_2Mc\left(1 + 2\frac{q_3}{p}A_2Mc\right)^p \tag{219}$$

Comparison of equation 218 with experimental data is shown in Figure 9; for the data given, $q_3 \approx 0.5$.

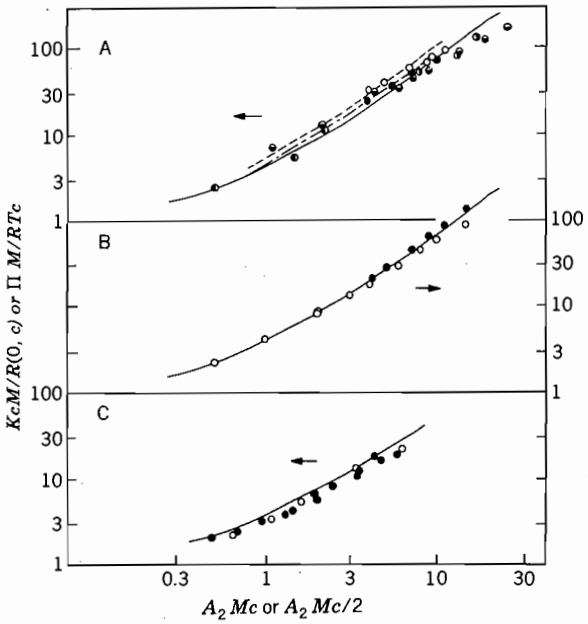

Fig. 9. A, Bilogarithmic plot of $KcM/R(0,c)$ vs A_2Mc for solutions of polystyrene in benzene. ○, discussed in Ref. 31; ◒, ◐, ◑, and ● discussed in Ref. 55. ----- and — - — - represent similar data for polystyrene in toluene (56,57). ——— represents equation 218 with $p = 0.39$ and $q = 0.45$; B, bilogarithmic plots of $KcM/R(0,c)$ vs A_2Mc, 0, and $\Pi M/RTc$ vs $A_2Mc/2$, 0, for solutions of poly(α-methyl styrene) in toluene (58). The curve is the same as is A; C, bilogarithmic plot of $KcM/R(0,c)$ vs A_2Mc for solutions of polystyrene in cyclopentane for $T = 313$K and 328K. ○, Mol wt 2.1×10^6; ●, mol wt 8.6×10^5 (55). The curves are the same as in A, except that $p = 0.28$ and $q = 0.45$.

If $A_2 = 0$, equation 194 is not useful, but A_3, and higher order coefficients, may not be zero; therefore

$$\frac{\Pi M}{RTc} = 1 + A_3Mc^2 + \cdots \tag{220}$$

or with equation 192

$$\mathbf{R}(0) = KcM(1 + 3A_3Mc^2 + \cdots)^{-1} \tag{221}$$

$$c\Gamma(c) = 3A_3Mc^2 + \cdots = 3\Psi_3([\eta]c)^2 + \cdots \tag{222}$$

where $\Psi_3 = A_3M/[\eta]^2$. For a system with $A_2 = 0$, $\psi_3 \approx 0.17$ (55).

Formally, for a homogeneous solute, $\partial\Pi/\partial c$ is related to the repeat-unit-pair correlation function $g(\mathbf{r})$ through the expression (50)

$$RT\left(\frac{\partial\Pi}{\partial c}\right)^{-1} = M[1 + c\Gamma(c)]^{-1} = m_0 \int_v g(\mathbf{r})d\mathbf{r} \tag{223}$$

where m_0 is the molecular weight of a repeating unit. For flexible chain polymers at concentration such that $[\eta]c \gg 1$, the copious intertwining of the chains permits a useful representation of the integral in equation 223 in terms of a correlation length ξ_0 where the subscript 0 denotes $q = 0$. In this representation, it is assumed

that $g(\mathbf{r})$ is such that (50)

$$\lim_{[\eta]c\gg 1} \int_V g(\mathbf{r})d\mathbf{r} \approx \int_{V_{\xi 0}} g(\mathbf{r})d\mathbf{r} \tag{224}$$

where $V_{\xi 0} = \pi\xi_0^3/6$ is the correlation volume. Since the integral gives the number of monomers per correlation volume, this approximation gives

$$\lim_{[\eta]c\gg 1} \int_V g(\mathbf{r})d\mathbf{r} \approx (cN_A/m_0)V_{\xi 0} \tag{225}$$

At infinite dilution, $V_{\xi 0}$ reduces to the volume spanned by the segments of one chain, and $(N_A c/m_0)V_{\xi 0}$ is equal to the number of monomers per chain, M/m_0. For a concentrated solution, $V_{\xi 0}$ is given by

$$cN_A V_{\xi 0} = M[1 + c\Gamma(c)]^{-1} \tag{226}$$

Thus, equations 223–226 give

$$\xi_0 = K_\xi R_H([\eta]c)^{-[(2+p)/3]}[S([\eta]c)]^{-1/3} \tag{227}$$

where the proportionality constant K_ξ given by

$$K_\xi = \left[\frac{6M[\eta]}{\pi N_A R_H^3}\right]^{1/3} = \left[6K_\eta\left(\frac{R_G}{R_H}\right)^2\right]^{1/3} \tag{228}$$

which is equal to 2.0 in the limit for large hydrodynamic parameter X_ν (eq. 167), with K_η defined by equation 1, and

$$S([\eta]c) = \frac{1 + c\Gamma(c)}{([\eta]c)^{1+p}} \tag{229}$$

With $\Gamma(c)$ given by equation 219, $S([\eta]c)$ is a constant $S(\infty)$ for $[\eta]c \gg 1$, and in this range the correlation length ξ_0 is proportional to $([\eta]c)^{-[(2+p)/3]}$. Thus, ξ_0 is proportional to $([\eta]c)^{-1}$ for $A_2 = 0$, or to $([\eta]c)^{-3/4}$ for $A_2 \gg 0$. The correlation length ξ_0 is used below in the discussion of the dynamic scattering for $[\eta]c \gg 1$.

Anisotropic Identical Scatterers. At zero scattering angle, the polarized and depolarized scattering may be represented as (1,5)

$$\mathbf{R}_{Vv}(0) = \mathbf{R}_{\text{iso}}(0) + \tfrac{4}{3}\mathbf{R}_{\text{aniso}}(0) \tag{230}$$

$$\mathbf{R}_{Hv}(0) = \mathbf{R}_{\text{aniso}}(0) \tag{231}$$

where $R_{\text{iso}}(0)$ is given by the relation discussed previously for isotropic scatterers. For low concentrations, eg, $[\eta]c < 1$, the orientation correlation among the scattering elements of different solutes is negligible, and $\mathbf{R}_{\text{aniso}}(0) \propto c$, even though A_2Mc may be large. If c is large enough, intermolecular correlations may develop, making interpretations of $\mathbf{R}_{\text{aniso}}(0)$ more complicated. For the case discussed above, with cylindrically symmetric scattering elements, $\mathbf{R}_{\text{aniso}}(0)$ may be written in the form

$$\mathbf{R}_{\text{aniso}}(0) = \frac{3}{5}K'\tilde{n}_s^2\left(\frac{\partial\tilde{n}}{\partial c}\right)^2 cm_0\delta_0^2 G_2 \tag{232}$$

where all the scattering centers have anisotropy δ_0, molecular weight m_0, and refractive-index increment $(\partial\tilde{n}/\partial c) \neq 0$. The function G_2 may be expressed in

terms of the angle $\beta_{i\nu,j\mu}$ between scattering element i on chain ν and element j on chain μ:

$$G_2 = G_{2,\text{intra}} + G_{2,\text{inter}} \tag{233}$$

$$G_{2,\text{intra}} = \frac{1}{m_0} \sum_{\nu}^{C} w_\nu M_\nu D_{\nu\nu} \tag{234}$$

$$G_{2,\text{inter}} = \frac{N_A c}{m_0} \sum_{\nu}^{C} \sum_{\substack{\mu \\ \nu \neq \mu}}^{C} w_\nu w_\mu D_{\nu\mu} \tag{235}$$

$$D_{\nu\mu} = \frac{1}{n_\nu n_\mu} \sum_{i\nu}^{n_\nu} \sum_{j\mu}^{n_\mu} P_2(\cos \beta_{i\nu,j\mu}) \tag{236}$$

$$P_2(x) = \frac{3\langle \cos^2 x \rangle - 1}{2} \tag{237}$$

where $\langle \cdots \rangle$ represents an ensemble average. Equation 234 was used above in the form of equations 53 to 54. Theoretical estimates of $G_{2,\text{inter}}$ are not available, but $G_{2,\text{inter}}$ may not be negligibly small if c is large enough. The interpretation of such data is complicated by factors not explicitly included in this discussion, eg, induced optical anisotropy caused by effects on the local electric field. Typically, for $[\eta]c < 1$, $G_{2,\text{inter}}$ is negligibly small since, as shown by equation 236, $G_{2,\text{inter}}$ involves orientational correlations among scattering elements on different solutes. In such a case, $\mathbf{R}_{Hv}(0)/c$ is independent of c (35,59). In some cases, for concentrated solutions of small molecules, $\mathbf{R}_{Hv}(0)/c$ appears to increase with c (60).

Static Scattering at Arbitrary Angle. The scattering at arbitrary angle and concentration emphasizes interference effects among rays scattered from all the scattering elements. Thus, both intramolecular and intermolecular correlations among these elements are important. Definitive treatment of this complex behavior is lacking. In the following discussion, some semiempirical relations are considered, including a concentration-dependent correlation length given by the limit of $-\partial \ln \mathbf{R}(q)/\partial q^2$ for small q, and a correlation length ξ_q that reduces to ξ_0 for small q. For larger q, ξ_q is expressed in terms of $[\eta]c$ and certain functions of q.

For concentrations high enough that intermolecular interactions are important, and for $q > 0$, equation 183 for isotropic scatterers becomes (13,16)

$$\mathbf{R}(q) = K' \tilde{n}_s^2 c \left[\sum_{\nu}^{C} w_\nu \psi_\nu^2 M_\nu P_\nu(q,c) - c \sum_{\nu}^{C} \sum_{\substack{\mu \\ \mu \neq \nu}}^{C} w_\nu w_\mu \psi_\nu \psi_\mu M_\nu M_\mu B_{\nu\mu} P^{(q)}_{\parallel,\nu\mu} \right] \tag{238}$$

where $P_{\parallel,\nu\mu}(q,c)$ is defined in terms of the radial distribution function $g_2(\nu,\mu)$ of equation 186:

$$P_{\parallel,\nu\mu}(q,c) = \frac{1}{n_\nu n_\mu} \sum_{i_\nu}^{n_\nu} \sum_{\substack{i_\mu \\ \mu \neq \nu}}^{n_\mu} \frac{\int g_2(\nu,\mu) \exp(i\mathbf{q}\cdot\mathbf{r}_{i\nu,i\mu}) d(\nu) d(\mu)}{\int g_2(\nu,\mu) d(\nu) d(\mu)} \tag{239}$$

Here, $r_{i\nu,i\mu}$ is the separation of elements i_ν and i_μ on solutes ν and μ, respectively, and it is assumed that all scattering elements on the ν^{th} solute have refractive index increment ψ_ν; $P_\nu(q,c)$ and $B_{\nu\mu}(c)$, given by equations 66a and 185, respectively, may depend on c (13).

For a monodisperse solute, equation 238 may be rewritten in the form

$$\mathbf{R}(q) = KcM\,P(q,c)F(q,c) \tag{240}$$

$$F(q,c) = 1 - c\mathbf{B}(c)P_\parallel(q,c)/P(q,c) \tag{241}$$

with $P_\parallel(q,c)$ given by equation 239 with $n_\nu = n_\mu = n$; $F(q,c)$ is called the static structure factor. Both $P(q,c)$ and $P_\parallel(q,c)$ may depend on c. For example, the chain dimensions can depend on c for flexible chain polymers (13) resulting in dependence of $P(q,c)$ on c. It is convenient to express $F(q,c)$ in the form

$$F^{-1}(c,q) = 1 + P(q,c)Q(q,c)c\Gamma(c) \tag{242}$$

where

$$Q(q,c) = \left[\frac{P_\parallel(q,c)}{P^2(q,c)}\right]\left\{(1 - c\Gamma(c)\left[\left(\frac{P_\parallel(q,c)}{P(q,c)}\right) - 1\right]\right\}^{-1} \tag{243}$$

$$c\Gamma(c) = \frac{M}{RT}\frac{\partial\Pi}{\partial c} - 1 \tag{193}$$

With this representation for $F(q,c)$, $\mathbf{R}(q)$ may be expressed in a simple form analogous to equation 187:

$$\frac{KcM}{\mathbf{R}(q)} = \frac{1}{P(q,c)} + cQ(q,c)\Gamma(c) \tag{244}$$

With monodisperse spheres interacting through a hard-core potential, $P(q,c) = P^0(q)$, $P(q,c)Q(q,c) \approx [P^0(2q)]^{1/2}$, and $\Gamma(c)$ is given by equation 214 (6).

For $[\eta]c < 1$, expansion of $P(q,c)$, $Q(q,c)$, and $\Gamma(c)$ in power series in c gives (13,36)

$$\frac{Kc}{\mathbf{R}(q)} = \frac{1}{M}\left[\frac{1}{P^0(q)} + 2A_2MQ^0(q)c + \cdots\right] \tag{245}$$

$$Q^0(q) = \lim_{c=0} Q(q,c) = \frac{P_\parallel^0(q)}{[P^0(q)]^2} - \frac{[\partial P(q,c)/\partial c]^0}{2A_2M[P^0(q)]^2} \tag{246}$$

With the random-flight chain model, $Q^0(q) = 1$ (13,36), but for flexible chains with excluded volume $U = 2A_2M^2/N_A$ (eq. 203) (13)

$$Q^0(q) = 1 - 0.008(U/R_G^3)u + \cdots \tag{247}$$

A concentration-dependent correlation length b, defined by

$$b^2 = -\lim_{q=0}\frac{\partial \ln \mathbf{R}(q)}{\partial q^2} \tag{248}$$

may be determined experimentally (6). With equation 244

$$b^2 = \frac{1}{1 + c\Gamma(c)}\lim_{q=0}\left[-\frac{\partial P(q,c)}{\partial q^2} + c\Gamma(c)\frac{\partial Q(q,c)}{\partial q^2}\right] \tag{249}$$

$$(b^2)^0 = \lim_{c=0} b^2 = R_G^2/3 \tag{250}$$

For coil-like chains, the relation

$$P(q,c) = [1 + (aq)^2]^{-2} \tag{251}$$

is suggested by analogy with equation 89, where a is an intramolecular correlation length that may depend on c (55). At infinite dilution, equation 251 with $(a^2)^0 = R_G^2/6$ is a good approximation to equation 89 for the random-flight chain for $R_G q < 2.5$. With equation 251, $-\partial P(q,c)/\partial q^2 = 2a^2$ for small q.

For solutions of flexible chain polymers with $A_2 > 0$, both a^2/R_G^2 and b^2/R_G^2 are expected to scale with A_2Mc (50,52,53,55,57)

$$\lim_{A_2 \gg 0} a^2 = (a^2)^0 \mathbf{A}(A_2Mc) \tag{252}$$

$$\lim_{A_2 \gg 0} b^2 = (b^2)^0 \mathbf{B}(A_2Mc) \tag{253}$$

where $\mathbf{A}(A_2Mc)$ and $\mathbf{B}(A_2Mc)$ are each unity at infinite dilution. The general features of $\mathbf{A}(A_2Mc)$ may be assessed on the basis of the molecular weight independence of $a^2/(a^2)^0$ for large A_2Mc, eg, for large A_2Mc, $\partial \ln a^2/\partial \ln M = 1$, since $(a^2)^0 \propto M$ (28). Making use of the relations $a = \partial \ln [\eta]/\partial \ln M$, $a - 1 = \partial \ln A_2/\partial \ln M$ and $M[\eta] \propto R_G^3$ discussed above (55),

$$r = \left[\frac{\partial \ln \mathbf{A}(A_2Mc)}{\partial \ln (A_2Mc)}\right]_M = \frac{1 - 2a}{3a} \tag{254}$$

Thus $r = -1/4$, if $a = 4/5$ (28), corresponding to the behavior for very large A_2M. Calculations of a, including treatments using renormalization group methods, lead to similar results, with numerical or analytical representations for $\mathbf{A}(A_2Mc)$. For example, with one treatment (53,55)

$$\mathbf{A}(A_2Mc) \approx \exp [-0.05X(1 + X)^{-1/2}] \tag{255a}$$

$$X = 1.3A_2Mc \tag{255b}$$

As shown by equation (249), the dependence of b on c is more complex unless $\partial Q/\partial q^2$ is zero, as suggested by some studies (55–57,61,62). In that case,

$$\mathbf{B}(A_2Mc) = \frac{\mathbf{A}(A_2Mc)}{1 + c\Gamma(c)} \tag{256}$$

where $c\Gamma(c)$ is given by equation 219.

As mentioned previously, with flexible chain polymers at concentrations with $[\eta]c \gg 1$, the copious intertwining of the chains motivates the introduction of a correlation length ξ_0 to describe the scattering at zero q. Similarly, a correlation length ξ_q may be defined for nonzero q. In this case, the monomeric pair correlation function $g(\mathbf{r})$ is used in the relation (50)

$$M\,P(q,c)\,F(q,c) = m_0 \int_V g(\mathbf{r}) \exp (i\mathbf{q}\cdot\mathbf{r}) d\mathbf{r} \tag{257}$$

with $P(q,c)$ and $F(q,c)$ defined above. For $[\eta]c \gg 1$, the integral is approximated by (50)

$$\lim_{[\eta]c \gg 1} \int_V g(\mathbf{r}) \exp(i\mathbf{q}\cdot\mathbf{r})d\mathbf{r} \approx \int_{V_{\xi q}} g(r) \exp(iq\cdot r)dr \approx (cN_A/m_0)V_{\xi q} \quad (258)$$

where $V_{\xi_q} = \pi\xi_q^3/6$; $(cN_A/m_0)V_{\xi_q}$ represents the number of monomers in $V_{\xi q}$. With these relations,

$$\xi_q = \xi_0\left[\frac{S([\eta]c)}{S_q([\eta]c)}\right]^{1/3} \quad (259)$$

where ξ_0 and $S([\eta]c)$ are given by equations 227 and 229 (obtained in the limit of small q), and

$$S_q([\eta]c) = \frac{[P(q,c)F(q,c)]^{-1}}{([\eta]c)^{1+p}} \quad (260)$$

The ratio

$$\frac{S([\eta]c)}{S_q([\eta]c)} = \frac{1 + c\Gamma(c)}{P^{-1}(q,c)[1 + P(q,c)Q(q,c)c\Gamma(c)]} \quad (261)$$

tends to $Q^{-1}(q,c)$ for large $[\eta]c$ and small q, but for $qR_G \gg 1$, $S([\eta]c)/S_q[\eta]c) \propto c\Gamma(c)(q^2r)^{-1(1+\epsilon)}$, with r and ϵ defined by their use in equation 79. Consequently, $\xi_q = \xi_0$ in the limit as q tends to zero, and $\xi_q \propto q^{-2/(1+\epsilon)}$ for $qR_G \gg 1$. The correlation length ξ_q is used below in discussion of the dynamic scattering for $[\eta]c \gg 1$ and $q \neq 0$.

Dynamic Scattering at Arbitrary Angle. The effects of solute interactions on $g^{(1)}(\tau,q)$ are discussed here based on the values of $[\eta]c$ and qR_G: both $[\eta]c$ and qR_G small, facilitating the use of Taylor expansions; large $[\eta]c$, but small qR_G, and small τ; both $[\eta]c$ and qR_G large, but τ small; and finally, large $[\eta]c$, arbitrary qR_G, and larger τ. For most purposes, the first regime is the most important, as it provides a guideline for extrapolation of data to infinite dilution. Thus, a discussion of the dependence on c of an experimentally defined mutual diffusion constant $D_M(c)$ is given in the following. The subsequent sections may be principally of interest in more specialized studies of molecular dynamics.

With interacting solutes the approximation leading to equations 127–135 at infinite dilution are not appropriate. Formally, $g^{(1)}(q,\tau)$ in equation 24 is given by (1)

$$g^{(1)}(q,\tau) = \frac{S(q,\tau)}{S(q,0)} \quad (262)$$

$$S(q,\tau) = \sum_i^\eta \sum_j \langle \exp i\mathbf{q}\cdot[\mathbf{r}_i(0) - \mathbf{r}_j(\tau)]\rangle \quad (263)$$

where the summations are over the $\eta = cN_A/m_0$ scattering elements with dimension b, all assumed to be identical. The behavior may be separated into regimes of concentration, corresponding to $[\eta]c \ll 1$ or $[\eta]c > 1$; regimes of q, corresponding to $qb \ll 1$ or $qb > 1$; and regimes of τ, with $\tau/\tau_m \ll 1$ or $\tau/\tau_m > 1$, where τ_m^{-1} is related to $q^2D_T^0$ (see below). The following discussion is limited to a monodisperse solute.

Behavior for $[\eta]c \ll 1$ and $qR_G \ll 1$. In the limit as q goes to zero, for the behavior at infinite dilution, equation 263 involves only the center of mass trans-

lation, with

$$g^{(1)}(g,\tau) = \exp - \gamma\tau \tag{264}$$

$$\gamma = q^2 D_M(c) \tag{265}$$

However, the mutual diffusion constant depends on c (eg, compare eq. 137):

$$D_M(c) = \frac{M}{N_A\,\Xi(c)} \cdot \frac{\partial \Pi}{\partial c}\,(1 - \phi) \tag{266}$$

$$\frac{M}{RT}\frac{\partial \Pi}{\partial c} = 1 + c\Gamma(c) \tag{267}$$

with ϕ the volume fraction of solute and $\Xi(c)$ the friction factor at concentration c. Of course, $D_M(c)$ reduces to D_T^0 at infinite dilution. For $[\eta]c \ll 1$, $\Gamma(c)$ may be represented by equation 189, and $\Xi(c)$ may be expanded in a power series in $[\eta]c$ (1,13,20,25,50):

$$\Xi(c) = \Xi^0[1 + k_\Xi[\eta]c + \cdots] \tag{268}$$

where $\Xi^0 = kT/D_T^0$. Combination of these relations gives

$$D_M(c) = D_T^0[1 + k_D[\eta]c + \cdots](1 - \phi) \tag{269}$$

$$k_D = \frac{2A_2M}{[\eta]} - k_\Xi \tag{270}$$

In general, k_Ξ has the form

$$k_\Xi = c_1 + c_2A_2M/[\eta] \tag{271}$$

where c_1 and c_2 depend on the nature of the solute and therefore

$$\lim_{[\eta]c \ll 1} \frac{\partial D_M(c)}{\partial c} = D_T^0[(2 - c_2)A_2M - c_1[\eta] - v_2] \tag{272}$$

For spherical solutes interacting through a hard-core potential, $[\eta]c = 5\phi/2$ and $A_2M/[\eta] = 8/5$; thus $k_D[\eta]c = [(16/5) - k_\Xi][\eta]c = (5/2)[(16/5) - k_\Xi]\phi$. Long standing theoretical calculations give $5k_\Xi/2 = 6.55$ (or $k_\Xi = 2.62$) for hard spheres (63). A revised treatment (64) gives $5k_\Xi/2 = 7.90$ for this model. Values of c_1 and c_2 for spherical solute interacting through other potentials, eg, electrostatic interducing long-range repulsion or a potential with an attractive part, are less well established. For flexible chain polymers, one treatment gives $c_1 \approx 0.2$ and $c_2 \approx 1.2$ (13). In this case $\partial D_M/\partial c$ is negative if $A_2 = 0$, but positive if $A_2M/[\eta] > c_1/(2 - c_2)$, with neglect of $v_2/[\eta]$. With $A_2M/[\eta] \approx 1$, $k_\Xi \approx 1.4$ reflecting the "softer" intermolecular potential in comparison with that for hard spheres.

Behavior for $[\eta]c > 1$ and $qR_G < 1$. For larger $[\eta]c$ (but small q and τ), the power series expansion of $\Xi(c)$ and $\Pi(c)$ used above is often inadequate (eg, eq. 217 for Π). In addition, the possible viscoelastic character of concentrated solutions may result in additional temporal correlations. Although understanding of this area is incomplete, it appears that $D_M(c)$ determined from the first cumulant for small q may be approximated by (50,65–67)

$$D_M(c) = \frac{M}{N_A\Xi(c)} \cdot \frac{\mathbf{M}_{LS}(c)}{c} \cdot (1 - \phi) \tag{273}$$

$$\mathbf{M}_{LS}(c) = \mathcal{M}\left\{c\frac{\partial\Pi}{\partial c}, \frac{4}{3}[\overline{G(\tau)}]_{LS}\right\} \tag{274}$$

Here, $c\partial\Pi/\partial c$ represents the osmotic modulus of compression and $[\overline{G(\tau)}]_{LS}$ is an effective value of the shear modulus $G(t)$ for the time range of the light-scattering experiment; $\mathbf{M}_{LS}(\tau)$ may be compared with the longitudinal modulus $\mathbf{M}(t)$ in which $c\partial\Pi/\partial c$ is replaced by the bulk modulus $K(t)$ and $[\overline{G(\tau)}]_{LS}$ is replaced by $G(t)$, see below. With increasing q, additional effects must be considered.

It will be convenient to consider $D_M(c)/D_T^0$, where D_T^0 is given by equation 137. With equations 273 and 274,

$$\frac{D_M(c)}{D_T^0} = \frac{\zeta(0)}{\zeta(\phi)}\cdot(1 - \phi)\mathcal{M}[H^{\Pi}(c), H^{G}(c)] \tag{275}$$

where the functions

$$H^{\Pi}(c) = \frac{\zeta(\phi)}{\zeta(0)}\frac{\Xi^0}{\Xi(c)}\cdot\left(\frac{M}{RT}\frac{\partial\Pi}{\partial c}\right) \tag{276}$$

$$H^{G}(c) = \frac{4}{3}\frac{\zeta(\phi)}{\zeta(0)}\frac{\Xi^0}{\Xi(c)}\cdot\frac{[\overline{G(\tau)}]_{LS}}{cRT/M} \tag{277}$$

involve osmotic and viscoelastic contributions, respectively, to $D_M(c)$. These functions depend on $[\eta]c$. In equation 275, the factor $\zeta(\phi)/\zeta(0)$ represents the change in the local friction from its value at infinite dilution, as the volume fraction ϕ of the solution is increased. With most solutions (68,69),

$$\zeta(\phi)/\zeta(0) = \exp\left\{\frac{T_0(\phi) - T_0(0)}{C[T - T_0(\phi)][T - T_0(0)]}\right\} \tag{278}$$

where $T_0(\phi)$ may depend markedly on ϕ, and C is a system-dependent constant, about equal to the volumetric expansion factor for the solution. Typically, $\zeta(\phi)/\zeta(0)$ is close to unity for $\phi < 0.1$ and has the form

$$\zeta(\phi)/\zeta(0) \approx \exp B(T)\phi \tag{279}$$

for larger ϕ, where $B(T)$ is a temperature-dependent constant. (Though usually positive, $B(T)$ could be negative under certain circumstances.)

For *spherical particles* interacting through a hard-core potential, viscoelastic effects are generally unimportant in the time range used to study $G^{(2)}(q,\tau)$, unless ϕ approaches the volume fraction ϕ_m for close packing of the spheres. Thus, for small q, $\mathbf{M}_{LS}(c) \approx c(\partial\Pi/\partial c) = (1 + c\Gamma(c))RTc/M$ where $\Gamma(c)$ is given by equation 214. The dependence of $\Xi(c)$ on c for large $[\eta]c$ for hard-core spherical particles is not well established, but for $\phi < \phi_m$, a useful approximation might be given by

$$\frac{\Xi^0}{\Xi(c)} \approx \exp -\frac{(5k_{\Xi}/2)\phi_m\phi}{(\phi_m - \phi)} \tag{280}$$

where $k_{\Xi} = 2.62$ (or 3.16) and $\phi = (2/5)[\eta]c$.

With *flexible chain polymers*, the copious intermolecular interactions among the intertwining chains complicates the interpretation of $D_M(c)$, with effects on

$\Xi(c)$ and the terms $c\partial\Pi/\partial c$ and $[\overline{G(\tau)}]_{LS}$ appearing in $\mathbf{M}_{LS}(c)$. With flexible chain polymers $G(t)$ has the form (68,70,71)

$$G(t) \approx G_0 \sum_{p=1}^{m} h_p \exp(-t/\tau_p) \tag{281}$$

where the τ_p are called viscoelastic relaxation times, with τ_m the largest τ_p. For fluids, $G(t)$ is zero for $t \gg \tau_m$, but $G(t) \approx G_0$ for t less than the smallest τ_p. The character of $G(t)$ for polymer solutions depends strongly on a parameter E defined by (47,68–71)

$$E = \frac{c\alpha_c^2 M}{\hat{\rho}\mathbf{M}_c} \approx (c/\hat{\rho})^{1+r}\frac{M}{\mathbf{M}_c} \tag{282}$$

Here, $\mathbf{M}_c$ is a polymer-specific constant, $\hat{\rho}$, the solute density, α_c, the ratio of R_G for the polymer in solution at the experimental c to $(R_{G,0})^0$ for the same polymer at infinite dilution in a solvent with $A_2 = 0$, and r, given by equation 254, is $-1/4$ for $A_2 \gg 0$ or 0 for $A_2 = 0$. For example, the viscosity η, related to $G(t)$ by the expression (68)

$$\eta = \int_0^\infty G(u)du = G_0 \sum h_p\tau_p \tag{283}$$

takes the form (67–70)

$$\eta = \eta^{(R)}(1 + E^{2.4\epsilon})^{1/\epsilon} \tag{284a}$$

$$\eta^{(R)} = N_A(R_{G,0}^2)^0 c\alpha_c^2\zeta/6m \tag{284b}$$

for polymer solutions with $2 < \epsilon < 3$, and where ζ is the friction factor for the hydrodynamic chain unit with molecular weight m. The steady-state recoverable compliance $R^{(S)}$, given in terms of $G(t)$ by the relation (68)

$$R^{(S)} = \frac{\int_0^\infty uG(u)du}{\left[\int_0^\infty G(u)du\right]^2} = \frac{\sum h_p\tau_p^2}{G_0(\sum h_p\tau_p)^2} \tag{285}$$

may be represented by (68,70,71)

$$R^{(S)} = R^{(R)}\left[1 + \left(\frac{5}{2}\frac{\mathbf{M}_e}{\mathbf{M}_c'}\frac{R^{(R)}}{R_N}\right)^\epsilon\right]^{-1/\epsilon} \tag{286}$$

for polymer solutions, where $R^{(R)} = 2M/5cRT$, $\mathbf{M}_c'$ is a system-dependent constant, ($\mathbf{M}_c' \approx 2\mathbf{M}_c \approx 4\mathbf{M}_e$), ϵ is arbitrary (ca 2–3), and the network modulus G_N is given by (50,68,70,71)

$$G_N = R_N^{-1} = \frac{\hat{\rho}RT}{\mathbf{M}_e}(c/\hat{\rho})^{2+s} \tag{287}$$

with $s = 0$ for solutions with $A_2 = 0$. The value of s for systems for which $A_2 \gg 0$ is still uncertain, but appears to be about equal to p given by equation 215 for moderately concentrated solutions (50). The constant $\tau_c = \eta R^{(S)}$ used below may

be computed from equations 284 and 285. For $t > \tau_e$, equation 281 reduces to

$$\lim_{t \gg \tau_e} G(t) \approx G_N \sum_{p=p_e}^{m} h_p \exp(-t/\tau_p) \tag{288}$$

where $\tau_e = (\eta_c^{(R)}/\eta)\tau_c$ with $\eta_c^{(R)}$ the value of $\eta^{(R)}$ for $M = M_c$, and p_e is the value of p for which $\tau_p \approx \tau_e$. Thus, the expression for $\mathbf{M}_{LS}(c)$ is conveniently represented by

$$\mathbf{M}_{LS}(c) = \frac{cRT}{M}\mathcal{M}\left\{1 + c\Gamma(c), \frac{4}{3}\frac{M}{M_e}(c/\hat{\rho})^{1+s}\frac{[\overline{G(\tau)}]_{LS}}{G_N}\right\} \tag{289}$$

where $[\overline{G(\tau)}]_{LS}/G_N \approx 1$, if the experimental time scale used to determine $D_M(c)$ is near τ_e, whereas $[\overline{G(\tau)}]_{LS} \approx 0$ if the time scale exceeds $\tau_c = \eta R^{(S)}$. The relation $\tau_e = [\eta_c^{(R)}/\eta]\tau_c$ provides an estimate for τ_e/τ_c, and τ_c may be calculated as $\eta R^{(S)}$, or approximated as κ_0^{-1}, where κ_0 is the shear rate for the onset of non-Newtonian behavior in the steady-state viscosity (71).

The relation for $\Xi(c)$ in the range $[\eta]c > 1$ is not well established. In one approximate treatment, $\Xi(c)$ is represented in terms of the monomer pair correlation $g(\mathbf{r})$ introduced in equation 223, through a hydrodynamical calculation giving the relation (50)

$$\frac{\Xi^0}{\Xi(c)} \approx \frac{R_H}{M}\frac{\zeta(0)}{\zeta(\phi)}\left[m_0 \int_{V_{\xi 0}} g(\mathbf{r})|r|^{-1}d\mathbf{r}\right] \tag{290}$$

Using equation 290 and the correlation length ξ_0 defined by equation 227, the relation for $\Xi^0/\Xi(c)$ may be recast in the form

$$\frac{\Xi^0}{\Xi(c)} \approx \frac{R_H}{\xi_0}\frac{\zeta(0)}{\zeta(\phi)}[1 + c(\Gamma)]^{-1}\frac{m_1}{m_2} \tag{291}$$

where

$$m_n = \int_0^\infty x^n g(x)dx \tag{292}$$

(If the Ornstein-Zernike relation (72) $g(x) \propto x^{-1}\exp(-x)$ is used, $m_1/m_2 = 1$; this value is assumed here.) Using the estimate for ξ_0 given by equation 227,

$$\frac{\Xi^0}{\Xi(c)} = K_\xi^{-1}\frac{\zeta(0)}{\zeta(\phi)}([\eta]c)^{-\frac{1-p}{3}}[S([\eta]c)]^{-2/3} \tag{293}$$

where $S([\eta]c)$ is given by equation 229; $S([\eta]c)$ tends to a constant $S^{(\infty)}$ for large $[\eta]c$. The discussion is confined to the model with $X_\nu = \infty$, for which $K_\xi = 2.0$.

In terms of the functions $H^\Pi(c)$ and $H^G(c)$ in equations 275–277, for small q,

$$H^\Pi(c) = R_H/\xi_0 = K_\xi^{-1}([\eta]c)^{(\gamma+p)/3}[S([\eta]c)]^{1/3} \tag{294}$$

$$H^G(c) = \frac{4}{3}H^\Pi(c)\frac{(c/\hat{\rho})^{s-p}}{([\eta]_e\hat{\rho})^{1+p}}\left\{\frac{[\overline{G(\tau)}]_{LS}/G_N}{S([\eta]c)}\right\} \tag{295}$$

In equation 295, $[\eta]_e$ is the intrinsic viscosity for a polymer with molecular weight M_e.

Discussion of $D_M(c)$ given by equations 275, 294, and 295 is conveniently separated into two cases: $A_2 = 0$ and $A_2 \gg 0$. Some experimental results with $D_M(c)/D_T^0$ are shown in Figure 10 in terms of the reduced concentration $[\eta]c$. It may be seen that the dependence of $D_M^{(c)}/D_T^0$ on $[\eta]c$ changes character as $[\eta]c$ exceeds unity. If $[\eta]c \gg 1$ and $A_2 > 0$, then according to equation 294, $H^{\Pi}(c)/([\eta]c)^{(2+p)/3}$ is a constant, and $H^{G}(c)/[\eta]c)^{(2+p)/3}$ is proportional to $(c/\rho)^{s-p}[\overline{G(\tau)}]_{LS}/G_N \approx [\overline{G(\tau)}]_{LS}/G_N$. For $\tau \approx \tau_e$, $[\overline{G(\tau)}]_{LS} \approx G_N$, but for $\tau \gg \tau_c$, $[\overline{G(\tau)}]_{LS} \approx 0$. In either case, $D_M(c)\zeta(\phi)/D_T^0\zeta(0)(1 - \phi)$ is expected to be proportional to $([\eta]c)^{(2+p)/3}$, with the exponent tending to ¾ as A_2 increases. Typically, the exponent is closer to 0.7 for solutions for which $A_2 > 0$, as shown in Figure 10. If $A_2 = 0$, the $c\Gamma(c) \approx 3(\psi_3[\eta]c)^2$, where $\psi_3 = A_3M/[\eta]^2$, and $p = 1$ since $a = ½$. Thus, for large $[\eta]c$, $S([\eta]c) \approx 3\psi_3^2$, and $H^{\Pi}(c) \propto [\eta]c$. Since $s \approx 0$ in this case, $H^G(c) \propto ([\eta]/[\eta]_e)\{[\overline{G(\tau)}]_{LS}/G_N\}$ is independent of c. If $\tau \approx \tau_e$, then $H^G(c) \propto [\eta]/[\eta]_e$, whereas $H^G(c) \approx 0$ if $\tau > \tau_c$.

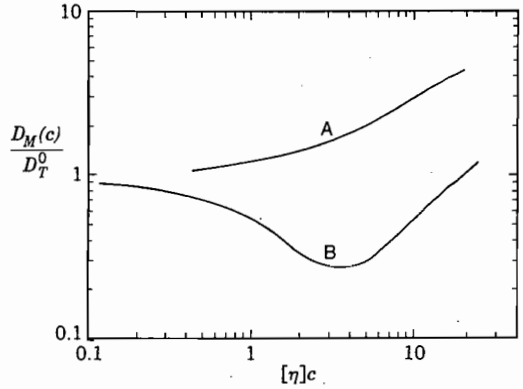

Fig. 10. The mutual diffusion constant $D_M(c)$ divided by its value D_T^0 at infinite dilution as a function of $[\eta]c$ for polystyrene solutions. *A*, $D_M(c)$ in tetrahydrofuran (73) for which $A_2M \approx [\eta]$; B, $D_M(c)$ in cyclohexane (74,75) for which $A_2 = 0$. The various features of these data are discussed in the text following equation 295.

Behavior for $[\eta]c > 1$ and $qR_G > 1$. With increasing q, the length scale probed by the scattered radiation is shortened and approximations made above are not valid. The first cumulant K_1 gives an apparent diffusion constant $D_{app}(c,q) = K_1/q^2$

$$D_{app}(c,q) = \frac{M}{N_A\,\Xi(c,q)}\,\frac{\mathbf{M}_{LS}(c,q)}{c}\,(1 - \phi) \tag{296}$$

For spherical particles interacting through a hard-core potential, and for $\phi < \phi_m$,

$$\mathbf{M}_{LS}(c,q) \approx \frac{cRT}{M}\,F(q,c) \tag{297}$$

where $F(q,c)$ is given by equation 242. The relation for $\Xi(c,q)$ is less well established, but with some approximations (76)

$$\Xi(c,q) \approx \Xi(c)W[F(q,c)] \tag{298}$$

For interacting flexible chain polymers, one effect of increased q is to reduce the effective volume V_ξ over which intermolecular and intramolecular correlations are important in $\Xi(c,q)$. In a treatment of this effect related to that discussed above for small q, $\Xi(c,q)$ for $qR_G > 1$ is given by (50)

$$\frac{\Xi^0}{\Xi(c,q)} \approx \frac{R_H}{M}\frac{\zeta(0)}{\zeta(\phi)}\left[m_0 \int_{V_{\xi q}} g(\mathbf{r}) \exp\,(i\mathbf{q}\cdot\mathbf{r})|r|^{-1}d\mathbf{r}\right] \tag{299}$$

which reduces to equation 290 for small q. Using equations 257–259, this relation may be written in the form (similar to 291):

$$\frac{\Xi^0}{\Xi(c,q)} = \frac{R_H}{\xi_q}\frac{\zeta(0)}{\zeta(\phi)}[P(q,c)F(q,c)]\frac{m_1(q\xi_q)}{m_2(q\xi_q)} \tag{300}$$

where

$$m_n(q\xi_q) = \int_0^\infty |\mathbf{x}|^n g(\mathbf{x})\exp\,(i\xi_q\mathbf{q}\cdot\mathbf{x})d\mathbf{x} \tag{301}$$

utilizing equation 257. With ξ_q given by equation 259,

$$\frac{\Xi^0}{\Xi(c,q)} = \frac{\Xi^0}{\Xi(c)}\left[\frac{S([\eta]c)}{S_q([\eta]c)}\right]^{2/3}\frac{m_1(q\xi_q)}{m_2(q\xi_q)} \tag{302}$$

where $\Xi^0/\Xi(c)$, $S([\eta]c)$, and $S_q([\eta]c)$ are given by equations 293, 229, and 260, respectively. Similarly, $\mathbf{M}_{LS}(q,c)$ is given by

$$\mathbf{M}_{LS}(c,q) \approx \frac{cRT}{M}\mathcal{M}\left\{[P(q,c)F(q,c)]^{-1}, \frac{4}{3}\frac{M}{M_e}\left(\frac{c}{\hat{\rho}}\right)^{1+s}\frac{[\overline{G(\tau)}]_{LS}}{G_N}\right\} \tag{303}$$

and finally,

$$\frac{D_{app}(c,q)}{D_T^0} \approx \frac{\zeta(0)}{\zeta(\phi)}(1 - \phi)\mathcal{M}[H^\Pi(q,c), H^G(q,c)]\frac{m_1(q\xi_q)}{m_2(q\xi_q)} \tag{304}$$

where the functions $H^\Pi(q,c)$ and $H^G(q,c)$, are given by

$$H^\Pi(q,c) = H^\Pi(c)[S_q([\eta]c)/S([\eta]c)]^{1/3} \tag{305}$$

$$H^G(q,c) = H^G(c)[S([\eta]c)/S_q([\eta]c)]^{2/3} \tag{306}$$

with $H^\Pi(c)$ and $H^G(c)$ given by equations 294 and 295, respectively. With the Ornstein-Zernicke relation $g(x) \propto x^{-1}\exp(-x)$,

$$\frac{m_1(z)}{m_2(z)} = (1 + z^2)^{1/2}\sigma(z) \tag{307}$$

$$\sigma(z) = \frac{3}{4}(1 + z^2)^{1/2}\left[\frac{1}{z^2} + \frac{1}{z}\left(1 - \frac{1}{z^2}\right)\arctan z\right] \tag{308}$$

where $\sigma(z)$ is unity for small z and approaches $\sigma(\infty) \approx 1.2$ for large z (77). Thus, for small q, $m_1/m_2 \approx 1$, but for large $q\xi_q$, $m_1/m_2 \approx q\xi_q$.

Combination of these results gives (50)

$$\lim_{q\xi_q \gg 1}\frac{D_{app}(c,q)}{D_T^0} \approx \frac{\zeta(0)}{\zeta(\phi)}(1 - \phi)qR_H \tag{309}$$

$$\frac{H^G(\infty,c)}{H^{\Pi}(\infty,c)} = \frac{H^G(c)}{H^{\Pi}(c)} \lim_{q\xi_q \gg 1} \frac{S([\eta]c)}{S_q([\eta]c)} = 0 \tag{310}$$

where the relation $S([\eta]c)/S_q([\eta]c) \propto c\Gamma(c)q^{-2}$ is applied for large q. Thus, for large q, $D_{app}(c,q)$ is expected to be proportional to q and independent of c, with the exception of the factor $(1 - \phi)\zeta(0)/\zeta(\phi)$; $D_{app}(c,q)$ given by equation 309 is equal to Ω_ν/q^2 given by equation 169 for infinite dilution, an expected result, since the scattered radiation probe distances are too short to be affected by intermolecular interactions, eg, $\xi_q \ll R_G$. The q needed to observe this behavior may be difficult to attain in light-scattering experiments.

Behavior for $[\eta]c > 1$ and $\tau > \tau_e$. Frequently, $g^{(1)}(q,\tau)$ is not an exponential function for $[\eta]c > 1$, but can be represented as a sum of two exponential contributions (73)

$$g^{(1)}(q,\tau) \approx [1 - r_L(c,q)] \exp[-\gamma_s(c,q)\tau] + r_L(c,q) \exp[-\gamma_L(c,q)\tau] \tag{311}$$

where $\tau_L = [\gamma_L(c,q)]^{-1}$ and $\tau_s = [\gamma_s(c,q)]^{-1}$ represent long- and short-time constants, respectively, ie, $\tau_L > \tau_s$. With equation 311, the first cumulant is given by

$$K_1 = \gamma_s(c,q) + r_L(c,q)[\gamma_L(c,q) - \gamma_s(c,q)] \tag{312}$$

and therefore $D_M(c) = K_1/q^2$ or $D_{app}(c) = K_1/q^2$ discussed previously may be expressed in terms of the functions introduced in equation 311. In some cases, it appears that with polymer solutions, $\gamma_L(c,q)$ reaches a limiting value τ_L^{-1}, which is independent of q for solutions with $[\eta]c \gg 1$ and for $qR_G > 1$, indicating a relaxational process for $\gamma_L(c,q)$ (78). The constant τ_L is similar to τ_c, indicating long time-scale (terminal) viscoelastic relaxations. This behavior is similar to predicting a treatment in which viscoelastic effects lead to equation 312 with (66,78)

$$r_L(c,q) = \frac{\tau_L - \tau_R}{\tau_L - \tau_s} \tag{313}$$

where τ_L is expected to be independent of q, $\tau_R \approx \tau_c$ and $K_1 = \tau_R/\tau_L\tau_s \approx \tau_s^{-1}$. Although behavior in this range remains to be fully documented, it appears that a contribution to $g^{(1)}(q,\tau)$ with $\gamma_L(q,\tau) \approx \tau_c^{-1}$ is most important for A_2 nearly zero and $[\eta]c \gg 1$.

Brillouin Scattering

Inelastic scattering associated with vibrational modes of the entire sample gives rise to Brillouin scattering with an intensity doublet shifted by $\pm\ \omega_B$ from the frequency of the incident radiation. The frequency shift is related to the adiabatic sound velocity $V_s(q)$ for phonons with wavelength selected by the scattering vector **q**:

$$\omega_B = qV_s(q) \tag{314}$$

For dilute solutions, $V_s(q)$ is given essentially by the viscoelastic properties of the solvent at frequency equal to ω_B, as modified by the solute (21,22).

Brillouin scattering is most conveniently discussed in terms of the normal-

ized power spectrum $S_{X_y}(q,\omega)$ given by

$$S_{X_y}(q,\omega) = \frac{I_{X_y}(q,\omega)}{I_{X_y}(q)} \tag{315}$$

$$I_{X_y}(q,\omega) = \int_{-\infty}^{\infty} I_{X_y}(q,t) \exp(i\omega t)dt \tag{316}$$

$$I_{X_y}(q) = \int_{-\infty}^{\infty} I_{X_y}(q,\omega)d\omega \tag{317}$$

where $I_{X_y}(q,\omega)$ is the intensity at wave number q and shift ω from the incident frequency, with the analyzer and polarizer orientation indicated by the notation X_y, eg, $X_y = V_v$ or H_v, respectively, for the vertical and horizontal components of the scattering in the transverse plane with vertically polarized incident light. As distinct from the preceding discussion, here the total scattering intensity is described as opposed to the excess scattering obtained by subtracting the scattering from the solvent from the total.

A useful approximation for Brillouin scattering follows:

$$S_{V_v}(q,\omega) = S_{\text{iso}}(q,\omega) + \tfrac{4}{3}S_{\text{aniso}}(q,\omega) \tag{318}$$

$$S_{H_v}(q,\omega) = S_{\text{aniso}}(q,\omega) \tag{319}$$

This relation is only strictly valid if $q = 0$. Both $S_{\text{iso}}(q,\omega)$ and $S_{\text{aniso}}(q,\omega)$ exhibit unshifted or central bands with line widths (at half height) dependent on a variety of properties (1,21,22,79). Contributions to $S_{\text{iso}}(q,\omega)$ and $S_{\text{aniso}}(q,\omega)$ due to translational and orientational diffusion of the solute in a solution have been mentioned previously. In addition, much broader central peaks appear in $S_{\text{iso}}(q,\omega)$ with line widths determined by thermal diffusion or the frequency dependence of the longitudinal modulus and the specific heat (22). Contributions to comparably broad central peaks appearing in $S_{\text{aniso}}(q,\omega)$ are determined by the relaxation of intramolecular orientational fluctuations, a coupling between shear and optical anisotropy, and other effects. All of these are essentially properties of the solvent in the binary solvent–solute mixture.

Although frequency-shifted peaks may appear in $S_{\text{aniso}}(q,\omega)$, these have low intensity in comparison with those in $S_{\text{iso}}(q,\omega)$ and are not discussed here. The latter may be represented as

$$S_{\text{iso}}(q,\omega) = S_{\text{iso}}^{(C)}(q,\omega) + S_{\text{iso}}^{(B)}(q,\omega) \tag{320}$$

where $S_{\text{iso}}^{(C)}(q,\omega)$ represents the contributions to $S_{\text{iso}}(q,\omega)$ of bands centered at the incident frequency and $S_{\text{iso}}^{(B)}(q,\omega)$ is the Brillouin scattering given for the q in the light scattering range by

$$S_{\text{iso}}^{(B)} \propto \frac{\Gamma_B q^2}{(\omega + \omega_B)^2 + (\Gamma_B q^2)^2} + \frac{\Gamma_B q^2}{(\omega - \omega_B)^2 + (\Gamma_B q^2)^2} \tag{321}$$

where Γ_B is the line width of the Lorentzian bands comprising the Brillouin doublets, and ω_B is given by equation 314. The adiabatic sound velocity may be expressed in terms of the storage longitudinal modulus $\mathbf{M}'(\omega)$ as (22,68)

$$\gamma \mathbf{M}'(\omega_B) = \rho V_s^2(q)\left\{\frac{1 - (\Gamma_B/qV_s(q))^2}{[1 + (\Gamma_B/qV_s(q))^2]^2}\right\} \tag{322}$$

$$V_s(q) \approx \left[\gamma \frac{\mathbf{M}'(\omega_B)}{\rho} + 3(\Gamma_B/q)^2\right]^{1/2} \approx \left[\gamma \frac{\mathbf{M}'(\omega_B)}{\rho}\right]^{1/2} \tag{323}$$

where $\gamma = c_P/c_V$, with c_P and c_V the heat capacities at constant P and V, respectively. The storage longitudinal modulus may be expressed in terms of the longitudinal modulus $\mathbf{M}(t)$ by the relations (68)

$$\mathbf{M}'(\omega) = \omega \int_0^\infty \mathbf{M}(t) \sin(\omega t) dt \tag{324}$$

$$\mathbf{M}(t) = K(t) + \tfrac{4}{3}G(t) \tag{325}$$

where $K(t)$ and $G(t)$ are, respectively, the bulk and shear moduli.

Based on equation 322 the frequency dependence of $\mathbf{M}'(\omega)$ underlies the experimental ω_B. In principle, $\mathbf{M}'(\omega)$ can be determined by measurement of ω_B over a range of q. The limiting values of $\mathbf{M}'(\omega)$ for large and small ω are given by

$$\mathbf{M}_I = \lim_{\omega=\infty} \mathbf{M}'(\omega) = \lim_{t=0} \mathbf{M}(t) = K_I + (\tfrac{4}{3})G_I \tag{326}$$

$$\mathbf{M}_e = \lim_{\omega=0} \mathbf{M}'(\omega) = \lim_{t=\infty} \mathbf{M}(t) = K_e + (\tfrac{4}{3})G_e \tag{327}$$

where K_I and G_I are $K(t)$ and $G(t)$, respectively, for small t, and K_e and G_e are $K(t)$ and $G(t)$, respectively, for large t; K_e^{-1} is the equilibrium isothermal compressibility, $G_e = 0$ for a fluid, and typically, $K_I/K_e \approx 1.2$–1.7 (68). Frequently, $K(t)$ and $G(t)$ are represented in the forms (68,71)

$$K(t) = K_e + \Sigma K_i \exp(-t/\kappa_i) \tag{328}$$

$$G(t) = G_e + \Sigma G_i \exp(-t/\tau_i) \tag{329}$$

with $\Sigma K_i = K_I - K_e$ and $\Sigma G_i = G_I - G_e$. Thus,

$$\mathbf{M}'(\omega) = \mathbf{M}_I - \Sigma K_i[1 + (\omega\kappa_i)^2]^{-1} - (\tfrac{4}{3})\Sigma G_i[1 + (\omega\tau_i)^2]^{-1} \tag{330}$$

For ω large enough that $\omega\kappa_i \gg 1$ and $\omega\tau_i \gg 1$ for all terms in equation 330, $\mathbf{M}'(\omega) \approx \mathbf{M}_I = K_I + (\tfrac{4}{3})G_I$. For smaller ω, $\mathbf{M}'(\omega)$ decreases from this limit toward $\mathbf{M}_e = K_e + (\tfrac{4}{3})G_e$ (or $M_e = K_e$ for fluids).

For solutions, the parameters in equation 321 dominant for $\omega \approx \omega_B$ are those of the solvent. However, addition of a solute at volume fraction ϕ may modify both κ_i and τ_i through expressions of the form (68,71)

$$\tau_i(\phi) = \tau_i(0)\zeta(\phi)/\zeta(0) \tag{331}$$

where $\zeta(\phi)/\zeta(0)$, given by equation 278, may be either smaller or larger than unity, depending on the nature of solvent and solute, with a similar expression for $\kappa_i(\phi)$. Consequently, addition of a solvent may result in variation of ω_B from one extreme, for which all $\omega\kappa_i$ and $\omega\tau_i$ are large, and $\mathbf{M}'(\omega) \approx \mathbf{M}_I$ to the other extreme for which $\omega\kappa_i$ and $\omega\tau_i$ are small enough that $\mathbf{M}'(\omega)$ tends to K_e, with G_e being zero for a fluid. In this case, the Brillouin scattering provides information on the change of the local mobility (80).

The attenuation coefficient Γ_B is more complicated, including dependence on the storage longitudinal modulus $\mathbf{M}''(\omega)$

$$\mathbf{M}''(\omega) = \omega \int_0^\infty (\mathbf{M}(t) - \mathbf{M}_e) \cos(\omega t) dt \tag{332}$$

In some cases, for example, Γ_B and ω_B may be used to estimate $\mathbf{M}''(\omega_B)$

$$\tan \delta(\omega_B) = \frac{\mathbf{M}''(\omega_B)}{\mathbf{M}'(\omega_B)} = \frac{2\Gamma_B \omega_B^{-1}}{1 - (\Gamma_B \omega_B^{-1})^2} \tag{333}$$

Methods

Instrumentation

Optical Components. The requirements for elastic and quasielastic light scattering may be satisfied by a single instrument, provided that certain design features are adopted (Fig. 11). Measurement of the inelastic Brillouin scattering requires a different type of instrument, employing a high quality monochromator (21,22).

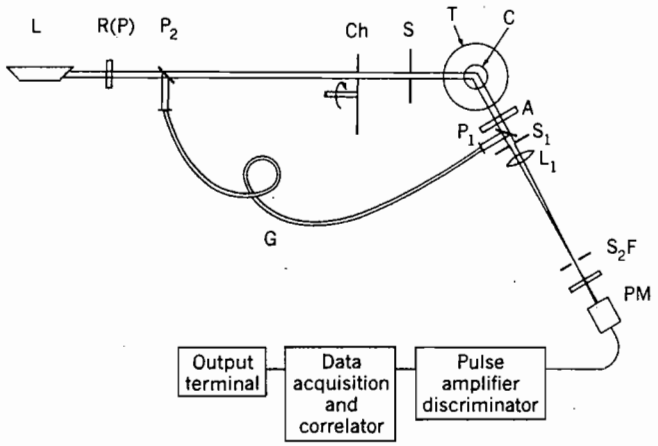

Fig. 11. Principal components of a light-scattering photometer; L, laser; R, half-wave plate (or P, polarizer); P_2, beam splitter; G, light guide; Ch, chopper; S, slit; T, thermostat; C, cell; A, analyzer; P_1, beam splitter; S_1, slit; L_1, lens; S_2, slit; F, monochromatic filter; and PM, photomultiplier.

A photometer to measure static or dynamic light scattering must be equipped with a laser light source. Other sources, eg, arc lamps, may be used if only the elastic scattering is to be studied, but the coherent properties of laser light are necessary for the quasielastic scattering experiment. Photon-count correlation methods are usually employed in dynamic light scattering studies.

Although basically similar, the optical requirements for elastic and quasi-elastic light scattering differ significantly. Therefore, the photometer should be equipped with interchangeable components if a single instrument is to be used for both. For elastic-scattering studies the effects of mechanical vibrations are

seldom serious, but in certain situations, vibrations may cause problems in studies of quasielastic scattering. In the latter case, vibrations are usually not a problem in fluid experiments using the self-beat mode, ie, no reference beam unless the fluid has a long viscoelastic time constant, but may result in periodic contributions to the measured $G^{(2)}(\tau)$ in experiments using a reference beam. Thus, it is desirable to arrange for pneumatic isolation of the optical components of the photometer when required.

The Incident Beam. For elastic scattering, it is necessary to compute $\mathbf{R}(q)$ from an instrument response, such as the average photon-count rate or an analogue signal. This requires consideration of a number of factors, ie, the scattering volume, the solid angle of acceptance of the scattered beam, effects attenuating the incident or scattered intensities, the incident intensity, and the means to convert the instrument response (suitably corrected for the preceding) to an absolute value of $\mathbf{R}(q)$. These needs are simplified by using a beam size larger than that of the usual continuous-wave laser source (ca 1 mm). For this reason, as shown in Figure 12, the beam from the laser, L, is expanded to a collimated beam using a suitable optical component E before entering the sample cell C. It is convenient to place a component D to allow direction of the laser beam to facilitate alignment of the incident beam. A beam stop S is used to define the height and width of the expanded beam, which is typically 5–10 mm high and 1–3 mm wide. Optical means to form a collimated beam with an arc lamp are discussed in Refs. 16 and 81. A laser with Brewster windows B is preferable since it provides for a plane polarized source. In this case, a half-wave retarder R in the incident beam may be used to rotate the plane of polarization. With an unpolarized source, a suitable polarizer P must be used, eg, a Nicol prism or equivalent. The chopper Ch shown in Figure 11, serves to modulate the beam at a convenient frequency to aid discrimination of the signal from the scattered beam.

For quasielastic scattering, it is not necessary to compute the absolute in-

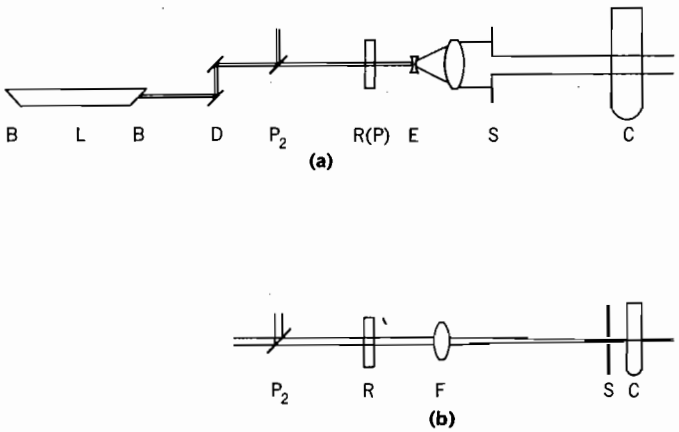

Fig. 12. Typical components of incident-beam optics for a light-scattering photometer. (**a**) Optical components for static scattering: B, Brewster window; L, laser; D, beam director; P_2, beam splitter; R, half-wave plate (or P, polarizer); E, beam expander; S, slit; and C, cell; (**b**) optical components for dynamic scattering: as in (**a**) for L, laser; P_2, beam splitter; R, half-wave plate; F, focus lens; S, slit; and C, cell.

tensity, but it is desirable to have a high energy density in the scattering volume. For this reason, the laser beam is either used directly, or is focused in the scattering volume with a large focal-length lens F with some compromise of the definition of q. A stop S is used to reduce stray light.

Detector Optics. The optical arrangements suitable for elastic or quasielastic scattering are shown in Figure 13 (16,81). In either case, a suitable analyzer A eg, a Nicol prism or a polaroid sheet, etc, may be placed as shown to select the polarization plane of the scattered light. Usually the optical axis of the detector is placed in the transverse scattering plane, ie, the plane containing the incident beam which is perpendicular to the polarization plane of vertically polarized incident light.

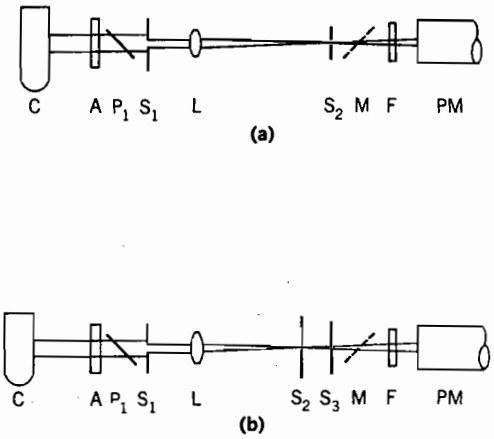

Fig. 13. Typical components of the detector optics for a light-scattering photometer. (**a**) C, cell; A, analyzer; P_1, beam splitter; S_1, slit; L, lens; S_2, slit at focal plane of L; M, retractable mirror; F, monochromatic filter; and PM, photomultiplier; (**b**) same optical components as in (**a**), with the addition of slit S_3.

With the arrangement in Figure 13a, the dimensions of the scattering volume perpendicular to the detector optic axis are set by S_1, and the angular resolution is fixed by S_2, which is placed at the focal plane of lens L in either arrangement shown. With the arrangement shown in Figure 13b, the same situation prevails if S_3 is large, but for small S_3 the dimensions of the scattering volume are set by S_2 and the angular resolution is controlled with S_3. With elastic scattering, the scattering volume is usually made as large as possible to meet the requirements that the vertical dimension of the scattering volume is less than the height of the volume illuminated in the cell, and that the width of the scattering volume is small enough to exclude reflections from the incident beam on the cell walls at the smallest scattering angle of interest. An angular resolution of ~1°C is usually acceptable for elastic scattering. When using quasielastic scattering, the coherence of the scattered rays must be high, lest the coherence factor $f(A)$ become so small that the signal-to-noise is too low. With the arrangement in Figure 13, for fixed S_1, the coherence may be adjusted by S_2, with $f(A)$ decreasing with increasing S_2. Values of $f(A)$ obtained as a function of the diameter D of pinhole S_2 are shown in Figure 14 for an apparatus in which L is a

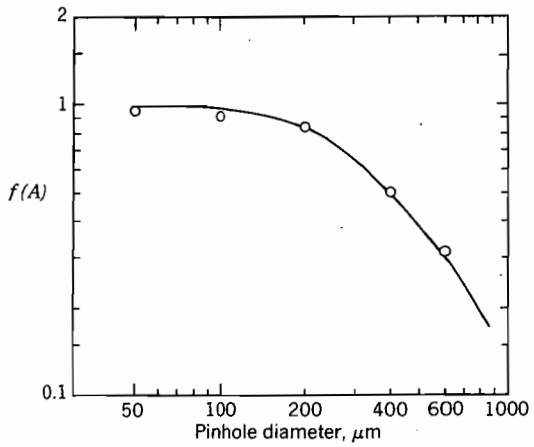

Fig. 14. Coherence factor $f(A)$ in equation 22 as a function of the pinhole diameter (eg, slit S_2 in Figure 13a). The curve represents a theoretical relation (43), and the points are from experimental data (47).

lens with a 25-cm focal length (47). The solid curve is based on a theoretical expression for $f(A)$ using a constant for A/D^2 chosen to obtain a best fit between experiment and theory (43). In typical experiments, S_1 is selected to place $f(A)$ in the range 0.2–0.5. This choice minimizes the time required to accumulate enough data to attain an acceptable signal-to-noise ratio. With the optical arrangements in Figure 13a, the value of $f(A)$ is only weakly dependent on S_1, with $f(A)$ decreasing with increasing S_1.

The detector optics are usually mounted on a goniometer, along with the photomultiplier. It is convenient to place a selective wavelength filter in front of the photomultiplier. For elastic or quasielastic scattering, this should be a bandpass interference filter selected to pass the wavelength of the incident light. To measure fluorescence, a band-reject interference filter may be selected to reject the incident beam but pass other wavelengths; an interference filter with bandpass wavelength graded along its length may serve as a crude monochrometer as the filter is translated across the detector optic axis. A retractable mirror or similar device permits inspection of the scattered beam.

In some cases it is desirable to mix a reference beam with the scattered beam in quasielastic experiments, eg, in electrophoretic light scattering. This is accomplished by placing an inclined thin glass plate P_1 on the optic axis of the scattered beam, as shown in Figure 13. A similar inclined plate P_2 may be placed in the incident beam to provide a reference beam. In order to avoid certain difficulties, this beam should be expanded, and a center portion of the expanded beam used as the reference beam. The latter may be directed to P_1 with mirrors or a coherent fiber-light guide.

The Sample Cell. Since the diffusion constant is inversely proportional to the solvent viscosity, and the latter depends markedly on temperature, it is necessary to thermostat the scattering cell. In addition, in some cases the thermodynamic and conformational properties of the solute may also depend on T, eg, for solutions with A_2 close to zero. This may conveniently be accomplished by immersing the scattering cell in a thermostat bath. The latter should have

flat entrance and exit windows to avoid undesirable focusing of the incident beam and should otherwise be cylindrical. The latter feature permits measurements at arbitrary angles and simplifies certain refraction corrections. In special experiments, eg, scattering angles below ca 10°C or in electrophoretic scattering, other arrangements are used. A low transmission filter placed in the thermostat bath between the cell and the exit window reduces the effects of back reflection at the glass–air interface; this amounts to ca 5% of the intensity of the incident beam. A curved low transmission filter, or blackened mask placed behind the cell aids in the attenuation of reflections, etc.

The light scattering cell is frequently a cylindrical tube suitable for centrifuging the sample before the scattering experiment in order to reduce extraneous matter, such as dust. Cells with a more complex shape are shown in Figure 15 (59). Because of their conical shape, these cells must be immersed in a liquid with a refractive index close to that of the solution (not the glass) in order to eliminate refraction effects. The conical shape serves to minimize reflections at the liquid–glass interface where the incident beam enters and leaves the cell; the bulb provides buoyancy, allowing the cell to float in a liquid during centrifugation using a swinging-bucket rotor. Design (**b**) in Figure 15 (appropriate for quasielastic scattering) typically requires 0.5 mL of fluid. The small diameter of this cell serves to suppress convection currents which may distort $G^{(2)}(q,\tau)$. Design (**a**) may be used for elastic or quasielastic experiments and typically requires 7–10 mL of sample.

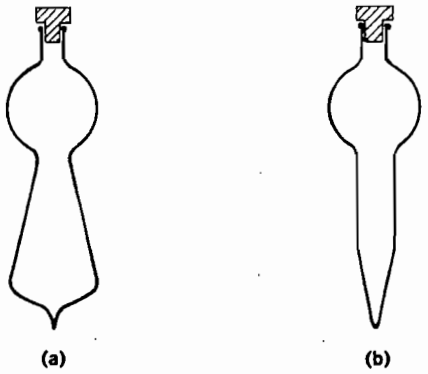

Fig. 15. Light-scattering cells suitable for swinging-bucket centrifuge to aid clarification. The scattered rays are collected from the conical parts of the cell to be immersed in a cylindrical cell in a liquid with a refractive index matching that of the solution. (**a**) Cells for static scattering; (**b**) cells for dynamic scattering (59).

For experiments confined to small angles, a slablike geometry is preferred with the sample confined as a slab between two thick flat windows. Refraction of the scattered beam at the sample–glass interface and the glass–air interface makes the scattering angle (θ_s) in the sample differ from the angle (θ_a) between the detector axis and the incident beam direction:

$$n_s \sin \theta_s = \sin \theta_a \qquad (334)$$

where n_s is the refractive index of the sample. In addition, the scattered beam is displaced a distance Δ perpendicular to the incident beam:

$$\Delta = t \times \tan\left(\arcsin\frac{\sin\theta_a}{n_g}\right) \tag{335}$$

where n_g is the refractive index of the glass plate and t, its thickness. This displacement helps to discriminate between the scattered ray and stray light coming from the incident beam as it exits the cell. In this arrangement, the center of the cell is displaced along the incident beam from the center of rotation of the detector. In one application of this geometry, the scattered light is collected around the solid cone rather than solely in the transverse plane.

Electrophoretic light scattering cells are specially designed to handle the problems of resistive-heating, the need for a well-defined potential field, bubble formation at the electrodes caused by electrolysis of the solvent, and secondary flows produced by ion transport near the cell surface in ion-containing samples (24,26,82). These problems are considerably reduced in studies of weakly charged particles dispersed in organic solvents. The sample cell shown in Figure 16 may be used with such systems. The central part of the cell may be conveniently formed with commercially available rectangular tubing. The sintered glass frits are not necessary if electrolysis is absent. The cell should be immersed in a large rectangular cell containing fluid with a refractive index close to that of glass to

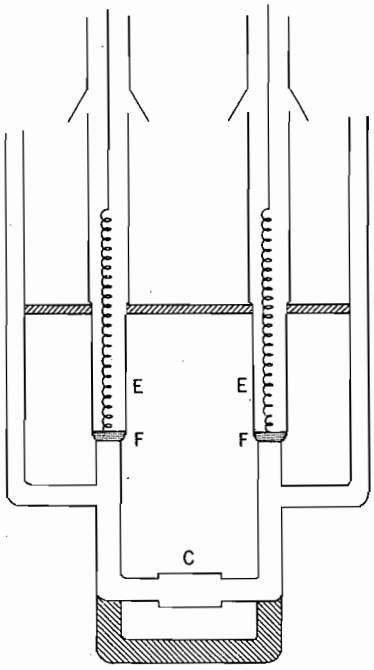

Fig. 16. A cell suitable for electrophoretic scattering in nonaqueous solutions: C, a thin rectangular tube section connected to frits F by narrow tubing, with electrodes E above the frits.

aid heat transfer and minimize surface reflections, which in some cases, may be used as a reference beam.

Signal Detection. Photon-counting methods are amenable to both elastic and quasielastic scattering studies. Analogue methods suitable for elastic scattering are discussed in Refs. 2, 14, and 16. Photon-counting methods place more severe restrictions on the choice of the photomultiplier tube than are necessary with analogue methods; in addition, costs may be higher. The photomultiplier should deliver a single pulse (ca 20–50 ns wide) for each photon event at the cathode and have a low thermal emission and high cathode sensitivity at the wavelength of the incident beam. Cooling lowers thermal emission, but is usually not required. A small cathode area and a magnetic shielding for the tube are useful. The power supply should be stable and supply voltage E selected to maximize the signal-to-noise for typical use conditions. For a given light intensity, the count rate tends to reach a plateau as E is increased above a threshold characteristic of the tube. Increase of E beyond this range results in enhanced thermionic emission and is to be avoided. The photomultiplier output should be processed by a pulse amplifier–discriminator to deliver a shaped, 20–50 ns pulse to a suitable data acquisition system (DAS) (2,14).

The DAS output could be estimates $\tilde{G}^{(2)}(\tau)$ and $\tilde{N}^{(r)}(\Delta\tau)$ (for $r = 1,2$, etc) of $G^{(2)}(\tau)$ and $N^{(r)}(\Delta\tau)$, respectively, computed as

$$\tilde{G}^{(2)}(k\,\Delta\tau) = \frac{1}{M}\sum_{j=1}^{M}\tilde{G}_j^{(2)}(k\Delta\tau) \tag{336}$$

$$\tilde{G}_j^{(2)}(k\Delta\tau) = \left(\frac{1}{T}\sum_{i=1}^{T} n_i n_{i+k}\right)_j \tag{337}$$

$$\tilde{N}^{(r)}(\Delta\tau) = \frac{1}{MT}\sum_{i=1}^{TM}[n(n-1)\cdots(n+r+1)]_i \tag{338}$$

for an experiment with sampling intervals of duration $\Delta\tau$, where $\tau = k\Delta\tau$, in which $\tilde{G}_j^{(2)}(k\Delta\tau)$ is computed for a subset of T such intervals, with $\tilde{G}_j^{(2)}(k\Delta\tau)$ for M such subsets being averaged to give $\tilde{G}^{(2)}(k\Delta\tau)$. In some arrangements $M = 1$, whereas in others $M > 1$. An estimate $\tilde{p}_1(n,\Delta\tau)$ of the photon-count distribution $p_1(n,\Delta\tau)$ may also be made available as the number of intervals for which exact n photon counts occurred, divided by MT. In order to compute these quantities, it is necessary that the DAS be able to accept and utilize the largest value of n appearing in $\tilde{p}_1(n)$. For experiments with a reference beam such a value may be large. Examples of $\tilde{p}_1(n,\Delta\tau)$ obtained for several values of $\Delta\tau$ (recorded as $q^2D_M\Delta\tau$) are given in Figure 17 (47). The solid curves in Figure 17 are calculated with the semiempirical relation (83)

$$\tilde{p}_1(n\Delta\tau) = \frac{\Gamma(n+s)}{N!\Gamma(s)}\left(1+\frac{s}{\langle n\rangle}\right)^{-n}\left(1+\frac{\langle n\rangle}{s}\right)^{-s} \tag{339}$$

$$s = \left[\frac{\tilde{N}^{(2)}(\Delta\tau)-1}{\langle n\rangle^2}\right]^{-1} \tag{340}$$

where $\langle n\rangle = \tilde{N}^{(1)}(\Delta\tau)$. As shown in Figure 17, n may be rather large, for large $\Delta\tau$, even without a reference beam. Consequently, calculation of $N^{(2)}(\Delta\tau)$, etc, requires the ability to handle large n.

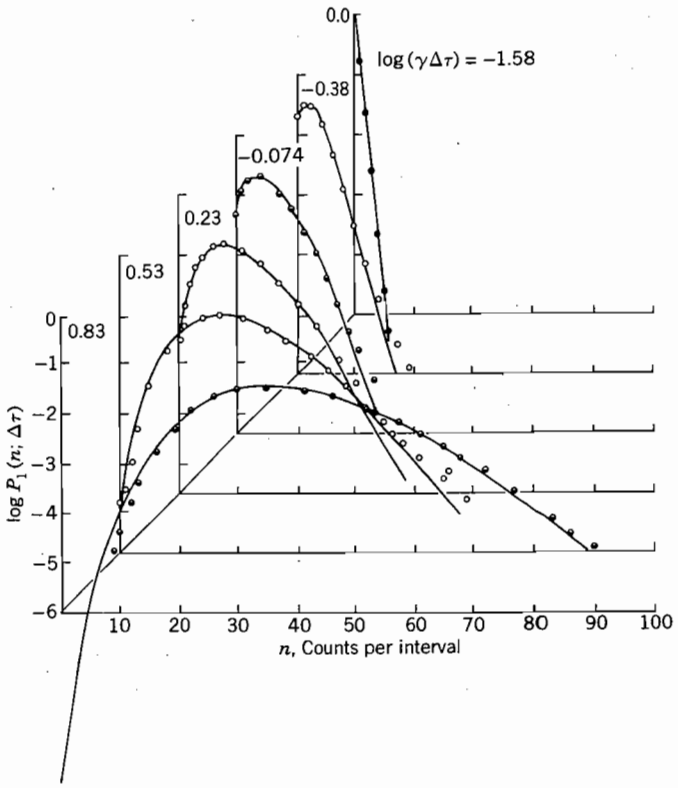

Fig. 17. Photon-count distribution $\tilde{p}_1(n;\Delta\tau)$ determined for several values of $\gamma\Delta\tau$, curves are computed with equation 339, and the points are from a polystyrene-solution experiment; n is the number of photon counts, $\Delta\tau$, the sample interval, and γ, an inverse coherence time (eq. 135) (47).

The estimator $\tilde{g}^{(2)}(\tau) = \tilde{G}^{(2)}(\tau)/\tilde{G}^{(2)}(\infty)$ for the normalized correlation function $\tilde{g}^{(2)}(q,\tau;\Delta\tau,A)$ requires an estimate $\tilde{G}^{(2)}(q,\infty;\Delta\tau,A)$ of the limiting value of $G^{(2)}(q,\tau;\Delta\tau,A)$ for large τ. Possible estimates (for a given $\Delta\tau$) include

$$\tilde{G}^{(2)}(q,\infty;\Delta\tau,A) = [\tilde{N}^{(1)}(q,\Delta\tau;A)]^2 \tag{341}$$

$$\tilde{G}^{(2)}(q,\infty;\Delta\tau,A) = \frac{1}{M}\sum_{j=1}^{M} [\tilde{N}_j^{(1)}(q,\Delta\tau;A)]^2 \tag{342}$$

$$\tilde{G}^{(2)}(q,\infty;\Delta\tau,A) = \lim_{k=\infty} \tilde{G}^{(2)}(q,k\Delta\tau;\Delta\tau,A) \tag{343}$$

For an idealized set of data, these would all be equal if the total number of counts $MT\tilde{N}^{(1)}$ is large, eg, $MT\tilde{N}^{(1)} > 10^6$. Slow variations in the count statistics during the data accumulation period result in differences among these estimators for $\tilde{G}^{(2)}(q,\infty;\Delta\tau,A)$.

If $\langle n\rangle$ is small, contributions from the thermionic emission may distort $\tilde{g}^{(2)}(\tau)$ and $\tilde{n}^{(2)}(\Delta\tau) = \tilde{N}^{(2)}/[\tilde{N}^{(1)}]^2$. Thus, if $\underline{\epsilon}$ is the fraction of the total counts arising from thermionic emission (47),

$$\tilde{n}^{(2)}(\Delta\tau) - 1 = [n^{(2)}(\Delta\tau) - 1](1 - \underline{\epsilon})^2 + [n_d^{(2)}(\Delta\tau) - 1]\underline{\epsilon}^2 \tag{344}$$

$$\tilde{g}^{(2)}(\tau) - 1 = [g^{(2)}(\tau) - 1](1 - \underline{\epsilon})^2 + [g_d^{(2)}(\tau) - 1]\underline{\epsilon}^2 \quad (345)$$

where $n_d^{(2)}$ and $g_d^{(2)}$ are properties of the thermionic emission count statistics. Usually, $n_d^{(2)} \approx g_d^{(2)} \approx 1$ in the experimental time range of interest, and therefore their effect does not introduce any error in the properties calculated from $\tilde{n}^{(2)}(\Delta\tau)$ and $\tilde{g}^{(2)}(\tau)$. Another source of error is introduced by the truncation of $\tilde{p}_1(n,\Delta\tau)$ by the digital nature of the experiment. Thus, if m is the largest value of n represented in $\tilde{p}_1(n,\Delta\tau)$ (ie, $TM\ \langle n\rangle\ p_1(m + 1,\Delta\tau) < 1$), then (47)

$$\tilde{N}^{(S)}(\Delta\tau) = \sum_{n=s}^{m} \frac{n!}{(n-s)!}\,\tilde{p}_1(n\Delta\tau) \quad (346)$$

Using equation 339 for $\tilde{p}_1(n,\Delta\tau)$ demonstrates that $m \approx \ln(TM\ \langle n\rangle)/\ln\langle n\rangle^{-1}$ for small $\langle n\rangle$. Consequently, m may be increased, and the error made negligible by increase of the total number of counts $TM\langle n\rangle$.

The total count rate $\langle n\rangle_T$ comprises several contributions, principally $\langle n\rangle_{SC}$ for the scattered light intensity, $\langle n\rangle_F$ from any fluorescence from the solution that reaches the photomultiplier, $\langle n\rangle_D$ from the thermionic emission, $\langle n\rangle_R$ from light reflected from the incident beam, and $\langle n\rangle_r$ from reflected light from any other light source. This total count rate is given by $N^{(1)} = \langle n\rangle_T$. (Here and in the following, the notation used above is suppressed to indicate an estimate for the true value.) If the incident beam is modulated with a period P, eg, using a rotary chopper exposing the scattering cell alternately to the beam for duration P/2, followed by no beam for duration P/2), then $G^{(2)}(\tau)$ appears as a triangular wave with period P and peak-to-peak amplitude $(\frac{1}{2})\langle n\rangle_C^2$, where $\langle n\rangle_C$ is the count rate for all sources modulated at period P. Usually $\langle n\rangle_C = \langle n\rangle_{SC} + \langle n\rangle_F + \langle n\rangle_R$ with $\langle n\rangle_C$ being free of contributions from $\langle n\rangle_D$ and $\langle n\rangle_r$. The slope $\partial G^{(2)}(\tau)/\partial\tau = \langle n\rangle_C^2/2P$ provides a means to compute $\langle n\rangle_C$ free from the effects of distortions at the extreme of $G^{(2)}(\tau)$, which may be caused by imperfections in the chopper edges, etc. The ratio $\langle n\rangle_C/\langle n\rangle_{REF}$ with $\langle n\rangle_{REF}$ proportional to the incident-beam intensity may be determined directly from $G^{(2)}(\tau)$ using a suitable rotary chopper design and a reference beam brought to the detector in the manner described above for quasi-elastic scattering with a reference beam. In this case, the chopper is equipped with ports to pass the incident beam to the scattering cell (duration P_C), to block the beam (duration $P_D \approx P_C$), to reflect the beam with a mirror to a mirror or light guide to inclined plate P_1 in the detector optic axis (duration $P_r \approx P_C/6$), and to block the beam (duration P_D). In this arrangement $G^{(2)}(\tau)$ is a waveform with slopes $S_1 = \partial G_2(\tau)/\partial\tau$ for $0 < \tau < P_R$ and $S_2 = \partial G_2(\tau)/\partial\rho$ for $P_R < \tau < P_S$, which may be used to compute $\langle n\rangle_C/\langle n\rangle_{REF} = [S_2/(S_1 - S_2)]^{1/2}$.

Intensity Calibration. In order to determine the absolute molecular weight from the elastic scattering, it is necessary to compute the Rayleigh ratio **R** from the count rate $\langle n\rangle_{SC}$ from the scattering. By contrast, other parameters, such as R_G, A_2, b, etc, may be determined without an absolute value for **R**. Several factors must be considered to compute **R** from the observed count rate, eg, from $\langle n\rangle_C$ (16,84): 1, the contribution of the solvent (**R** is defined as the excess scattering caused by solute); 2, the scattering volume; 3, the effects of refraction; 4, attenuation of the incident and scattered intensities; 5, fluorescence contributions, ie, $\langle n\rangle_F$; 6, and a calibration constant giving the proportionality between **R** and the count rate (or other instrument response) corrected for the preceding effects.

In terms of the count rate $\langle n(q)\rangle_C$ defined above, (and for $\langle n\rangle_R = 0$) these effects can be expressed by the relation

$$\mathbf{R}(q) = k\,\langle n(q)\rangle_{corr}/\langle n\rangle_{inc} \tag{347}$$

$$\langle n(q)\rangle_{corr} = C_n f_V(\theta)(\{f_A(\theta)[\langle n(q)\rangle_C - \langle n(q)\rangle_F]\}_{soln} - \{f_A(\theta)[\langle n(q)\rangle_C - \langle n(q)\rangle_F]\}_{solv}) \tag{348}$$

Here, $\langle n\rangle_{inc}$ is the count rate for the incident beam, and the subscripts designate solution and solvent, respectively, with the subtraction accounting for the first factor listed above. The parameters $f_V(\theta)$, C_n, $f_A(\theta)$, $\langle n(q)\rangle_F$, and k refer to factors 2, 3, 4, 5, and 6, respectively.

In the preceding, $\mathbf{R}_{V_v}(q)$ is defined in terms of the polarized scattering determined with plane-polarized incident light. If, instead, $\mathbf{R}_{V_v}(q)$ is defined in terms of unpolarized or natural incident light, eg, as would be obtained with an arc lamp, then $\langle n\rangle_{inc}$ or I_{inc} is increased twofold and K' in equation 26 must be replaced by $K'_U = K'/2$. Furthermore, if no analyzer is used and $R_{Uu}(q) = R_{Vu}(q) + R_{Hu}(q)$ is measured, K'_U must be multiplied by $(1 + \cos^2\theta)$.

It is convenient to include the scattering volume V_{90} for $\theta = 90°C$ in k, and to define $f_V(\theta)$ as the function

$$f_V(\theta) = (V_{90}/V_\theta) \tag{349}$$

where V_θ is the volume at scattering angle θ. With most instruments $f_V(\theta)/\sin\theta$ is within a few percent of unity at all useful angles. Since fluorescence emission is independent of θ, a convenient means to measure $f_V(\theta)$ is to determine the fluorescence from a dilute solution of a fluorphor using a filter (F) in the detector to reject completely any contributions to $\langle n(q)\rangle_C$ at the incident wavelength, eg, $\langle n\rangle_R$ in the preceding. For example, a dilute solution of fluoroscein may be excited by blue light (eg, the 480 nm line of an argon-ion laser, or the 436 nm line of a mercury arc) to give fluorescence at longer wavelengths. Light with the wavelength of the incident beam may be easily removed with a yellow optical cutoff filter.

The factor C_n accounts for refraction at the glass–air interface, which alters the scattered volume and the solid angle of the cone of acceptance of the scattered beam. In general, this factor is a complex function of θ, but for a cylindrical glass–air interface and for detector optics adjusted in such a way that the field of view lies completely within the height and width of the volume illuminated by the incident beam, $C_n = \tilde{n}^2$. This is one reason for the use of an expanded beam for elastic-scattering measurements.

The count rate $\langle n\rangle_F$ from fluorescence from the solution (or solvent) may be minimized by inserting a band-pass filter for the wavelength λ_0 of the incident beam in the detector optics, eg, filters F in Figure 13. However, if the fluorescence is strong, this may not make $\langle n\rangle_F$ negligible, especially for studies of $\mathbf{R}_{Hv}$. In such cases, it is useful to measure $\langle n\rangle$ over a range of $\lambda > \lambda_0$ to give $\langle n\rangle_F$ as a function of λ that may be extrapolated to give $\langle n\rangle_F$ at $\lambda = \lambda_0$ for use in computing $\langle n\rangle_{corr}$; this procedure is best done with Hv polarization to minimize the contribution of the elastic scattering to $\langle n\rangle$ for λ near λ_0.

The factor $f_A(\theta)$, which accounts for attenuation of the incident and scattered rays, may depend on θ if the attenuation is strong enough, but usually under

such conditions additional effects invalidate the relations given above (16). However, if λ_0 is not near the wavelength for a maximum extinction coefficient μ_A for absorption, the relations given above are valid and the attenuation is small enough that $f_A(\theta)$ is a constant f_A, independent of θ, except for possible variation of the path length ℓ_θ with scattering angle due to the design of the scattering cell:

$$\ln f_A = -\ell_\theta(\mu_A + \tau_S) \tag{350}$$

where τ_S is the turbidity caused by scattering; for cells with cylindrical symmetry, ℓ = the cell diameter D. For small isotropic scatterers, eg, $qR_G \ll 1$, the latter is given by

$$\tau_S = (16\pi/3)\mathbf{R}_{90} \approx (16\pi/3)k\langle n\rangle_{90} \tag{351}$$

where $\mathbf{R}_{90}$ is the value of $\mathbf{R}$ for $\theta = 90°$C. Since τ_S is usually small, equation 351 serves as a useful approximation for τ_S even if qR_G is not small enough to neglect the effects of intramolecular interference on $\mathbf{R}(q)$. An estimate of ℓ_θ is conveniently made by comparison of $\langle n(q)\rangle$ for a polymer solution with $\mu_A = 0$ to that for the same solution containing a low concentration of a (small molecule) dye, selected to give μ_A and, if possible, an extinction band similar to that for the polymer solution to be studied. The ratio of $\langle n(q)\rangle$ for the solutions with and without the dye may be used to compute ℓ_θ provided μ_A is low enough so that geometric effects, other than that in equation 350, are unimportant in $f_A(\theta)$.

Methods available for determination of the calibration constant k include (16) the use of the instrument geometry to calculate k; measurement of $(\langle n\rangle_{90})_{SP}/\langle n\rangle_{inc}$ for the scattering $(\langle n\rangle_{90})_{SP}$ in the transverse plane at 90°C from internal reflections from an integrating sphere (eg, a hollow sphere with a MgO surface) to permit experimental determination of k; and measurement of the reduced count rate $\langle n(q)\rangle_{STD}/\langle n\rangle_{inc}$ for a standard scatterer with known Rayleigh ratio $\mathbf{R}_{STD}(q)$, permitting k to be calculated as

$$k = \frac{\mathbf{R}_{STD}(q)}{[\langle n(q)\rangle_{STD}]_{corr}/\langle n\rangle_{inc}} \tag{352}$$

Although possible in principle and practice, the first two methods are rarely used to determine k. Rather a variety of standards are employed to establish k by the third method, including the use of a substance for which $\mathbf{R}(q)$ is reported in the literature, usually $\mathbf{R}_{90}$ for $\theta = 90°$C (eg, pure solvent or a standard polymer solution for which $\mathbf{R}_{90}$ has been measured on an instrument calibrated by some independent method); a colloidal suspension of small isotropic spheres, for which $\mathbf{R}_{90}$ may be determined by separate photometric transmission experiments of the turbidity (eq. 351); and solutions of a polymer with accurately known $\overline{M}_w$ and $(\partial\tilde{n}/\partial c)_w$, permitting k to be calculated as

$$k = K' n_s^2 \left(\frac{\partial \tilde{n}}{\partial c}\right)^2 \overline{M}_w \langle n\rangle_{inc} [c/\langle n(0)\rangle_{corr}]^0 \tag{353}$$

where $[c/\langle n(0)\rangle_{corr}]^0$ is obtained by extrapolation of $[c/\langle n(q)\rangle_{corr}]$ to infinite dilution and $q = 0$.

A combination of these methods best establishes k since each method has

its advantages and limitations. For example, whereas $\mathbf{R}_{90}$ may be well established for a pure liquid, fluorescent impurities in the sample used to determine k may result in error, and the weak scattering from the pure liquid makes measurement of k less precise than desired. With colloidal suspensions, chromophoric impurities may vitiate determination of τ_S, and aggregation of the spheres may cause the assumed proportionality between τ_S and $\langle n\rangle_{\text{corr}}$ to be in error. Use of a polymer solution may lead to an imprecise estimate for $[c/\langle n(0)\rangle_{\text{corr}}]^0$ unless A_2 is small or zero, and the accuracy in k is limited by the accuracy by which $\overline{M}_w$ and $(\partial\tilde{n}/\partial c)_w$ are known. The former may be well established using polymers prepared by methods, eg, anionic polymerization, with $\overline{M}_n$ determined by osmometry and $\overline{M}_w/\overline{M}_n$ by fractionation methods.

In practice, a secondary standard for which the reduced count rate $\langle n\rangle_{\text{sec}}/\langle n\rangle_{\text{inc}} = k_{\text{sec}}$ is known at the experimental conditions is used on a routine basis to avoid direct determination of $\langle n\rangle_{\text{inc}}$. In this case,

$$\mathbf{R} = kk_{\text{sec}}\langle n\rangle_{\text{corr}}/\langle n\rangle_{\text{sec}} \tag{354}$$

Since $\langle n\rangle_{\text{inc}}$ does not appear in this expression, it is evident that measurement of $\langle n\rangle_{\text{corr}}/\langle n\rangle_{\text{sec}}$ for systems with known $\mathbf{R}$ to establish kk_{sec} serves as an alternative to the measurement of $\langle n\rangle_{\text{corr}}/\langle n\rangle_{\text{inc}}$ to establish k. Secondary standards frequently include scattering at 90°C from a polymer solution, a pure liquid, eg, benzene), or a turbid glass block, or the scattering of 0°C from an opalescent glass.

The last two methods are not well suited for use with a laser source since the coherent light results in variations of the scattered light unless the scattering blocks are placed in precisely the same position for each measurement. (This variability is caused by the long coherence lengths characteristic of such materials.) The scattering from a pure liquid is frequently used as a secondary standard, but may have the disadvantage that $\langle n\rangle_{\text{sec}}$ is smaller than $\langle n(q)\rangle$ obtained with the sample, causing undesirable inaccuracy in $\langle n(q)\rangle/\langle n\rangle_{\text{sec}}$. The scattering from a polymer solution may be made large enough to circumvent the latter difficulty, and may serve well as a secondary standard if polymer and solvent are stable and well sealed to avoid change in the concentration. The latter may also be advantageous in that kk_{sec} may depend only weakly on λ_0 and the temperature.

Other Procedures. The alignment of the polarizer and analyzer (Figs. 12 and 13) must be precise, especially for measurement of $\mathbf{R}_{Hv}(q)$. This alignment can also be achieved by using the property that $\mathbf{R}_{Hv}(q) = \mathbf{R}_{Vh}(q)$ is negligible for a solution of a flexible chain polymer [eg, polystyrene, poly(vinyl acetate), etc], and that $\mathbf{R}_{Hh}(q) \approx \mathbf{R}_{Vh}(q)$ for the scattering at 90°C. The orientation of the polarizer may be set in the horizontal plane by adjustment to give a minimum count rate for the scattering from such a solution, either with or without an analyzer. With this orientation established, the polarizer may be set to give vertically polarized light, and the horizontal orientation of the analyzer may be adjusted to give a minimum count rate, corresponding to $\mathbf{R}_{Hv}(q)$. Since multiple scattering may result in increased $\mathbf{R}_{Hv}(q)$, a dilute solution should be used for this alignment procedure.

The use of fluorescence to establish $f_V(\theta)$ and $f_A(\theta)$ was discussed previously. Fluorescence may also be used to evaluate instrument performance in quasielastic scattering. For the time scale of usual interest in quasielastic scattering (eg,

$\tau > 100$ ns), the correlation function $G^{(2)}(q,\tau)$ should equal $G^{(2)}(q,\infty)$ for all τ, unless the concentration of the fluorophor is so low that the number of fluorophors in the scattering volume varies appreciably. Deviations from this behavior may reveal laser instability, periodic electronic disturbance, or other difficulties.

With samples that absorb light, the use of the unexpanded or focused laser beam may cause heating of the sample in the beam. This results in a radial temperature gradient, which results in a radial refractive-index gradient, which, in turn, results in a radial refractive-index gradient. In this case, the transmitted incident beam is transformed into a series of concentric rings (or related image distorted by the optics of the cell and thermostat), the diameters of which are related to the temperature rise. Thus, the ring diameters decrease as the energy of the laser beam is reduced, and an observable time is required to establish the pattern after illumination of the dark, thermally equilibrated sample. The heating may also result in a sinusoidal oscillation of $G^{(2)}(q,\tau)$, with a period related to the temperature rise. Heating effects of this sort are undesirable and should be avoided by changing the experimental conditions.

Sample Preparation

Solvent. Solvent purity is important. Impure solvents may contain fluorescent species that compromise measurement of the scattering; (this is especially true of $\mathbf{R}_{Hv}(q)$, which is generally small). Solvent impurities may affect the thermodynamic properties of the solutions, eg, absorbed water appreciably alters the properties of polystyrene in cyclohexane, especially for conditions with $A_2 = 0$. Solvent impurities may enhance degradation of the solvent or the solute, leading to irreproducible and erroneous results, and the impurities may be colloidal in nature, resulting in undesirably high and θ-dependent solvent scattering. Freshly purified solvents must be used and solvent scattering frequently checked.

Solute. For determination of $\overline{M}_w$ and A_2, the concentration c (weight per volume) must be known. Thus, if for no other reason, the solute must be rigorously free of entrained or adsorbed components. In addition, any such components may also affect the thermodynamic properties of the solution. In some cases, it is difficult to determine c accurately. For example, it may not be possible to completely remove water from a hydrated polymer under conditions that do not degrade the polymer. If studied in aqueous solution, the water of hydration would have no consequence except to cause an erroneous estimate for c determined by gravimetric analysis, and consequently erroneous estimates of $\overline{M}_w$ and A_2. In such cases, measurement of the optical density may provide an alternative means to measure c if the extinction coefficient is known.

Solution Dialysis. With mixed solvents, it is desirable to carry out measurements of $\mathbf{R}(q)$ and $(\partial\tilde{n}/\partial c)_\mu$ with solutions brought to osmotic equilibrium with the solvent mixtures. A simple arrangement to prepare such a dialyzed solution is shown in Figure 18. The dialysis should be carried out until the solvent composition in the solution reaches equilibrium. In practice, it is satisfactory to prepare dilutions of the dialyzed solution by addition of the mixed solvent; ideally, each solution is dialyzed separately.

Clarification of Solutions. The preparation of a solution free from extraneous scattering sources is among the most important, and at times frustrating,

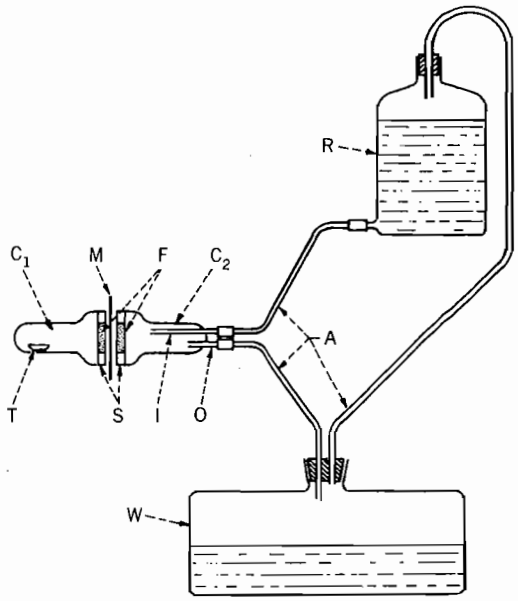

Fig. 18. Schematic drawing of an apparatus to dialyze a solution against a mixed solvent: C_1 is the solution chamber; C_2, solvent chamber; M, dialysis membrane; F, supporting frits; S, ground glass surface; T, magnetic stirring bar; I, solvent inlet; O, solvent outlet; A, Teflon tubing; R, fresh solvent reservoir; and W, solvent waste (85).

procedures in light-scattering work. Extraneous matter originates in several ways, particularly from incompletely dissolved solute (occurs especially with a crystalline solute), and colloidally dispersed particles with a composition different from that of the solute. In some cases, incompletely dissolved solute may be reduced or eliminated by changing the dissolution temperature, usually by increasing T, and by subjecting the solution to weak ultrasonic vibration.

Centrifugation or filtration, or both, are applied to reduce the concentration of extraneous matter to an acceptable range, eg, where an extraneous particle is rarely to be found in the scattering volume. For centrifugation to be effective, the centrifugal field must be large enough to cause sedimentation (or flotation) of the extraneous matter without causing appreciable concentration gradient in the solution. In some cases, the solution is centrifuged in the scattering cell (similar to the cells shown in Fig. 15), whereas in other situations, an aliquot of the centrifuged sample must be transferred to the light scattering cell. In either case, the light scattering cell is rinsed thoroughly with well-filtered solvent, or with the condensing vapors from a still. If the solution is centrifuged in the cell, remixing of the removed component must be prevented. In some cases, the sedimented material is trapped by a special cell design.

Frequently, filtration through a porous membrane (0.1–0.5 μm pore size) is more effective than centrifugation in reducing the concentration of extraneous matter, particularly if the entire contents of the scattering cell may be purged several times with filtered solution. Difficulties encountered in filtration include possible change in the solution concentration caused by adsorption of the solute on the membrane or evaporation of the solvent; the need to hold the temperature

in a range for complete miscibility if near a condition for a phase segregation (ie, a condition for which $A_2 < 0$); degradation of the polymer molecular weight by mechanical rupture; clogging of the filter by a microgel fraction in the solute; and degradation of the filter in the solution. The first difficulty is rarely a problem, but it indicates that filtration should be aided by positive pressure above the filter rather than a vacuum below the filter. Mechanical degradation of the polymer molecular weight is rarely a problem with flexible chain polymers unless $\overline{M}_w > 10^7$. Clogging of a membrane filter by microgel components may be reduced by placing a coarse glass fiber mat on top of the membrane filter. Since porous membranes are available from a variety of materials, it is usually possible to select a membrane that is stable in the light scattering solution; care should be exercised to ensure stability of any backing material, etc, as well as the membrane itself.

Data Manipulation

Static Scattering. For dilute solutions, the basic relations used to determine $\overline{M}_w$, R_G, and A_2 for isotropic scatterers are given by equations 61 and 194. Following these relations, plots of $Kc/\mathbf{R}(q)$ vs q^2 for each c are extrapolated to $Kc/\mathbf{R}(0)$ for $q = 0$, with initial tangent

$$\lim_{q=0} \frac{\partial Kc/\mathbf{R}(q)}{\partial q^2} = \frac{1}{3}S(c) \tag{355}$$

with $R_{G,X}^2/\overline{M}_w = S(0)$. Moreover, if equation 245 is valid with $Q(q) = 1$, $S(c)$ is independent of c and the curves $Kc/\mathbf{R}(q)$ vs q^2 at each c should be parallel to each other. If they are not parallel, $R_{G,X}^2/\overline{M}_w$ should be calculated by extrapolation $S(c)$ to infinite dilution. A plot of $Kc/\mathbf{R}(0)$ vs c can be extrapolated to $\overline{M}_w^{-1}$ for $c = 0$ (for isotropic scatterers), with initial tangent

$$\lim_{c=0} \frac{\partial Kc/\mathbf{R}(0)}{\partial c} = 2A_2^{(R)} \tag{356}$$

A double extrapolation of $Kc/\mathbf{R}(q)$ vs $k_1c + k_2q^2$ is sometimes used (a so-called Zimm plot) to give curves parametric in c and q, with k_1 and k_2 selected to optimize the display. If equation 245 is valid with $Q(q) = 1$, the curves parametric in c should be parallel, as should those parametric in q.

For monodisperse flexible chain polymers, $P^{1/2}(q)$ is more nearly linear in q^2 than is $P(q)$. In this case, a plot of $[Kc/\mathbf{R}(q)]^{1/2}$ vs q^2 for each c is extrapolated to $[Kc/\mathbf{R}(0)]^{1/2}$, with initial tangent (16)

$$\lim_{q=0} \frac{\partial [Kc/\mathbf{R}(q)]^{1/2}}{\partial q^2} = \frac{1}{6} \frac{R_{G,X}^2}{\overline{M}_w^{1/2}(1 + A_2Mc + \cdots)} \tag{357}$$

Thus, the plots at different c are not parallel in this case, and extrapolation to $c = 0$ is necessary to determine $R_{G,X}^2$. Similarly, for rodlike chains long enough that $qR_G > 1$ for the experiment q-range, $P(q)$ is more nearly linear in q than in q^2 for large q. In this case, plots of $Kc/\mathbf{R}(q)$ vs q for each c have tangent $1/\pi M_L$ for a monodisperse solute. Plots of $Kc/\mathbf{R}(0)$ vs c may exhibit considerable curvature if c is large. According to equation 95, a plot of $[Kc/\mathbf{R}(0)]^{1/2}$ vs c should be

more nearly linear, with intercept $\overline{M}_w^{-1/2}$ *for* $c = 0$ and initial tangent $A_2^{(R)}\overline{M}_w^{1/2}$. These examples illustrate the need to use judgment and care in the methods used to analyze experimental data. A double extrapolation of $[Kc/\mathbf{R}(q)]^{1/2}$ vs $k, c + K_2q^2$ is not recommended as the parametric curves are not expected to be parallel.

With samples containing small fractions of large supramolecular structure (eg, microgels or aggregates), or other large extraneous matter, $\mathbf{R}(q)$ may frequently be represented as

$$\mathbf{R}(q) = \mathbf{R}_1(q) + \mathbf{R}_2(q) \tag{358}$$

where $\mathbf{R}_1(q)$ and $\mathbf{R}_2(q)$ arise from the large structures and the molecularly dispersed solute, respectively. Thus, owing to the effects of intramolecular interference, for small q, $\mathbf{R}_1(q) > \mathbf{R}_2(q)$, but for large q, $\mathbf{R}_2(q) > \mathbf{R}_1(q)$. The effect is to give plots of $Kc/\mathbf{R}(q)$ vs q^2 that decrease markedly with decreasing q for q below some value q^* related to the size of the large structure. In such cases, analysis of the data at small q may yield $\overline{M}_w$ *and* $R_{G,X}^2$ for the composite (if the extrapolations can be carried out reliably), but not provide information on the fully dissolved solute. If $\mathbf{R}_1(q) \ll \mathbf{R}_2(q)$ for $q > q^*$, analysis of the data for $q > q^*$ by equations 61 and 194, with neglect of the data for $q < q^*$, may yield $R_{G,X}^2$ and $\overline{M}_w(1 - w_1)$ for the dissolved solute, where w_1 is the weight fraction of the large species. Frequently, w_1 is close to zero, even though $\mathbf{R}_1(q) > \mathbf{R}_2(q)$ for small q.

General procedures to apply in the analysis of data on concentrated solutions are not well established. With solutions of flexible chain polymers, plots of $Kc/\mathbf{R}(q)$ vs q^2 frequently begin to depart from parallelism as c increases to the range for $[\eta]c > 1$, but the change is slow, and plots of $Kc/\mathbf{R}(q)$ or $[Kc/\mathbf{R}(q)]^{1/2}$ vs q^2 parametric in c are useful in evaluating $Kc/\mathbf{R}(0)$ and the correlation length b (eq. 248). In other cases, plots of $\ln \mathbf{R}(q)/c$ vs q^2 may be more nearly linear, and better suited for evaluation of $Kc/\mathbf{R}(0)$ and b.

Dynamic Scattering. With use of equation 155, the unnormalized correlation function $G^{(2)}(\tau,q)$ has the form

$$\left[\frac{G^{(2)}(q,\tau) - G^{(2)}(q,\infty)}{G^{(2)}(q,\infty)}\right]^{1/2} = f^{1/2}(A) \sum_{\nu}^{C} r_\nu D(\Omega_\nu\tau) \exp(-\Omega_\nu\tau) \tag{359}$$

for data extrapolated to infinite dilution (and in the absence of a reference beam) where the fraction r_ν of the light from component ν may depend on q. Accordingly, if $G^{(2)}(q,\infty)$ is accurately known, and the data extend to small enough τ to permit accurate extrapolation to $\tau = 0$, the intercept $[G^{(2)}(q,0) - G^{(2)}(q,\infty)]/G^{(2)}(q,\infty)$ should be dependent only on the optical arrangement. If $qR_G \ll 1$, or the scatterers lack intramolecular motions on the time scale of the experiment, $\Omega_\nu = \gamma_\nu = q^2D_{T,\nu}^0$ and $D(\Omega_\nu\tau)$ is unity. In this case, a plot of $\ln [G^{(2)}(q,\tau) - G^{(2)}(q,\infty)]$ vs τq^2 is linear, with tangent $-2D_T^0$ and intercept $\ln [G^{(2)}(q,\infty)f(A)]$. Arbitrary adjustment of $G^{(2)}(q,\infty)$ to achieve such linearity is not recommended, as departure from linearity may be caused, for example, by heterodispersity and intramolecular motion.

If the plots of $\ln [G^{(2)}(q,\tau) - G^{(2)}(q,\infty)]$ vs τq^2 for data parametric in q are not linear or independent of q, the first cumulant given by equation 146 may depend on q. If the solute is known to be monodisperse, K_1 may be interpreted in terms of the intramolecular dynamics (eg, $k^{(2)}$ in equation 162). Conversely, if it is known that the intramolecular dynamics are unimportant, eg, rigid solute

or small qR_G, the first and second cumulants may be interpreted in terms of molecular weight polydispersity (eqs. 147 and 148). In this case, it may be possible to interpret the nonlinear character of ln $[G^{(2)}(q,\tau) - G^{(2)}(q,\infty)]$ versus τ in terms of the distribution of the fraction r_ν of the scattering from components characterized by γ_ν. In this analysis, r_ν may depend on q, and γ_ν/q^2 should be independent of q. In the first approximation, r_ν is represented as a distribution of a discrete number of components (typically <5). In this procedure, r_1 and γ_1 for the component with smallest γ_ν are evaluated from the tangent to ln $[G^{(2)}(q,\tau 0) - 1]^{1/2}$ vs τ for the data at large τ, and r_1 is obtained from the extrapolation of the tangent to $\tau = 0$ (47). This process is repeated to determine r_2 and γ_2 for the component with next smallest γ_ν using data on ln $[g^{(2)}(q,\tau) - 1)^{1/2} - f^{1/2}r_1 \exp - \gamma_1\tau]$ vs τ, and so on, until the difference plot is linear for the component with smallest γ_ν. Typical results of an analysis of this type are shown in Figure 19, giving r_ν and γ_ν/q^2 for a range of q. More sophisticated procedures have been developed to obtain the distribution of γ_ν and r_ν, including continuous representations (25,44,45,86,87).

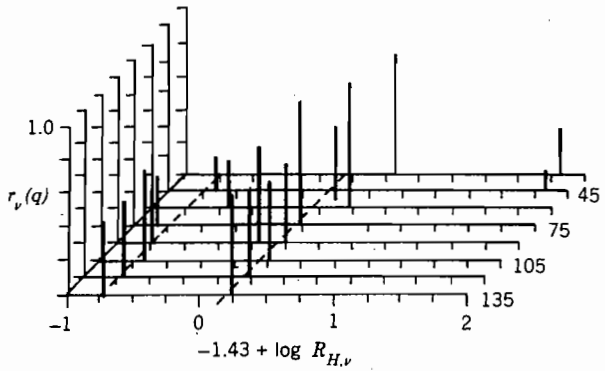

Fig. 19. Components determined from analysis of the photon-count correlation function, showing the hydrodynamic radius $R_{H,\nu}$ and the corresponding weight factor r_ν for several scattering angles (shown on the right-hand side) (37).

Conversion of the data on the r_ν and γ_ν to a molecular weight distribution requires some representation of the dependence of r_ν and c_ν and M_ν and of γ_ν on M_ν. For data at infinite dilution,

$$r_\nu = \frac{w_\nu M_\nu P_\nu(q)}{\overline{M}_w P_X(q)} \tag{360}$$

$$\gamma_\nu/q^2 = kT/6\pi\eta_s R_{H,\nu} \tag{361}$$

where, for example, $R_{H,\nu} \propto M_\nu^\alpha$.

Nomenclature

a	= Mark-Houwink exponent equal to $\partial \ln [\eta]/\partial \ln M$
a	= ionic radius in equation 178
a	= correlation length defined in equation 251

A = illuminated area on the photomultiplier (eq. 13)
$A_2, A_3, \cdots$ = second, third, etc, virial coefficients (eq. 191)
A_2^R, A_2^Π = averages of A_2 (eqs. 208 and 210)
$A(A_2Mc)$ = ratio $a^2/(a^2)^0$ (eq. 252)
b = an experimental correlation length defined by equation 248
b = dimension of a scattering element
$B(T)$ = temperature-dependent coefficient in equation 279
$\mathbf{B}(c)$ = see equations 183 and 184
$B_{\nu\mu}(c)$ = interaction function for solutes ν and μ (eq. 185)
$B^0_{\nu\mu}$ = limiting value of $B_{\nu\mu}(c)$ for small c
$B(A_2Mc)$ = ratio $b^2/(b^2)^0$ (eq. 253)
c, c_ν = concentration (wt/vol) of the solute, or the same for component ν
c_p, c_V = heat capacities at constant p and V, respectively
C = number of solute molecules in the scattering volume
C = constant in equations 100 and 101
C_n = parameter to account for refraction effects
d = hydrodynamic diameter (eq. 166 and Table 1)
d = ratio R_H/R_G
$D(\Omega_\nu\tau)$ = function defined by equation 155
$D_M(c)$ = mutual diffusion constant determined as the limit of $D_{app}(c,q)$ for small q (eq. 265)
D^0_R, $D^0_{R,\nu}$ = rotational diffusion constant at infinite dilution, or the same for component ν
D^0_T, $D^0_{T,\nu}$ = translational diffusion constant at infinite dilution, or the same for component ν
$D_{app}(c,q)$ = apparent diffusion constant determined as K_1/q^2
$D_{\nu\mu}$ = function defined by equation 236
e = electron charge
E = parameter defined by equation 282
$\mathbf{E}, E_i$ = electric field, or its components
$\mathscr{E}, \mathscr{E}$ = applied field in electrophoretic light scattering or its magnitude
f, f_{cyl}, f_{sp} = geometric factor in a relation for the excluded volume (eq. 197) and its values for cylinders and spheroids
$f(A)$ = coherence factor (eq. 22)
$f_A(\theta)$ = factor accounting for attenuation of the scattered and incident rays (eq. 350)
$f_V(\theta)$ = ratio V_{90}/V_θ
$f_{i,\nu}$ = for $i = 1 - 3$, parameters in eq. 113 and 114 (Fig. 6)
$F(q,c)$ = function defined by equation 241
$F_1(\nu), F_2(\nu,\mu)$ = molecular distribution functions (eq. 186)
$g(\mathbf{r})$ = repeat unit-pair correlation function (eq. 223)
$g_2(\nu,\mu)$ = radial distribution function (eq. 186)
$g^{(1)}(q,\tau), g^{(1)}_\nu(q,\tau)$ = function defined by equation 24, or the same for component ν
$g^{(2)}(q,\tau;\Delta\tau)$ = function defined by equation 20
$g^{(2)}(q,\tau;\Delta\tau,A)$ = function defined by equation 22
$g^{(2)}_d(\tau)$ = see equation 345
G_0 = see equation 281
G_i = see equation 329
G_I, G_e = limits of $G(t)$ for small and large t, respectively
G_N = network modulus defined by equation 287
$G(t)$ = linear shear-relaxation modulus
$[\overline{G(\tau)}]_{LS}$ = average value of $G(t)$ for the time scale in a light-scattering experiment
$G_2, G_{2,intra}, G_{2,inter}$ = see equations 232–235
$G_{s,\nu}(\mathbf{R},\tau)$ = Van Hove self-space–time correlation
$G^{(2)}(q,\tau;\Delta\tau)$ = photon-count correlation function (eq. 17); sometimes denoted $G^{(2)}(q,\tau)$
$\hat{G}^{(2)}(q,\omega;A)$ = see equation 181

$h(\gamma)$ = function defined by equation 141
h = parameter in equation 72
h_p = see equation 281
$H_\mu(x)$ = see equation 150
$H(Z)$ = factor in equation 218; nearly equal to unity
$H^{\Pi}(c), H^{G}(c)$ = contributions to $D_M(c)$ (eq. 275)
i = square root of -1
I = ionic strength in equation 179
$I(q)$ = time-averaged scattered intensity
$I(q,t;\mathbf{R})$ = instantaneous scattered intensity at position $\mathbf{R}$
$I(q,t)$ = instantaneous scattered intensity
$I(q,\omega)$ = transform of $I(q,t)$ given by equation 316
I_{inc} = incident intensity
$J(\delta_\nu)$ = function defined by equation 114
k = Boltzmann's constant
k = calibration factor defined by equation 347
$\mathbf{k},\mathbf{k}_0$ = vectoral wave numbers for the scattered and incident rays, respectively
k_{sec} = see equation 354
$k(X_\nu)$ = function of X_ν appearing in equation 165
$k_\nu^{(2)}$ = parameter appearing in equation 158
K = see equation 183
K' = see equation 26c
K_1, K_2, etc = first, second, etc, cumulants (eq. 146)
K_η = parameter defined by equation 1
K_ξ = parameter defined by equation 228
K_i = see equation 328
K_l, K_e = limits of $K(t)$ for small and large t, respectively
$K(t)$ = linear bulk-relaxation modulus
l_θ = cell-path length in equation 350
L, L_ν = contour length of a (linear) polymer chain, or the same for component ν
m = molecular weight of a hydrodynamic unit (eq. 284b)
m_0 = molecular weight of a chain-repeating unit
m_1, m_2 = constants appearing in equation 291, defined by equation 292
$m_{i,\nu}$ = molecular weight of monomer i on chain ν
m_ν = parameter M_ν/n_ν
$m_1(q\xi_q), m_2(q\xi_q)$ = parameters appearing in equation 300, defined by equation 301
$\Delta m_{i,\nu}$ = see equation 36
M, M_ν = molecular weight, or the same for component ν
M_L = parameter M/L
$\overline{M}_n, \overline{M}_w, \overline{M}_z$ = number, weight, and z-average molecular weights for a polydisperse solute (eq. 33)
$\overline{M}_{n,A}, \overline{M}_{w,A}$ = see equation 48
M_{LS} = see equation 32
$\mathbf{M}_c$ = polymer-specific constant in equation 282
$\mathbf{M}_c'$ = polymer-specific constant in equation 286
$\mathbf{M}_e$ = polymer-specific constant in equation 287
$\mathbf{M}_l, \mathbf{M}_e$ = limits of $M(t)$ for small and large t, respectively
$\mathbf{M}(t)$ = linear longitudinal-relaxation modulus
$\mathbf{M}_{LS}(c)$ = see equation 274
$\mathbf{M}_{LS}(c,q)$ = see equation 296
$\mathbf{M}'(\omega), \mathbf{M}''(\omega)$ = storage and loss longitudinal moduli (eqs. 324 and 332)
n, n_ν = number of scattering elements in a solute, or the same for component ν
n_A, n_B = number of scattering elements of type A and B in a copolymer

n_{jk} = number of scattering elements between elements j and k on a polymer chain

$\tilde{n},\tilde{n}_s$ = refractive index and the same for the solvent

$\mathbf{n}_r,\mathbf{n}_s$ = unit vectors defining polarization of the incident and scattered beams, respectively

n_n,n_w,n_z,etc = the number, weight, or z-average, etc of n for a polydisperse solute (eqs. 73–75)

$n(q,t;\Delta\tau)$ = count rate at time t averaged over duration $\Delta\tau$ (eq. 13)

$\langle n\rangle_T,\langle n\rangle_{SC},\langle n\rangle_F,\langle n\rangle_D,\langle n\rangle_R,\langle n_r\rangle$ = contributions to the observed average count rate

$\langle n\rangle_{inc},n_{inc}$ = average count rate for the incident beam

$\langle n\rangle_{ref}$ = average count rate of a reference beam mixed with the scattered light

$\langle n\rangle_{sec}$ = average count rate from a secondary standard

$\langle n(q,\Delta\tau)\rangle,\langle n\rangle$ = average count rate at q with sample interval $\Delta\tau$

$n^{(r)}(q,\Delta\tau)$ = normalized r^{th} factorial moment (eq. 21)

$n^{(2)}(q,\Delta\tau;A)$ = function defined by equation 23

$n_d^{(2)}(\Delta\tau)$ = see equation 344

N_A = Avogadro's number

$N^{(r)}(q,\Delta\tau)$ = rth factorial moment (eq. 16)

p = exponent defined by equation 216

p = parameter in equation 39

$p(q,\Delta\tau)$ = see equations 25b and 139

P_e = see equation 288

$p_i(x_\nu)$ = for i = 1,2,3, functions defined by equations 115–117

$p_1(n)$ = probability density for the count rate

$p_2(n,m)$ = bivariant probability density for the count rate

$\tilde{p}_1(n,\Delta\tau)$ = estimate of $p_1(n)$ (eq. 339)

P = pressure

$\mathbf{P},P_i$ = polarizability or its components (eq. 3)

$P(A_2Mc)$ = see equation 215

$P(q,c),P_\nu(q,c)$ = intramolecular interference function at concentration c, or the same for component ν (eq. 66a)

$P^0(q),P_\nu^0(q)$ = intramolecular interference function at infinite dilution, or the same for component ν (eq. 66b)

$P_A^0(q),P_B^0(q),P_{AB}^0(q)$ = interference functions in equation 104 for a copolymer

$P_X^0(q)$ = average of $P_\nu^0(q)$ defined by equation 65

$P_{V,A}^0(q),P_{H,A}^0(q)$ = see equations 110 and 111, respectively

$P_{V,\nu}^0(q),P_{H,\nu}^0(q)$ = see equations 112 and 113, respectively

$P_{\parallel,\nu\mu}(q,c)$ = see equation 239

$\mathbf{q},q$ = scattering vector and its magnitude (eq. 9)

q = parameter in equation 39

q_3 = parameter A_3/A_2^2M (eqs. 194 and 195)

$q_i(X_\nu)$ = for i = 1–4, functions defined by eqs. 118–121

$Q(q,c)$ = see equation 243

$Q^0(q)$ = limit of $Q(q,c)$ for small c (eq. 246)

Q_a,Q_a^0 = see equations 4 and 6

$Q_{rs}(\mathbf{q},t)$ = see equation 10

r = exponent defined by equation 254

r = parameter defined by equation 78

r = position vector

$\mathbf{r}_i,\mathbf{r}_i(\tau)$ = position of the i^{th} scattering element, or its value at time τ

$\mathbf{r}_{ij},\mathbf{r}_{i\nu,i\mu}$ = vector between scattering elements i and j, the same for elements on separate solutes

r_0 = fraction of the total count rate due to a reference beam

r_ν = fraction of the scattered light due to component ν

$r_L(c,q)$ = see equation 311

$\langle r_{jk}^2\rangle$ = mean-square distance between scattering elements

R = distance between the scattering elements and the photomultiplier
R = gas constant kN_A
$\mathbf{R}$ = position on a photomultiplier
R_N = see equation 286
$R^{(s)}$ = steady-state recoverable compliance (eq. 285)
$R^{(R)}$ = parameter $2M/5cRT$ (eq. 286)
$R_G, R_{G,\nu}$ = root-mean-square radius of gyration, and the same for component ν (eq. 68)
$R^2_{G,X}$ = average of $R^2_{G,\nu}$ defined by equation 67
$R_{G,A}, R_{G,B}$ = parameters in a relation for $R^2_{G,X}$ for copolymers (eq. 86)
$R_H, R_{H,\nu}$ = hydrodynamic radius, the same for component ν (eq. 136)
$\mathbf{R}(q)$ = Rayleigh ratio defined by equation 15
$\mathbf{R}_{iso}(q), \mathbf{R}_{aniso}(q), \mathbf{R}_{cross}(q)$ = components in the expression for the Rayleigh ratio for anisotropic scatterers (eqs. 106 and 107)
s = exponent introduced in equation 287
$\mathbf{s}_i, \mathbf{s}_i(\tau)$ = vector distance of scattering element i from the center of mass of the molecule (or particle), and the same at time τ
$s^{(2)}_\nu(u_\nu)$ = structure-dependent parameter in equation 158
$\mathbf{S}(\tau)$ = position of the center of mass at time τ
$S([\eta]c)$ = function defined by equation 229
$S_q([\eta]c)$ = function defined by equation 260
$S_\nu(q,\tau)$ = see equation 127
$S(q,\omega)$ = see equation 315
$S_{iso}(q,\omega), S_{aniso}(q,\omega)$ = see equations 318 and 319
$S^{(C)}_{iso}(q,\omega), S^{(B)}_{iso}(q,\omega)$ = see equation 320
t = time
T = temperature
$T_0(\phi)$ = concentration-dependent parameter in equation 278
u, u_ν = product $R^2_G q^2$ or $R^2_{G,\nu} q^2$
U = excluded volume defined by equation 196
$U_{\nu\mu}$ = potential appearing in equation 186
$\mathbf{v}$ = velocity
V = volume
V_p = particle volume used in equation 197
$V_{\xi 0}, V_{\xi q}$ = correlation volumes appearing in equations 224 and 258, respectively
V_θ, V_{90} = scattering volume at angle θ or $\theta = 90°$C
$V_S(q)$ = adiabatic sound velocity in equation 314
w, w_ν = weight fraction of the solute, or the same for component ν
w_A, w_B = see equation 43
$w_{A,\nu}$ = see equation 43
Δw_ν = see equation 43
$W[F(q,c)]$ = see equation 298
x, x_ν = parameter in equations 90, 124, and 125
X = parameter in equation 255 equal to $1.3\, A_2 Mc$
$X_H(\kappa a)$ = see equation 178
X_ν = see equation 166
y, y_ν = parameter in equation 92
z, z_ν = parameter in equation 91
Z = charge on a solute in equation 178
Z = product $A_2 Mc$ (eqs. 217 and 218)
$Z_{eq}, Z_{eq,\nu}$ = equivalent charge per solute, or the same for component ν (eqs. 177 and 178)
α = exponent in equation 150
$\boldsymbol{\alpha}, \boldsymbol{\alpha}_\nu$ = excess isotropic polarizability of a solute, or the same for component ν (eq. 27)
$\boldsymbol{\alpha}, \alpha_{ij}$ = excess polarizability, or its components
$\boldsymbol{\alpha}_\nu(t)$ = excess polarizability of component ν at time t

$\alpha_{\parallel},\alpha_{\perp}$ = principal excess polarizabilities for scattering elements with cylindrical symmetry (eq. 56)

$\Delta\alpha_{rs}(\mathbf{q},t),\Delta\alpha_{rs}^{*}(\mathbf{q},t)$ = function defined by equation 11 and is complex conjugate

α_c = parameter defined in connection with equation 282

β = parameter defined in connection with equation 151

$\boldsymbol{\beta},\beta_{ijk}$ = hyperpolarizability tensor and its components

β_{ij} = see equation 55

γ = exponent in equation 212

γ = ratio c_p/c_V in equation 323

γ,γ_ν = inverse coherence time $q^2D_T^0$, or the same for component ν (eq. 135)

$\langle\gamma_\nu^2\rangle$ = mean-square optical anisotropy per molecule of component ν in equations 51 and 52

$\gamma_L(c,q),\gamma_S(c,q)$ = see equation 311

$\langle\gamma\rangle_n^{(2)}$ = see equation 149

Γ_2,Γ_3 = virial coefficients equal to A_2M, A_3M, etc

Γ_B = see equation 321

$\Gamma(c)$ = see equation 188

δ,δ_ν = see equation 55

δ_0 = see equation 56

δ_X^2 = see equation 54

$\delta(\omega_B)$ = see equation 333

Δ_{AB} = see equation 86

ϵ = exponent used in equation 284

ϵ = exponent, defined by its use in equation 78

$\underline{\epsilon}$ = see equations 344 and 345

$\mathscr{E}$ = electric field in electrophoresis (eq. 175)

$\zeta,\zeta(\phi)$ = friction factor of a chain element

η = as a summation limit, the total number of scattering elements (eq. 11)

η,η_s = viscosity or viscosity of a solvent (diluent)

$[\eta],[\eta]_\nu$ = intrinsic viscosity of a solute, or the same for component ν; $[\eta]$ being the limiting value of $\partial\ln\eta/\partial c$ at infinite dilution

$[\eta]_e$ = value of $[\eta]$ for $M = M_e$

$\eta^{(R)}$ = see equation 284b

$\eta_c^{(R)}$ = value of $\eta^{(R)}$ for $M = M_c$

θ = scattering angle (Fig. 1)

κ = in equation 178, a parameter defined by equation 179

κ_i = see equation 328

λ,λ_0 = wavelength of light in a dielectric or in vacuum ($\lambda = \lambda_0/\tilde{n}$)

μ = subscript denoting osmotic equilibrium in equation 34

μ_A = extinction coefficient for absorption

μ_ν = electrophoretic mobility in equation 176, defined by equation 177

ξ_0,ξ_q = correlation lengths defined by equations 227 and 259

Ξ^0,Ξ_ν^0 = molecular friction coefficient at infinite dilution

$\Xi(c)$ = molecular friction coefficient at finite concentration (eqs. 266 and 268)

$\Xi(c,q)$ = see equation 296

Π = osmotic pressure

ρ = persistence length (eq. 69)

$\hat{\rho}$ = density

σ = constant in equation 13

σ = parameter $\partial\ln R_H/\partial\ln R_G$

$\sigma(z)$ = see equation 308

τ = time in dynamic scattering

τ_C = product $\eta R^{(S)}$

τ_e = parameter $[\eta_c^{(R)}/\eta]\tau_C$

τ_p = see equation 281

τ_i = see equation 329

τ_s = in equation 350, the turbidity defined by equation 351
τ_L, τ_S = see equation 313
τ_m = see equation 281
$\tau_\nu^{(2)}$ = see equation 160
$\Delta\tau$ = time interval (eqs. 13 and 25)
ϕ = volume fraction of a solute
ϕ = in equation 176, the angle between $\mathbf{q}$ and ϵ
ϕ_m = limiting volume fraction for close packing of spheres
Ψ, Ψ_ν = refractive index increment or the same for component ν (eq. 28)
Ψ_A, Ψ_B = refractive index increments for monomers A and B in a copolymer or blend
ψ_3 = parameter $A_3M/[\eta]^2$
$\psi(U/R_G^3)$ = see equation 203
ω = frequency difference between scattered and incident light
ω_B = see equation 314
ω_L = frequency of the incident light
ω_S = frequency of the scattered light
ω_ϵ = see equation 79
$\Delta\omega_\nu$ = parameter $\mathbf{q}\cdot\nu_\nu$ in equation 174
Ω_a = see equation 7
Ω_ν = see equation 155

Subscripts

V_V, H_V = vertical and horizontally polarized components of light scattered with vertically polarized incident light
V_h, H_h = same as the preceding, but with horizontally polarized incident light
X = averaged parameter computed as shown in equation 62
ν, μ = components in a heterodisperse solute

Superscripts

(1) = see equation 24
(2) = see equations 17 and 23
0 = parameter evaluated at infinite dilution (eq. 26b)
~ = experimental estimate of a parameter, except to denote the refractive index (eqs. 336–339)

Standard Symbols

$J_1(z)$ = first-order Bessel function
$0(x^d)$ = function with the property that $0(x^d)/x^d$ is of order unity
$P_2(z)$ = Legendre polynomial of the second kind (eq. 237)
$\mathrm{Si}(z)$ = sine integral (eq. 93)
$\Gamma(z)$ = gamma functions in equations 72, 81, 84, 150, and 151
$\delta(z - z_0)$ = Dirac delta function
δ_{ij} = Kronecker delta
∇^2 = Laplacian operator

BIBLIOGRAPHY

"Light Scattering" in *EPST* 1st ed., Vol. 8, pp. 231–233, by Jo Conrad, *Encyclopedia of Polymer Science and Technology.*

1. B. J. Berne and R. Pecora, *Dynamic Light Scattering,* Wiley–Interscience, New York, 1976.
2. B. Chu, *Laser Light Scattering,* Academic Press, Inc., New York, 1974.
3. H. Z. Cummins and E. R. Pike, eds., *Photon Correlation and Light Beating Spectroscopy,* Plenum Publishing Corp., New York, 1974.
4. B. E. Dahneke, ed., *Measurement of Suspended Particles by Quasi-Elastic Light Scattering,* Wiley–Interscience, New York, 1983.
5. P. J. Flory, *Statistical Mechanics of Chain Molecules,* Wiley–Interscience, New York, 1969.
6. A. Guinier and G. Fournet, *Small-Angle Scattering of X-Rays,* translation by C. B. Walker, John Wiley & Sons, Inc., New York, 1955; University Microfilms, Ann Arbor, Mich.
7. M. B. Huglin, ed., *Light Scattering From Polymer Solutions,* Academic Press, Inc., New York, 1972.
8. M. Kerker, *The Scattering of Light and Other Electromagnetic Radiation,* Academic Press, Inc., New York, 1969.
9. M. Kerker, ed., *Electromagnetic Scattering,* ICES I, Pergamon Press, Inc., Elmsford, N.Y., 1963.
10. D. McIntyre and F. Gornick, eds., *Light Scattering From Dilute Solutions,* Gordon and Breach Science Publishers, Inc., New York, 1964.
11. R. L. Rowell and R. S. Stein, eds., *Electromagnetic Scattering,* ICES II, Gordon and Breach Science Publishers, Inc., New York, 1967.
12. B. Sedlacek, C. G. Oberberger, H. F. Mark, and T. G. Fox, eds., *J. Polym. Sci. Polym. Symp.* **61,** 1977.
13. H. Yamakawa, *Modern Theory of Polymer Solutions,* Harper and Row Publishers, Inc., New York, 1971.
14. V. A. Bloomfield and T. K. Lim, *Methods Enzymol.* **48,** 415 (1978).
15. W. Burchard, *Adv. Polym. Sci.* **48,** 1 (1983).
16. E. F. Casassa and G. C. Berry in P. E. Slade, Jr., ed., *Polymer Molecular Weights,* Part 1, Marcel Dekker, Inc., 1975, Chapt. 5.
17. E. F. Casassa and H. Eisenberg, *Adv. Protein Chem.* **19,** 287 (1964).
18. B. Chu, *Pure Appl. Chem.* **49,** 941 (1977).
19. W. H. Flygare, S. L. Hartford, and B. R. Ware, *Electro-Opt. Syst. Des.* 1, 321 (1976).
20. A. M. Jamieson and M. E. McDonnell, *Advances in Chemistry Series No. 174,* American Chemical Society, Washington, D.C., 1979, pp. 163.
21. G. D. Patterson, *Adv. Polym. Sci.* **48,** 125 (1983).
22. W. L. Peticolas, *Adv. Polym. Sci.* **9,** 285 (1972).
23. E. R. Pike and E. Jakeman, *Adv. Quantum Electron.* **2,** 1 (1974).
24. B. A. Smith and B. R. Ware, *Contemp. Top. Anal. Clin. Chem.* **2,** 29 (1978).
25. J. M. Schurr, *CRC Crit. Rev. Biochem.* **4,** 371 (1977).
26. B. R. Ware, *Adv. Colloid Interface Sci.* **4,** 1 (1974).
27. P. Debye, *J. Appl. Phys.* **15,** 338 (1944); reprinted in Ref. 10, p. 1.
28. P. J. Flory, *Principles of Polymer Chemistry,* Cornell University Press, Ithaca, N.Y., 1953.
29. H. Eisenberg, *Biological Macromolecules and Polyelectrolytes in Solution,* Clarendon Press, Oxford, U.K., 1976.
30. C. Strazielle in Ref. 7, Chapt. 15.
31. H. Benoit in Ref. 9, p. 285.
32. H. Benoit and D. Froelich in Ref. 7, Chapt. 11.
33. H. Benoit and C. Wippler, *J. Chem. Phys.* **57,** 524 (1960); English translation in Ref. 10, p. 211.
34. M. V. Volkenstein, *Configurational Statistics of Polymer Chains,* Wiley–Interscience, New York, 1969.
35. G. C. Berry, *J. Polym. Sci.* **65,** 143 (1978).
36. B. H. Zimm, *J. Chem. Phys.* **16,** 1093, 1099 (1948); reprinted in Ref. 10, p. 149, 157.
37. R. Furukawa and G. C. Berry, *Pure Appl. Chem.* **57,** 913 (1985).
38. G. C. Berry in M. B. Bever, ed., *Encyclopedia of Materials Science and Engineering,* Pergamon Press, Oxford, 1986, p. 3759.
39. A. Peterlin in Ref. 9, p. 357.
40. P. Kratochvil in Ref. 7, Chapt. 7.
41. A. Holtzer, *J. Polym. Sci.* **17,** 432 (1965); reprinted in Ref. 10, p. 195.
42. W. Burchard, K. Kajiwara, D. Nerger, and W. H. Stockmayer, *Macromolecules* **17,** 222 (1984).

43. E. Jakeman in Ref. 3, p. 75.
44. B. Chu and A. Dinapoli in Ref. 4, Chapt. 3.
45. E. R. Pike, D. Watson, and F. McNeil Watson in Ref. 4, Chapt. 4.
46. D. E. Koppel, *J. Chem. Phys.* **57,** 4814 (1972).
47. Y. Einaga and G. C. Berry in P. Dubin, ed., *Microdomains in Polymer Solutions,* Plenum Publishing Corp., New York, 1985, Chapt. 11.
48. A. Z. Akcasu, M. Benmouna, and C. C. Han, *Polymer* **21,** 866 (1980).
49. G. Ronca, *J. Chem. Phys.* **79,** 1031 (1983).
50. P. G. de Gennes, *Scaling Concepts in Polymer Physics,* Cornell University Press, Ithaca, N.Y., 1979.
51. G. C. Berry and E. F. Casassa, *J. Polym. Sci., Part D* **4,** 1 (1970).
52. Y. Oono and M. Kohmoto, *J. Chem. Phys.* **78,** 520 (1983).
53. K. F. Freed, *Acc. Chem. Res.* **18,** 38 (1985).
54. N. F. Carnaham, K. E. Starling, *J. Chem. Phys.* **51,** 635 (1969).
55. B. L. Hager, G. C. Berry, and H. H. Tsai, *J. Polym. Sci. Polym. Phys. Ed.,* in press.
56. T. Amerzadeh and M. E. McDonnell, *Macromolecules* **15,** 927 (1982).
57. P. Wiltzuis, H. R. Haller, D. S. Cannell, and D. W. Schaefer, *Phys. Rev. Lett.* **51,** 1183 (1983).
58. G. D. Patterson and P. J. Flory, *J. Chem. Soc. Faraday Trans. 2* **68,** 111 (1972).
59. C. C. Lee, S. G. Chu, and G. C. Berry, *J. Polym. Sci. Polym. Phys. Ed.* **21,** 1573 (1983).
60. I. Noda, N. Kato, T. Kitano, and M. Nagasawa, *Macromolecules* **14,** 668 (1981).
61. A. J. Hyde in Ref. 7, Chapt. 7.
62. H. Benoit and M. Benmouna, *Polymer* **25,** 1059 (1984).
63. G. K. Batchelor, *J. Fluid Mech.* **52,** 245 (1972); **74,** 1 (1976); M. Muthukumar and K. F. Freed, *J. Chem. Phys.* **78,** 511 (1983).
64. J. M. Carter and G. D. F. Phillies, *J. Phys. Chem.* **89,** 5118 (1985).
65. F. Brochard and P. G. de Gennes, *Macromolecules* **10,** 1157 (1977).
66. F. Brochard, *J. Phys.* **44,** 39 (1983).
67. G. D. Patterson, J. P. Jarry, and C. P. Lindsey, *Macromolecules* **13,** 668 (1980).
68. J. D. Ferry, *Viscoelastic Properties of Polymers,* 3rd ed., John Wiley & Sons, Inc., New York, 1980.
69. G. C. Berry and T. G. Fox, *Adv. Polym. Sci.* **5,** 261 (1967).
70. W. W. Graessley, *Adv. Polym. Sci.* **16,** 1 (1975); **47,** 68 (1982).
71. G. C. Berry and D. J. Plazek in *Glass: Science and Technology,* Academic Press, Inc., New York, 1986, Chapt. 6.
72. L. S. Ornstein and F. Zernicke, *Phys. Z.* **19,** 134 (1918); **27,** 761 (1926).
73. W. Brown and R. M. Johnsen, *Macromolecules* **18,** 379 (1985).
74. J. Roots and B. Nystrom, *Macromolecules* **13,** 1595 (1980).
75. J. P. Munch, G. Hild, and S. Candau, *Macromolecules* **16,** 71 (1983).
76. B. J. Ackerson, *J. Chem. Phys.* **64,** 242 (1976); **69,** 684 (1978).
77. R. A. Ferrell, *Phys. Rev. Lett.* **24,** 1169 (1970).
78. M. Adam and M. Delsante, *Macromolecules* **18,** 1760 (1985).
79. C. H. Wang and E. W. Fischer, *J. Chem. Phys.* **82,** 632 (1985).
80. M. H. Birnboim, *Proceedings of the IUPAC, 28th Macromolecular Symposium,* Amherst, Mass., 1982, p. 872.
81. H. Utiyama in Ref. 7, Chapt. 3.
82. B. R. Ware, D. Cyr, S. Gorti, and F. Lani in Ref. 4, Chapt. 9.
83. M. Bertolotti in Ref. 3, p. 41.
84. H. Utiyama in Ref. 7, Chapt. 4.
85. G. C. Berry and M. A. Leech in D. A. Brant, ed., *Solution Properties Polysaccharine, ACS Symposium Series No. 150,* American Chemical Society, Washington, D.C., 1981.
86. E. F. Grabowski and I. D. Morrison in Ref. 4, Chapt. 7.
87. R. S. Stock and W. H. Ray, *J. Polym. Sci. Polym. Phys. Ed.* **23,** 1393 (1985).

GUY C. BERRY
Carnegie-Mellon University